



University of HUDDERSFIELD

University of Huddersfield Repository

Barragan, Inmaculada

TOPICAL SUBSTITUTION OF TRANSGLUTAMINASE 1 FOR THE TREATMENT OF CONGENITAL ICHTHYOSIS

Original Citation

Barragan, Inmaculada (2019) TOPICAL SUBSTITUTION OF TRANSGLUTAMINASE 1 FOR THE TREATMENT OF CONGENITAL ICHTHYOSIS. Masters thesis, University of Huddersfield.

This version is available at <http://eprints.hud.ac.uk/id/eprint/34946/>

The University Repository is a digital collection of the research output of the University, available on Open Access. Copyright and Moral Rights for the items on this site are retained by the individual author and/or other copyright owners. Users may access full items free of charge; copies of full text items generally can be reproduced, displayed or performed and given to third parties in any format or medium for personal research or study, educational or not-for-profit purposes without prior permission or charge, provided:

- The authors, title and full bibliographic details is credited in any copy;
- A hyperlink and/or URL is included for the original metadata page; and
- The content is not changed in any way.

For more information, including our policy and submission procedure, please contact the Repository Team at: E.mailbox@hud.ac.uk.

<http://eprints.hud.ac.uk/>



University of
HUDDERSFIELD

**TOPICAL SUBSTITUTION OF
TRANSGLUTAMINASE 1 FOR THE TREATMENT
OF CONGENITAL ICHTHYOSIS**

INMACULADA BARRAGÁN VÁZQUEZ

A thesis submitted to the University of Huddersfield in partial fulfilment of the requirements for the degree of Master's by Research (MSc) in Biological Sciences.

The University of Huddersfield

September 2018

Copyright statement

- i. The author of this thesis (including any appendices and/or schedules to this thesis) owns any copyright in it (the “Copyright”) and s/he has given The University of Huddersfield the right to use such copyright for any administrative, promotional, educational and/or teaching purposes.
- ii. Copies of this thesis, either in full or in extracts, may be made only in accordance with the regulations of the University Library. Details of these regulations may be obtained from the Librarian. This page must form part of any such copies made.
- iii. The ownership of any patents, designs, trademarks and any and all other intellectual property rights except for the Copyright (the “Intellectual Property Rights”) and any reproductions of copyright works, for example graphs and tables (“Reproductions”), which may be described in this thesis, may not be owned by the author and may be owned by third parties. Such Intellectual Property Rights and Reproductions cannot and must not be made available for use without the prior written permission of the owner(s) of the relevant Intellectual Property Rights and/or Reproductions

Abstract

Autosomal recessive congenital ichthyosis (ARCI) is a rare cornification disorder with impaired skin barrier function and with no causative treatment available. Eleven genes are involved in different ARCI phenotypes, all related to epidermal differentiation. Mutation in *TGMI* is the main cause of ARCI, and it encodes for the enzyme transglutaminase 1 (TGase1), which is involved in the keratinocyte differentiation and in the formation of the cornified cell envelope. Mutations in *TGMI* cause lamellar ichthyosis and congenital ichthyosiform erythroderma phenotypes, causing also self-healing collodion babies.

In this project, we aimed to study the fate of the protein-loaded thermoresponsive PNIPAM-dPG nanogel for cutaneous protein TGase1 delivery for restoring the skin barrier function in ARCI patients with *TGMI* mutation.

To accomplish this, TGase1 delivery was analysed in keratinocytes grown in a 2D monolayer and in 3D skin models. We first studied the gene expression of *TGMI* and other specific markers for ARCI on RNA level. As *TGMI* was expressed in all our cell models (human control, human ARCI-patient with *TGMI* mutation, and pig control keratinocytes), we subsequently developed three-dimensional skin models to evaluate the destiny of the TGase1/NG complex in the skin. Observing the successful delivery of TGase1 and nanogel in the epidermis, we carried out the study of their location in keratinocytes in a 2D monolayer. Our findings suggested that TGase1 and nanogel enter the keratinocytes, release one from each other, and they are located around the nuclei, in the cytoplasm and in the plasma membrane.

Table of contents

1. Introduction.....	11
1.1. Skin: structure and barrier function.....	11
1.1.1. Human skin.....	11
1.1.2. Porcine skin.....	17
1.2. ARCI.....	21
1.2.1. Classification of ARCI.....	21
1.2.2. Genetics of ARCI.....	25
1.2.3. Therapeutic strategies.....	28
1.3. Skin models.....	30
1.4. Skin Explants.....	32
2. Aim of the study.....	34
3. Materials and methods.....	36
3.1. Ethical approval.....	36
3.2. Materials.....	36
3.3. Methods.....	39
3.3.1. Cell culture.....	39
3.3.2. Analysis of 2D keratinocytes.....	48
3.3.3. Harvesting and analysis of 3D Skin models.....	49
3.3.4. RNA extraction.....	51
3.3.5. cDNA synthesis.....	53
3.3.6. TaqMan Real Time PCR (qRT-PCR).....	54
3.3.7. Statistical analysis.....	56
4. Results.....	57
4.1. Gene expression in differentiated and non-differentiated primary keratinocytes.....	57
4.2. 3D skin models characterization.....	59
4.2.1. Evaluation of skin structure in 3D skin models.....	60

4.2.2. Challenges in 3D skin model construction.....	60
4.3. Application of TGase1/NG complex in cells grown on a 2D monolayer	61
4.4. Characterization of Pig Skin Explants.....	68
5. Discussion.....	70
5.1. Comparison of human and pig keratinocytes growth conditions	71
5.2. TGase1 is expressed on RNA level in 2D keratinocytes.....	71
5.3. Control and diseased 3D skin models are good systems to test protein substitution	75
5.4. TGase1/NG complex enters the keratinocytes	79
5.5. Pig skin explants.....	82
6. Conclusion	84
7. Bibliography	86

List of figures

Figure 1. Schematic representation of normal skin structure.	13
Figure 2. Apoptosis and terminal differentiation in the epidermis..	15
Figure 3. Generation of acyl-Cer and protein-bound Cer in epidermis..	17
Figure 4. Comparison between human, pig, rat and mouse skin.	19
Figure 5. Phenotype of ARCI-patients.....	24
Figure 6. Schematic illustration of genomic organization of <i>TGM1</i>	27
Figure 7. Synthesis and chemical structure of the PNIPAM-dPG nanogels.....	30
Figure 8. Full thickness skin models.....	32
Figure 9. Schematic representation of extraction of pig skin cells.	42
Figure 10. Schematic representation of splitting.	43
Figure 11. Schematic representation of skin models.	46
Figure 12. Schematic representation of pig skin explant.	47
Figure 13. Schematic representation of RNA extraction.	53
Figure 14. Drawing of the plate with the samples and primers.	55
Figure 15. Gene expression in differentiated primary keratinocytes.	57
Figure 16. Gene expression in basal primary keratinocytes.....	58
Figure 17. Characterization of untreated and treated control, and ARCI-patient derived 3D skin models (day 13).....	60
Figure 18. Anti E-cadherin staining when application of labelled TGase1/NG complex in basal, control human keratinocytes.	62
Figure 19. Anti EEA1 staining when application of labelled TGase1/NG in basal, control human keratinocytes	63
Figure 20. Anti GM130 staining when application of labelled TGase1/NG in basal, control human keratinocytes.	63
Figure 21. LysoTracker deep red staining when application of labelled TGase1/NG in basal, control human keratinocytes.	64

Figure 22. Anti E-cadherin staining when application of labelled TGase1/NG complex in basal, control porcine keratinocytes.	65
Figure 23. Anti EEA1 staining when application of labelled TGase1/NG complex in basal, control porcine keratinocytes.	66
Figure 24. Anti GM130 staining when application of labelled TGase1/NG complex in basal, control porcine keratinocytes	67
Figure 25. LysoTracker deep red staining when application of labelled TGase1/NG complex in basal, control porcine keratinocytes.....	67
Figure 26. Pig skin explants.....	69

List of tables

Table 1. Advantages and disadvantages of human and porcine skin models	20
Table 2. Subtypes of inherited ichthyosis: nonsyndromic forms.....	21
Table 3. Subtypes of inherited ichthyosis: syndromic forms.....	22
Table 4. Reagents used in cell culture.	39
Table 5. Program used for paraffin embedding.	49
Table 6. Required volume of Lysis Buffer.	51
Table 7. Composition of PureLink® DNase mixture.	52
Table 8. Quantities of Master Mix, primer, cDNA and distilled water for every plate.	54
Table 9. Cycling conditions to run RT-PCR.....	55

Acknowledgment

I would like to acknowledge my supervisor, Dr Hans Christian Hennies, for his guidance, encouragement and advice he has provided throughout my time as his student. Thanks to him, I could work on an interesting project where I learned a lot of new and different techniques.

A special mention goes to Dulce and Sari for their support, guidance, and teaching me all what I know now about working in the lab.

I would also like to thank Gabriele for his support and for helping me in finalizing this project.

Abbreviations list

2D	Two-dimensional
3D	Three-dimensional
Acyl Cer	Acylceramides
ARCI	Autosomal recessive congenital ichthyosis
Arg	Arginine
Asp	Aspartic acid
BSA	Bovine serum albumin
BSI	Bathing suit ichthyosis
CaCl ₂	Calcium chloride
cDNA	Complementary DNA
CE	Cornified envelope
Cer	Ceramide
CIE	Congenital ichthyosiform erythroderma
CLE	Cornified lipid envelope
CO ₂	Carbon dioxide
CT	Cholera Toxin
CYP4F22	Protein of the cytochrome-P450 family 4, subfamily F, polypeptide 22
Cys	Cystine
DAPI	4',6-diamidino-2-phenylindole nuclear staining
DC	Dendritic cells
DMEM	Dulbecco's modified Eagle medium
DMSO	Dimethylsulfoxid
dPG	Di-polyglycerol
EDTA	Ethylenediaminetetraacetic acid
EGF	Human epidermal growth factor
FBS	Fetal Bovine Serum
FFA	Free fatty acids
FLG	Filaggrin
FTM	Full thickness human skin model
GAPDH	Glyceraldehyde 3-phosphate dehydrogenase
Gln	Glutamine
Gly	Glycine

HaCaT	Immortalized human keratinocyte line
HBSS	Hank's balanced salt solution
HC	Hydrocortisone
H&E	Haematoxylin and eosin
HI	Harlequin ichthyosis
His	Histidine
hOSEC	Human organotypic skin explanted culture
HSE	Human skin equivalents
KBM	Keratinocyte basal medium
KCM	Keratinocyte culture medium
KGM	Keratinocyte growth medium
KIFs	Keratin intermediate filaments
LC	Langerhans cells
LDH	Cellular lactate dehydrogenase
LI	Lamellar ichthyosis
LOX	Lysoxygenases
Lys	Lysine
MEDOC	Mendelian disorders of cornification
MTT	Dimethyl-thiazoldiphenyltetrazolium bromide
NAOH	Sodium hydroxide
NG	Nanogel
P/S	Penicillin-Streptomycin
PBS	Phosphate buffered saline
PECM	Pig explant culture medium
PNIPAm	Poly(N-isopropylacrylamide)
qPCR	Quantitative polymerase chain reaction
RH	Relative humidity
RNA	Ribonucleic acid
RT	Room temperature
RT-PCR	Real Time – Polymerase chain reaction
SC	Stratum corneum
SDS	Sodium dodecyl sulfate
SHCB	Self-healing collodion baby

SICI	Self-improving congenital ichthyosis
SPR	Small proline-rich protein
T	Treated
TG	Transglutaminase
TGase1	Transglutaminase 1 protein
TPM	Transportation medium
TRAIL	Tumor necrosis factor-related apoptosis-inducing ligand
UT	Untreated
UVR	Ultraviolet radiation
WHO	World Health Organization
ω -OH Cer	ω -hydroxyceramide

1. INTRODUCTION

1.1. SKIN: STRUCTURE AND BARRIER FUNCTION

1.1.1. HUMAN SKIN

Skin is the largest and one of our body's heaviest organ. Skin is the primary protective organ of the human body, with a measure about 1.5-2 m² in adults, covers the body's entire external surface and serves as a first-order physical barrier against the environment (Richardson, 2003; Lai-Cheong and McGrath, 2017; Lopez-Ojeda and James, 2017). The skin permeability barrier is located in the horny layer of the epidermis and serves a vital function by protecting against water loss from the body. It prevents the invasion of pathogens, allergens, UV light and chemicals, takes part in metabolic processes, and plays a thermoregulatory function. Barrier dysfunction can be involved in the pathophysiology of cutaneous disorders, for example, ichthyosis; infectious diseases, and dry skin, as this can be caused by certain mutations that can lead to an impairment of skin barrier formation (Landmann, 1988; Kolarsick, Kolarsick, and Goodwin, 2011; Boer et al., 2016; Kihara, 2016).

Looking at its structure, skin consists of three layers: the outer epidermis (a superficial epidermal layer), the inner dermis (a deeper, thicker dermal layer), and subcutaneous tissue that links the upper layers to the adjacent tissues and organs (Lai-Cheong and McGrath, 2009; Kolarsick, Kolarsick, and Goodwin, 2011; Eckl et al., 2013).

Each of these layers contains different cell types and is involved in specific functions (Figure 1). The epidermis is mainly formed by keratinocytes (95% of cells), that synthesize major structural elements of the epidermal barrier and catalytic proteins during a programmed process of differentiation. Keratins, filaggrin, involucrin and transglutaminases are these synthesized compounds. Keratinocyte differentiation is enhanced by calcium, hydrocortisone, and vitamin A depletion, and is usually suppressed by retinoids and low calcium levels. Keratinocytes form the outer skin layer and are therefore important in epidermal renewal as they participate in skin's immune defence, constituting the first line of defence against percutaneous pathogens. Melanocytes, Langerhans cells and Merkel cells constitute the remaining 5% of the cells. Melanocytes are cells originated from the neural crest that are important in skin's pigmentary system as they produce melanin. These cells can also secrete signalling molecules. They can be found at many locations in the body; specifically, in the skin, they are associated with the hair follicle, and in some mammals like humans, melanocytes are also found in the basal layer

of the interfollicular epidermis. Mature melanocytes make contact with around 30-40 keratinocytes forming the epidermal-melanin unit. In this way, melanocytes transfer melanin into keratinocytes, determining the skin colour. This also helps to protect against the damaging effects of ultraviolet radiation (UVR). Langerhans cells (LC), the skin epidermal contingent of dendritic cells (DC), constitute a group of mononuclear phagocytes that are seeded from macrophage precursors in the skin epidermis before birth. LC are cells that play an important role in local defence mechanisms and are thought to act as antigen-presenting cells. Merkel cells are located in the basal layer of the epidermis at certain different areas of hairy skin in mammals. They are cells with many features, such as neuroendocrine and epithelial characteristics that synapse with the dermal sensory axons and adjacent epithelial cells and are sensitive to mechanical stimuli. Merkel cells therefore act as an adapting mechanoreceptor through their Merkel nerve endings. Furthermore, those cells that are not associated to nerve, may participate in endocrine or paracrine secretion (Eckert and Rorke, 1989; Tsatmali, Ancans, and Thody, 2002; Fradette et al., 2003; Moll et al., 2005; Fore, 2006; Lai-Cheong and McGrath, 2009; Suter et al., 2009; Jaitley and Saraswathi, 2012; Cichorek et al., 2013; Arda, Göksügür, and Tüzün, 2014; Min et al., 2017; West and Bennett, 2018).

The dermis is 0.55 mm thick, depending on body site, and is embryologically originated from the mesoderm. It contains interstitial (collagen fibres, elastic tissue) and cellular (such as fibroblasts, plasma cell or histiocytes) components. It is also composed of lymphatic channels, blood vessels and sensory nerves (Lai-Cheong and McGrath, 2009; Krieg and Aumailley, 2011; Tracy, Minasian, and Catterson, 2016; Lopez-Ojeda and James, 2017). Collagen is the major stress-resistant material of skin and is a fibrous family constituted of at least 15 different types in human skin. Collagen types I and III are the prominent fibrillary protein in the human dermis, becoming about 70% of its dry weight. Elastic fibres account for about 5% and consist of elastin and elastic microfibrils, maintaining elasticity (Meigel, Gay, and Wever, 1977; Gelse, Pöschl, and Aigner, 2003; Lai-Cheong and McGrath, 2009; Kolarsick, Kolarsick, and Goodwin, 2011). Fibroblasts are a heterogeneous and dynamic cell lineage that can be found in most tissues in the body. They play a key role in normal wound healing, as they produce big amounts of collagenous matrix helping to isolate and repair the damaged tissue. Apart from its importance in wound healing, they also regulate extracellular matrices, interstitial fluid volume and pressure. Their survival, metabolism and migration are influenced by the action of extracellular matrix components. They have also the ability of differentiating into other

members of the family (Alberts et al., 2002; McAnulty, 2007; Tracy, Minasian, and Caterson, 2016).

The subcutaneous layer or hypodermis is mainly formed by fat and connective tissue, and it is the deepest layer of the skin (Ahn and Kaptchuck, 2011; Yousef and Sharma, 2017).

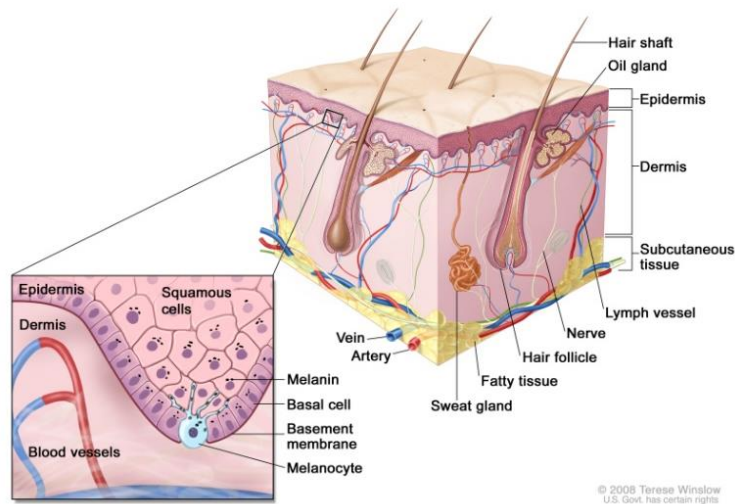


Figure 1. Schematic representation of normal skin structure. Different layers of the skin and their components (from National Cancer Institute at the National Institute of Health).

Mammalian epidermis is composed of four layers, or “strata”: stratum basale, stratum spinosum, stratum granulosum and stratum corneum. The inner layer, called basal layer, is a germinal epithelium that produce all the cells of the epidermis. It is separated from dermis by basal lamina or basement membrane (a specialized extracellular matrix structure) and attached by hemidesmosomes and integrin-based adhesions. The keratinocytes proliferate in this layer and migrate outward while differentiating into cell layer-specific cells. Melanocytes can be identified in the stratum basale. While basal cells of the basal layer stay attached to an underlying matrix and proliferate, some of their daughter keratinocytes go to the stratum spinosum. The spinous layer is the layer next to the stratum basale and the basal cells move towards the surface producing a layer of polyhedral cells connected by desmosomes. Langerhans cells also sit within this layer. Keratinocytes in the stratum granulosum contain intracellular keratohyalin granules where profilaggrin, the precursor of filaggrin, is integrated. Cells get together a water-impermeable cornified envelope carrying the plasma membrane. The lipids are secreted by the cells into the intercellular space, being important for the barrier

function and intercellular cohesion within the stratum corneum (or horny layer). The stratum corneum is the outermost layer of the epidermis, is where the skin barrier is fundamentally formed, and forms a continuous sheet of protein-enriched cells (corneocytes) connected by corneodesmosomes and embedded in an intercellular matrix. The corneocytes are the migrated cells from the granular cell layer that have lost their nuclei and cytoplasmic organelles. It takes about 28 days, in healthy skin, for a basal keratinocyte to move through all the layers and differentiate to a corneocyte (Gilbert, 2000; Richard, 2004; Proksch et al., 2008; Venus, Waterman, and McNab, 2010; Eckl et al., 2013; Kihara, 2016; Yousef and Sharma, 2017).

Embryonic epidermis starts as a monolayer of ectodermal cells that will form a multilayered epithelium by stratification and in response to particular transcription factors. Once built, the epidermis is maintained by frequent stratification and differentiation of keratinocytes in adult life. Epidermal differentiation begins with the migration of keratinocytes from the basal layer and ends with the formation of the cornified layer at the late stages of keratinocyte differentiation (Figure 2). The cells become more permeable to calcium and other ions when they migrate into the upper skin layer. Calcium influence activates a keratinocyte-specific transglutaminase that catalyzes the formation of the cornified envelope (CE). CE serves a barrier function for the organism, helping to keep the structural integrity of the epidermis. The cornified layer is in the upper layer of epidermis and is composed of terminally differentiated, dead, cornified, flattened cells (corneocytes). The corneocytes are composed of keratin intermediate filaments (KIFs) embedded in a filaggrin matrix and surrounded by insoluble lipids (ceramides, cholesterol, fatty acids, cholesterol esters, glucosylceramides and phospholipids) which play an important role in the barrier function of the epidermis because of their prevention to water loss. In addition, to reinforce the cornified envelope just below the plasma membrane, there are structural proteins (involucrin, loricrin, trichohyalin and small proline-rich proteins) synthesized and crosslinked by transglutaminases (TGase1, TGase3 and TGase5) (Eckert and Rorke, 1989; Steven and Steinert, 1994; Richard, 2004; Candi et al., 2005; Akiyama, 2011; Simpson, Patel, and Green, 2011).

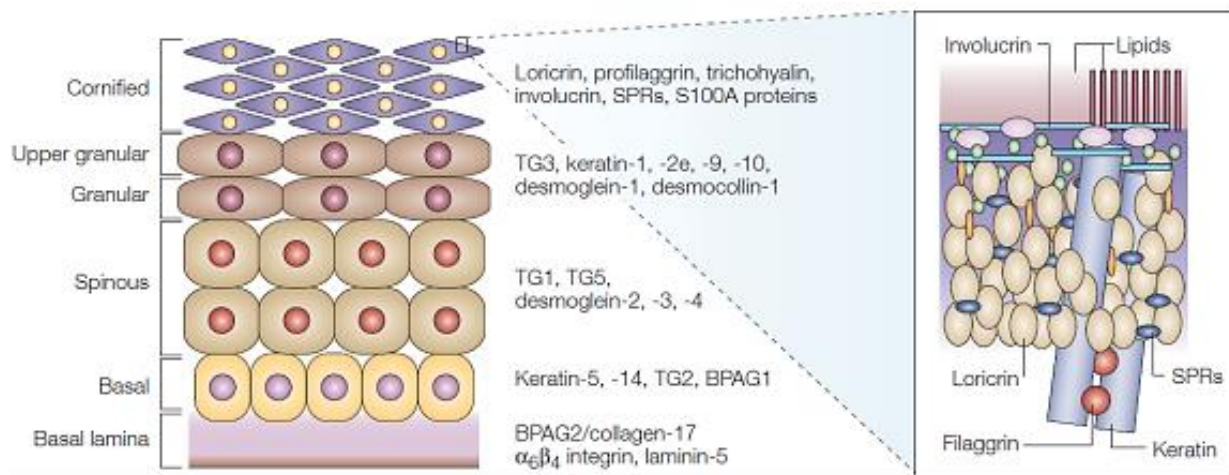


Figure 2. Apoptosis and terminal differentiation in the epidermis. The proteins expressed in specific locations in the epidermis during skin differentiation are shown. Apoptosis is limited to the basal layer and cornification takes place in the suprabasal layers (Candi et al., 2005).

Filaggrin (FLG) is formed from profilaggrin and is crosslinked to the epidermal cornified envelope. Its main function is to coordinate the structure of the cornified cells and it is rich in Arg and His residues (Candi et al., 2005). The profilaggrin system is proteolytically processed during keratinocytes differentiation (Aufenvenne et al., 2012) and participates in the alignment of KIFs, the control of significant changes in cell shape and the maintenance of epidermal texture. Involucrin is expressed throughout the suprabasal layers in stratified epithelia including epidermis. In humans, it consists mainly in Gly and Asp residues, and it is rich in α -helices. Loricrin in humans is the main component of the epidermal cornified envelope in the epidermis and is expressed in the granular layer during cornification (the process of terminal keratinocyte differentiation). Loricrin is rich in Gly, Ser and Cys residues. Small proline-rich proteins (SPRs) are a 14-member multigene family formed by three subgroups: SPR1, SPR2 and SPR3. The structure of SPRs is based in β -turn motifs and they contain head and tail domains that are rich in Gln and Lys residues. In addition, a central domain of variable numbers of repeating peptide units of highly enriched in Pro residues is presented in SPRs. It has been suggested that these proteins act as bridges to join together other precursors (Candi et al., 2005; Eckert et al., 2005).

Transglutaminases (TGase) are calcium-dependent enzymes that catalyze the formation of covalent bonds between the glutamyl residues and lysyl residues of either proteins or polyamines (Iizuka, Chiba and Imajoh-Ohmi, 2003), producing stable structures consisting of

polymerized proteins important in biological processes to maintain cell and tissue integrity (Yamada et al., 1997).

The cornified lipid envelope (CLE) is composed of a monolayer of long chain, ω -acylated-hydroxy-ceramides, with minor amounts of omega-hydroxy-fatty acids packaged, along with large amounts of other barrier lipids such as cholesterol and its esters, free fatty acids (FFA), and other ceramides (Cer) into their limiting membrane and central core (Figure 3). The insoluble proteins found in the cornified envelope are covalently bound to a layer of lipids, being these bonds ester linkages in which the carboxyl group of the arrayed glutamic acid (Glu) residues of involucrin is bound to the hydroxyl group of ceramides. At a later stage of differentiation, the lamellar body membranes unify with the apical plasma membrane, secreting the contents into the extracellular milieu. One of the products delivered into the plasma membrane are the ω -OH-Ce, generated by CYP4F22 (protein of the cytochrome-P450 family 4) (Kalinin, Marekov, and Steinert, 2001; Lopez et al., 2007; Elias et al., 2014).

CLE functions as a scaffold for the organization of the extracellular lamellar bilayers, as a semi-permeable membrane to transfer water and restricts the loss of hygroscopic molecules and contributes to the cohesion of the stratum corneum (SC) (Elias et al., 2014).

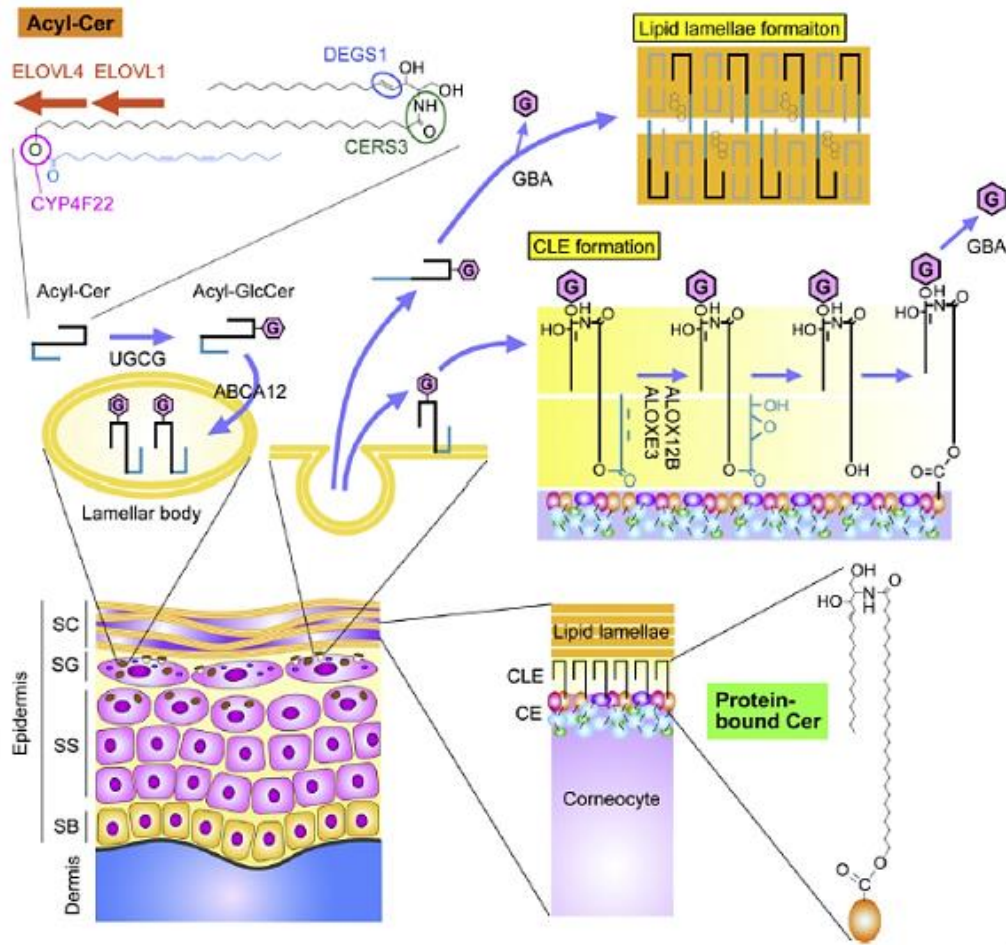


Figure 3. Generation of acyl-Cer and protein-bound Cer in epidermis. G, glucose; SB, stratum basale; SC, stratum corneum; SG, stratum granulosum; SS, stratum spinosum (Kihara, 2016).

The formation of the skin barrier is a complex process that involves a big number of proteins, lipids and enzymes. Mutations in genes that code for these molecules can result in diseases, such as autosomal recessive congenital ichthyosis (ARCI).

1.1.2. PORCINE SKIN

Biomedical research is extended and most of the studies carried out with animals in recent years have used the murine species due to their small size, fast reproductive cycles, and short lifespan. However, in many occasions murine species do not sufficiently act for human pathologies. In connection with the point previously mentioned, animals that better represent

human disorders are needed. Pigs and humans share many characteristics such as anatomy, size or physiology (Gutierrez et al., 2015).

Although rats and mice have been used very often in skin wound healing research, murine models are not ideal due to them being loose skinned animals. They also present immunologically significant differences in both innate and adaptive immune system, which is not surprising due to their small size and lifespan (comparing to humans) (Mestas and Hughes, 2004; O'Brien et al., 2014). Moreover, Wei et al. (2017) studied different mechanical properties and skin tissue structure in mice, pigs and humans, among others, observing similar skin strata thickness, and elastic and viscoelastic properties for pig and humans (*in vivo*), but thinner skin layers in mice.

Animal skin is different morphologically comparing to human skin, respecting to epidermis and dermis thickness, hair follicles, and other characteristics (Figure 4). Porcine and human skin have many similarities such as histological, physiological and immunological characteristics, but also some differences concerning structure, immunohistochemistry, and function. Despite the dissimilarities, porcine seems to be the most appropriate animal type to substitute human skin when doing models for testing, even if rat, mouse, and rabbit have been used in dermatological and toxicological studies due to their availability, their small size and low cost. In addition, pigs are the favorite nonrodent species of choice in the preclinical toxicological testing of drugs. (Avon and Wood, 2005; Swindle et al., 2012; O'Brien et al., 2014; Fujita et al., 2018). Drug *in vitro* permeability measurements and permeation studies have been carried out showing more similar results between pigs and humans than between mice and human beings (Todo, 2017). Pigs are therefore the major animal species used for translational research and they seem to be an alternative to the dogs or primates as nonrodent species used in research.

The skin of the pig is slightly hairless and has a fixed subcutaneous layer and dermal hair follicle like humans. Their skin is thicker, varies in different anatomic locations, and it is less vascular comparing to human skin, being structurally similar to human epidermal thickness and dermal-epidermal thickness ratios. They have also sweat glands and sebaceous glands throughout the skin with minimal functions in thermoregulation. Pigs contain dermal collagen and elastic content that is more similar to human than other animals used in research. Also, they show similar epidermal turnover kinetics, lipid constitution and carbohydrate biochemistry, and a similar microbiome to human beings. Porcine models are therefore used in

wound healing, plastic surgery, reconstructive techniques, burn models, stem cell research and artificial skin for transplantation surgically, as they give a more similar anatomy of the skin (Eaglstein and Mertz, 1978; Swindle, 1998; Avon and Wood, 2005; Liu et al., 2009; Swindle et al., 2012; Gutierrez et al., 2015).

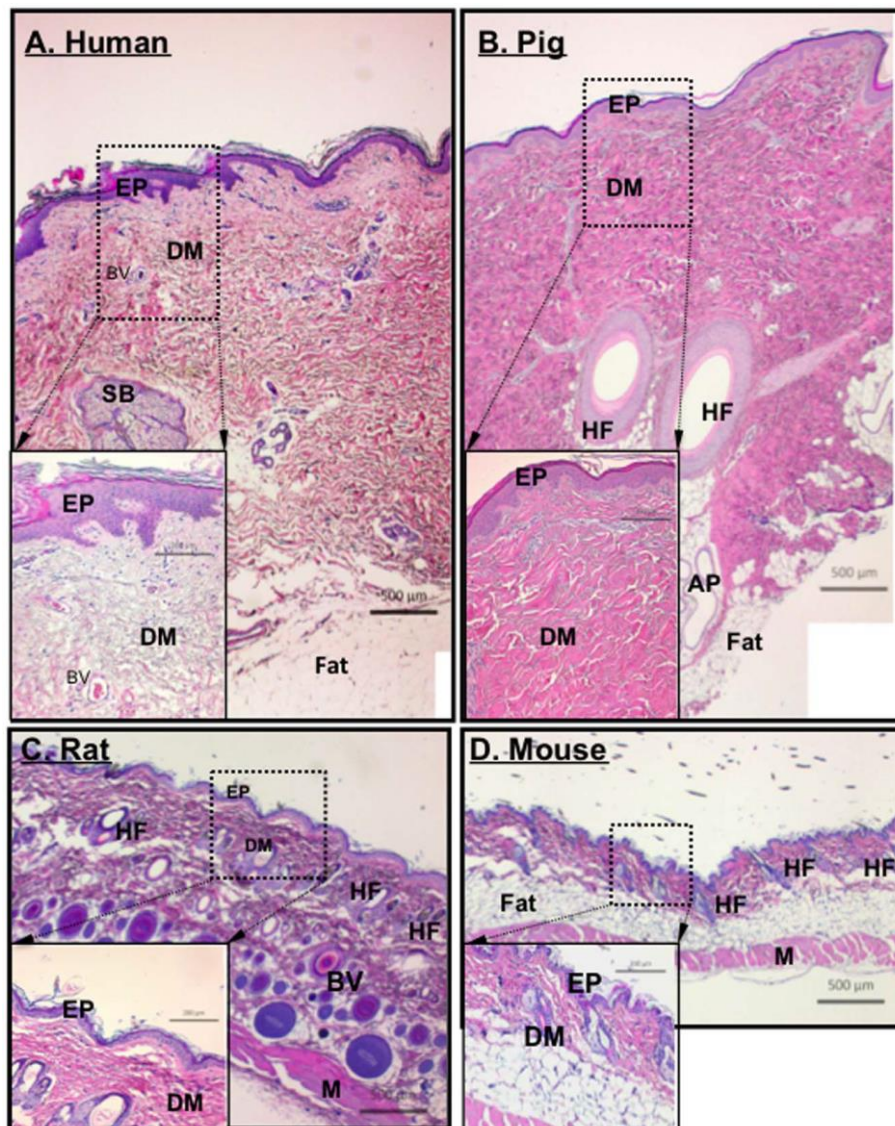


Figure 4. Comparison between human, pig, rat and mouse skin. Paraffin skin sections from healthy humans, pigs, rats and mouse tissue were stained with haematoxylin and eosin for structural comparisons. EP, epidermis; DM, dermis; BD, blood vessel; SB, sebaceous gland; HF, hair follicle; AP, sweat gland; M, muscle (O'Brien et al., 2014).

Nowadays, many researchers take in consideration porcine skin as an appropriate model to study human skin barrier and for pharmacological tests *in vivo* and *in vitro*.

Some researchers have studied the ear porcine skin through *in vitro* studies, using the pig ear as a model for human skin. Jacobi et al. (2007), for example, carried out studies with skin samples from different body areas (ear, back, abdomen, among others) for percutaneous absorption of substances that are applied topically, as the percutaneous absorption depends *in vivo* of the body region studied. Also, Sekkat, Kalia, and Guy (2002) evaluated the stratum corneum barrier function on porcine ear skin *in vitro* as a model for humans.

Ideally, one would like to use human skin to evaluate penetration properties of candidate drugs, but not all researchers have access to get human skin samples (figu 1). That is the reason why some studies have compared human skin, human living skin equivalents, human reconstructed epidermis, and/or animal skin models (Schmook, Meingassner, and Billich, 2001; Herron, 2009; Ranamukhaarachchi et al., 2016).

Table 1. Advantages and disadvantages of human and porcine skin models (Abd et al., 2016).

Model	Advantages	Disadvantages
Human skin:		
In vivo	Gold standard	Often precluded for ethical and practical reasons
Ex vivo skin	Best surrogate for in vivo humans	Not readily available, variability
Animal skin:		
In vivo	Reasonably easy to obtain animals, can be scaled up to humans	Pigs: similar barrier to humans, but difficult to handle
Ex vivo skin	Easy to obtain	Different barrier properties, variability
Reconstructed skin models:		
Reconstructed human epidermis	Built-in barrier properties	Usually more permeable than human skin
Living skin equivalents	Can be engineered to include a range of normal or disease characteristics	Usually more permeable than human skin

1.2. ARCI

1.2.1. CLASSIFICATION OF ARCI

Ichthyosis form part of a clinical and etiological group of Mendelian disorders of cornification (MEDOC) involved all or most of the entire integument. During the last years, progress has been made to define the molecular basis of these disorders and to establish a genotype-phenotype correlation. Nevertheless, there is not a classification of these diseases universally accepted. One of the revised classification (Table 2 and Table 3) is based on the diagnostic as main criteria for that classification, being nonsyndromic and syndromic ichthyosis the two subgroups. In nonsyndromic ichthyosis, the phenotypic expression of underlying genetic deficiency is only seen in skin, while in syndromic ichthyosis the deficiency is seen in skin and other organs (Oji and Traupe, 2009; Oji et al., 2010; Yoneda et al., 2016).

Table 2. Subtypes of inherited ichthyosis: nonsyndromic forms (Takeichi and Akiyama, 2016).

Nonsyndromic ichthyosis				
Common ichthyosis	ARCI		Keratinopathic ichthyosis	
	Major types	Minor types	Major types	Minor types
Ichthyosis vulgaris	Harlequin ichthyosis	Self-healing collodion baby (SHCB)	Epidermolytic ichthyosis	Annular epidermolytic ichthyosis
	Lamellar ichthyosis	Acral-SHCB	Superficial epidermolytic ichthyosis	Congenital reticular ichthyosiform erythroderma
Recessive X-linked ichthyosis	Congenital ichthyosiform erythroderma	Bathing suit ichthyosis		

Table 3. Subtypes of inherited ichthyosis: syndromic forms (Yoneda, 2016).

Syndromic ichthyosis				
Netherton syndrome	Sjogren-Larsson syndrome	Refsum syndrome	Multiple sulfatase deficiency ichthyosis	Keratitis-ichthyosis-deafness syndrome
Conradi-Hunermann-Happle syndrome	Dofman-Chanarin syndrome	Ichthyosis follicularis with alopecia and photophobia	Hystrix-like ichthyosis with deafness	Congenital hemidysplasia

ARCI is a genetically (Takeichi et al., 2015) heterogeneous group of keratinization disorders with an approximate prevalence of 1:100000 (Eckl et al., 2013; Pigg et al., 2016). Ichthyosis symbolize a group of cutaneous disorders with the common characteristic of abnormal epidermal differentiation. The word Ichthyosis comes from the Greek root *ichthys*, meaning fish, representing the cutaneous scaling presented in these disorders. These disorders are mostly nonsyndromic and limited to the skin (Fischer, 2009). They are characterized by abnormal skin scaling over the whole body, dry and thickened cornified layer (hyperkeratosis) (Oji and Traupe, 2009; Sugiura and Akiyama, 2015); and in many cases by inflammation presenting as erythroderma, for example, in bullous/keratinopathic ichthyosis (Oji and Traupe, 2009). The barrier function of the skin of these patients has a reduced capacity to protect against chemical and bacterial external components, and to prevent transepidermal water loss (Craiglow, 2013). It affects all racial groups and ethnic, and it is seen in more elevated incidence in societies in which consanguineous marriage is usual (Richard, 2017).

Depending on their causative genes or loci, ARCI is classified into a total of 11 subtypes (Oji et al., 2010; Shigehara et al., 2016; Bastaki et al., 2017; Takeichi et al., 2017). The main ARCI phenotypes are harlequin ichthyosis (HI), lamellar ichthyosis (LI) and congenital ichthyosiform erythroderma (CIE) (Figure 5).

Harlequin ichthyosis is the most severe form of autosomal recessive congenital ichthyosis and has a high perinatal mortality. Patients with HI show thickened and scaly skin on their entire body, and babies are covered with an armour of hyperkeratosis (Oji et al., 2010; Vahlquist, 2010; Maruthappu, Scott, and Kelsell, 2014; Numata et al., 2015; Sugiura and Akiyama, 2015). Other clinical characteristics of this form is eclabium (the turning outwards of a lip) and open mouth, ectropion (the eyelid is turned outwards away from the eyeball), hypoplastic fingers, and mobility limitation of the joints. In addition, these patients are at high risk for hypo/hyperthermia, dehydration, respiratory distress, and skin infection, among others (Salehin et al., 2013; Rathore et al., 2015; Shruthi et al., 2017). It has a frequency of 1:1000000, and it is due to nonsense mutations in the ATP-binding cassette A12 (*ABCA12*) gene (Oji and Traupe, 2009).

Currently there is no cure for HI. However, treatment can be carried out thanks to the developed medical care and progresses in the postnatal therapies, such as use of systemic retinoids. *ABCA12* gene mutations can be diagnosed in the fetus (Salehin et al., 2013; Mithwani et al., 2014; Rathore et al., 2015), a first step for an early detection of the disease (Salehin et al., 2013; Mithwani et al., 2014; Tekin, 2014).

Lamellar ichthyosis, also called as nonerythrodermic ichthyosis, causes severe abnormalities of the cornified layer. LI is characterized by the presence of a collodion membrane at birth covering the neonate, and large, dark, platelike, solidly adherent scales in the absence of erythroderma (Fischer et al., 2000; Louhichi et al., 2013; Richard, 2017). Most of LI patients are born as collodion babies (CB), in a hyperkeratotic translucent membrane, and frequently present a characterised involvement of the face and the ears. Other features of these patients are ectropion, eclabion, palmar and plantar hyperkeratosis, and alopecia (Fischer et al., 2000; Akiyama, Sawamura, and Shimizu, 2003; Al-Naamani et al., 2013). Its incidence is about 1:500000, and the most common cause of LI is inactivating mutations in the transglutaminase 1 (*TGM1*) gene. A defect in cornification or terminal epidermal differentiation can be observed in the skin of LI patients (Fischer et al., 2000; DiGiovanna and Robinson-Bostom, 2003; Louhichi et al., 2013).

Congenital ichthyosiform erythroderma is characterized by erythroderma with fine, white scale and often with palmoplantar hyperkeratosis (Al-Naamani et al., 2013; Sugiura and Akiyama, 2015; Richard, 2017). Also, eclabion, ectropion, and loss of eyebrows and lashes, are shown more frequent in this form, comparing to LI. About 90% of CIE patients present as collodion

babies at birth. It is an inflammatory form of ichthyosis that affects 1:300000 of the population. In some cases, the erythroderma and fine scaling decrease with age when using treatments such as retinoids or steroids (Akiyama, Sawamura, and Shimizu, 2003; Fischer et al., 2000).



Figure 5. Phenotype of ARCI-patients. (A) Neonate with HI (Glick et al., 2016). (B) Back and (C) dorsa of the feet of a CIE patient with fine, white scales and erythroderma (Akiyama, Sawamura, and Shimizu, 2003). (D) Collodion membrane in ARCI (Schmuth et al., 2013). (E) Leg and (F) dorsa of the feet of a LI patient with thick and dark brown scales without erythroderma (Akiyama, Sawamura, and Shimizu, 2003).

In about 10% of collodion babies, the disease can either evolve to a mild form of ARCI or there is a long-term clinical healing. One of these clinical types is the self-improving congenital ichthyosis (SICI) that has been described in patients with mutation in *TGMI* and those with 12R-LOX and eLOX-3 deficiencies. Mutations in *TGMI* related to temperature-sensitive activity can lead to bathing suit ichthyosis (BSI), also with collodion babies, but in this case the skin of the extremities “heals” in a long period of time (Vahlquist et al., 2010; Traupe, Fischer, and Oji, 2014; Takeichi and Akiyama, 2016).

1.2.2. GENETICS OF ARCI

ARCI follows an inherited autosomal recessive pattern. Eleven genes are reported in association with different ARCI phenotypes: *ABCA12*, *ALOXE3*, *ALOX12B*, *CERS3*, *CYP4F22*, *LIPN*, *NIPAL4*, *PNPLA1*, *SDR9C7*, *SULT2B1* and *TGM1*. In about 15% of families affected by ARCI, no mutations in any of the known genes have been identified (Richard, 2017).

ABCA12 gene is a keratinocyte lipid transporter ATP-binding cassette sub-family A member 12, located in a region of chromosome 2q34 (Annilo et al., 2002). Mutations in this gene are associated with all three forms of ARCI (HI, LI, and CIE). While HI is usually related to loss of function gene, LI and CIE are associated with disease. *ABCA12* transports lipids to cells that form the epidermis and the normal development of the skin, via lamellar granules. Lamellar granules reduction is shown in the skin of HI patients (Akiyama, 2010; Salehin et al., 2013; Maruthappu, Scott, and Kelsell, 2014), as a result of which, abnormal lipid-containing vacuoles form in the cytoplasm of the corneocytes, producing a thickened and not desquamate stratum corneum (Hovnanian, 2015). Therefore, a defective *ABCA12* leads to the disruption of lamellar granule lipid transport in the upper epidermal keratinocytes, and to the loss of the skin lipid barrier (Akiyama et al., 2005; Sugiura and Akiyama, 2015).

Lipoxygenase-3 (*ALOXE3*) and 12(R)-lipoxygenase (*ALOX12B*) are lipoxygenases (LOX) genes that are expressed in the epidermis and are located in the chromosome 17p13.1 (Jobard et al., 2002; Lefèvre et al., 2003). LOX oxygenates the linoleate moiety of ceramides, an important step for the synthesis of proteins of the cornified cell envelope and for the formation of the corneocyte lipid envelope, indispensables for barrier function and lipid metabolism of the skin. The genes for the human epidermal LOX are *ALOX15B*, *ALOX12B*, and *ALOXE3*, and mutations in *ALOX12B* and *ALOXE3* are linked to cases of CIE, LI or CB (Eckl et al., 2005; Eckl et al., 2009; Akbari and Ataei-Kachoui, 2015; Sugiura and Akiyama, 2015; Dick et al., 2017). There are also studies in which a possible participation of *ALOX15B* in ARCI has been investigated (Lesueur et al., 2007).

CERS3 encodes ceramide synthase 3, is located in the chromosome 15q26.3, and is involved in the combination of ceramides with very long-chain acyl parts. The deficiency in the metabolism of sphingolipids disorders the composition of lipids present in the epidermis, causing irregularities in the terminal differentiation (Radner et al., 2013; Kihara, 2016). Mutations in this gene are associated to LI patients. Human CerS3 is usually present in testis

and skin, specifically in the zone that marks the junction of stratum granulosum and stratum corneum (Eckl et al., 2013). Eckl et al. (2013) found the malfunction in ceramide synthesis only in diseased keratinocytes that were in the late stages of the differentiation.

Defects in *CYP4F22* (protein of the cytochrome-P450, family 4, subfamily F, polypeptide 22), which encodes an epidermal ω -hydroxylase decisive in the formation of acylceramides (Gruber et al., 2017), are related to LI and CB (Noguera-Morel et al., 2016). It is situated in the chromosome 19p13.12. Patients with mutation in this gene are born without collodion membranes, but they develop the ARCI phenotype later (Binamer, 2016). Ichthyosis-mutant proteins show a decrease of enzyme activity, which means that there is an association between activity and pathology. In addition, the acylceramide production in these patients is reduced (Ohno et al., 2015).

LIPN gene, which encodes lipase N, is thought to play a role in the differentiation of human keratinocytes. It is located on 10q23.31 locus and present in LI patients (Israeli et al., 2011; Ohno et al., 2015).

NIPAL4 (NIPA-like domain-containing 4) encodes for ichthyin, a protein proposed to be a magnesium transporter, a transmembrane receptor implicated in the formation or transport of lamellar bodies, and a membrane receptor for lipoxygenase products. It is located in the chromosome 5q33, and mutations have been identified as defects in LI or CIE phenotypes (Dahlqvist et al., 2007; Wajid et al., 2010; Li et al., 2013; Gruber et al., 2017). These patients are born either with or without collodion membrane, with fine brown scales on erythematous background with keratoderma and probable atopic diathesis (Binamer, 2016).

PNPLA1 (patatin-like phospholipase domain protein 1) has been identified as causative gene of ARCI, in particular in LI patients, and it is formed by eight exons at chromosome 6p21.31. *PNPLA1* plays an important role in lipid synthesis and metabolism during epidermal barrier formation, and its loss affects to the epidermal ceramide homeostasis (Oji and Traupe, 2009; Grall et al., 2012; Sugiura and Akiyama, 2015; Grond et al., 2016; Richard, 2017). Specifically, *PNPLA1* is related to the synthesis of ω -O-acylceramides, which are involved in epidermal cornified lipid envelope organization (Dökmeci-Emre et al., 2017).

SCR9C7 (short chain dehydrogenase/reductase family 9C, member 7) gene on chromosome 12q13.3 participates in the conversion of retinal into retinol. Mutations in this gene have been found in LI and CIE patients. It is highly expressed in the granular and cornified layers of

normal human skin, which means that mutation in *SCR9C7* submits an important role of vitamin A metabolism in terminal differentiation of the epidermis in humans (Shigehara et al., 2016; Karim, Murtaza, and Naeem, 2017; Takeichi et al., 2017).

SULT2B1 (Sulfotransferase family 2B, member 1) enzyme is a member of the cytosolic sulfotransferase superfamily that interacts in the synthesis and metabolism of steroids in humans. It is located on chromosome 19q13.33, and consists of two isoforms, SULT2B1a and SULT2B1b. The first isoform has not been detected in skin, while the isoform SULT2B1b is expressed in the human epidermis. It plays an important role in epidermal cholesterol metabolism and it participates in the maintenance of a functional cutaneous permeability barrier. Mutations in this gen cause ARCI, and the loss of SULT2B1 also affects the proper expression of cornified envelope proteins (Falany et al., 2006; Heinz et al., 2017).

TGM1 gene spans 15 exons (Louhichi et al., 2013) (Figure 6), and it encodes transglutaminase-1 (TGase1), a tissue-specific enzyme (Yamada et al., 1997) located at chromosome 14q11.2 in humans (Terrinoni et al., 2012). This enzyme has 817 amino acid residues, its molecular weight is approximately 89 kD, and is modified by myristoyl and palmitoyl adducts near the N-terminus of the protein (Terrinoni et al., 2012; Louhichi et al., 2013; Vaigundan et al., 2014). TGase1 expression is differentiation-dependent and it initiates in the spinous layer (Eckert et al., 2005). Therefore, TG is expressed in the upper spinous and granular layers below the stratum corneum of the epidermis and in hair follicles and is linked to the inner plasma membrane of keratinocytes (Yamada et al., 1997; Terrinoni et al., 2012; Aufenvenne et al., 2013; Vaigundan et al., 2014), being also involved in the formation of the cornified cell envelope (Farasat et al., 2009). *TGM1* mutations cause LI and CIE phenotypes, and it also causes self-healing collodion baby (SHCB), a baby who is born as a collodion baby, but improves spontaneously (Oji and Traupe, 2009; Richard and Bale, 2014; Sugiura and Akiyama, 2015).

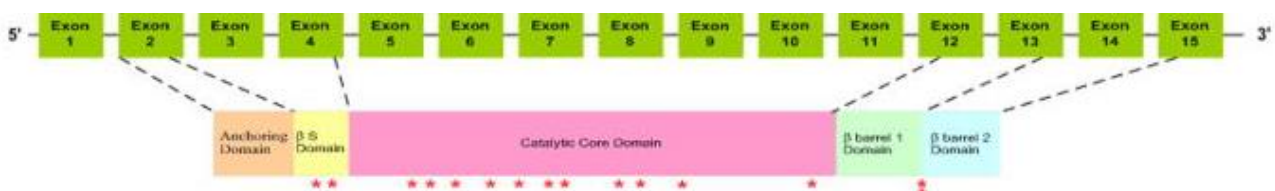


Figure 6. Schematic illustration of genomic organization of *TGM1* (Herman et al., 2009).

Other transglutaminases such as TGase3 or TGase5 are also present in different epidermal layers, but they cannot compensate the need of an active TGase1 in ARCI patients (Eckert et al., 2005; Aufenvenne et al., 2013).

1.2.3. THERAPEUTIC STRATEGIES

So far, the current available treatment for ARCI is symptomatic, and it is usually focused on patient's experience instead of disease pathogenesis. One of the main objectives in this kind of treatment is to keep the skin hydrated. For that, humidification with long baths are used to hydrate and facilitate scale removal by abrasives such as sponges. In neonates with congenital phenotypes, intensive care using humidified incubators is necessary. With these incubators, temperature instability and hypernatremic dehydration is avoided. In addition, vigilance to check possible cutaneous infections is important. For the skin care, petrolatum-based creams and ointments are used. When infants become older, and with the course of the disease, therapy is based in long baths, keratolytic agents such as urea preparations, and lubrication for the hydration of the stratum corneum. Some locations, like the outer ear canals or regions of hair growth, need special care and professionals to help with regular removal of scaling. Furthermore, there are some measures to have in consideration: prevention of infection in the newborn, prevention of dehydration, maintenance of body temperature, and high caloric diet, among others. In addition, skin irritants should be avoided (DiGiovanna et al., 2013; Schmuth et al., 2013; Richard, 2017).

Another therapy for ARCI patients is the modulation of epidermal differentiation by nuclear hormone receptor ligands such as topical vitamin A, topical and oral retinoids. Retinoids are a family of natural and synthetic compounds that share structural and functional characteristics with vitamin A. Retinoids are helpful in some locations including palms, soles and eyelids, for the treatment of ectropion. However, before starting retinoids treatment, some details from the patients like age, severity or psychological status have to be considered. Other factor to be taken into consideration is the type of retinoids, being the most common used etretinate, acitretin and isotretinoin. Depending of the chosen retinoid, the dose will vary, even if the goal of choosing a dose should be to find the lowest dose that the patient tolerates. One of the limitations of the treatment with retinoids is that the scaling comes back if the treatment is stopped. They are also highly teratogenic; it can disturb the development of the embryo or

fetus, so it should not be used in pregnant women or women planning a pregnancy. In addition, adverse effects such as hair loss, abnormalities in blood cell counts, neuromuscular effects like headache, renal dysfunction when using etretinate or bone toxicity may appear (Larsen et al., 1988; Mukherjee et al., 2006; Verfaillie, Borgers, and Van Steensel, 2008; Layton, 2009; Ormerod, Campalani, and Goodfield, 2010; DiGiovanna et al., 2013; Mortazavi et al., 2013; Schmuth et al., 2013).

Another kind of treatment is the administration of agents like liarazole, that is a novel imidazole derivative that seems to block the metabolism of retinoic acid by inhibition of the cytochrome P450-dependent 4-hydroxylation of retinoic acid, which is the physiological breakdown of all-trans-retinoic acid. Blocking the metabolism of retinoic acid, tissue levels of it increase. This treatment seems to be better tolerated in patients and shows less adverse effects (Lucker et al., 1997; Verfaillie et al., 2007; Verfaillie, Borgers, and Van Steensel, 2008).

As it has been mentioned above, available treatments only provide symptomatic relief to the patients, but they do not eliminate them. Therefore, a causative treatment has to be developed.

One way to find a causative treatment is by protein substitution. Aufenvenne et al. (2013) developed a targeted topical enzyme-replacement therapy for TGase1-deficient ARCI, for what a carrier system tagged is necessary. This carrier system is a liposome that delivers the recombinant human TGase1 enzyme at the site of action into keratinocytes in a skin-humanized mouse model for TGase1-deficient ARCI. In addition, Stout et al. (2014) described the topical introduction of recombinant FLG monomer protein linked to a cell penetrating peptide, for the treatment of ichthyosis vulgaris, which is a disorder of keratinization with mutations in *flaggrin*. They demonstrated this in FLG deficient animal model.

Liposomes can be unstable under environmental stress such as high temperature or high pressure. An alternative for these described carrier systems are the dendritic polyglycerol (PG) and poly(N-isopropylacrylamide (PNIPAm)-based nanogels. Dendritic molecules such as polylysine, polyester, polyamidoamine, triazine dendrimers, and polyglycerol are being used for biomedical studies to amplify or multiply pathopharmacological effects. PGs are water soluble, polyether-based and spherical nanomaterials with low anticoagulative and intrinsic anti-inflammatory function. PGs are obtained by ring-opening polymerization of glycerol, and stimuli-sensitive nanogels are polymeric particles formed by a cross-linked, three-dimensional network that can respond to local environmental conditions. By other side, PNIPAm is a nontoxic thermoresponsive polymer with inverse solubility and a reversible phase transition

upon heating. The use of PNIPAm in the biomedical field has been limited due to its deficiency of water solubility, and because it is not specific to protein absorption. However, PNIPAm has shown very positive results concerning temperature-sensitive applications, as it is soluble at room temperature, but its phase separates at body temperature (37°C) (Calderon et al., 2010; Cuggino et al., 2011; Lima, Morales, and Cabral, 2016; Pant et al., 2017). Witting et al. (2015) prepared protein-loaded thermoresponsive PNIPAM-dPG nanogel (Figure 7) for cutaneous protein TGase1 delivery in *TGMI*-knock -human skin model restoring the skin barrier function.

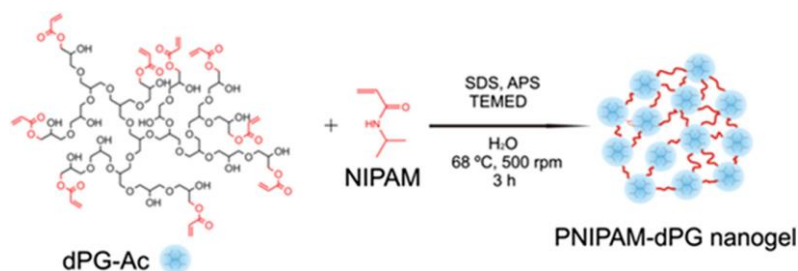


Figure 7. Synthesis and chemical structure of the PNIPAM-dPG nanogels (Witting et al., 2015).

1.3. SKIN MODELS

One of the main issues for the cosmetic industries has been the *in vitro* engineering of the human skin due to ethical and legal requests. Biomedical and pharmacological research also requires suitable test methods for the discovery of drugs and treatments. Two-dimensional (2D) skin cell cultures have been used since many years now, but main functions of skin such as barrier function, cell layering, or immune function are not summarized in these 2D cultures. *In vitro* human skin equivalents (HSE) are used for drug development, as the skin can be used to test systematically acting drugs, and for efficacy testing of drugs at sites of acting thanks to the construction of disease skin models (Mertsching et al., 2008; Mathes, Ruffner, and Graf-Hausner, 2014; Klicks et al., 2017). Human skin equivalents are therefore also used to study normal and abnormal skin biology, including infection, skin disease, and wound healing; and they constitute an alternative method to animal testing (Vörsmann et al., 2013; Abdallah, Pawar, and Harrad, 2015; Reijnders et al., 2015).

Human skin equivalents are three-dimensional (3D) organotypic models of the human skin, bioengineered substitutes, constituted of primary human skin cells (keratinocytes, fibroblasts and/or stem cells) and components of the extracellular matrix. After particular culture

conditions, a HSE can resemble the majority of the characteristics of the native human skin (El Ghalbzouri et al., 2009; Zhang and Michniak-Kohn, 2012; Planz, Lehr, and Windbergs, 2016; Mieremet et al., 2017). Specific advantages of these models include normal human cells, organotypic structure, barrier function, and real-life exposure options, among others (Leist et al., 2012).

Different systems can be used to create skin models. Some of these systems are: spheroids, 3D bioprinting, organ-on-a-chip, and hydrogels.

Spheroids or aggregates are formed by cells within a matrix, on a matrix, or in a suspension medium. 3D spheroids constitute cells in various stages including proliferating, apoptotic and necrotic cells, among others. These models are constructed using HaCaT cells or fibroblasts co-cultured with melanoma cells in the spheroid format to obtain tumor models and are useful for cancer research and development of treatment. However, some of their limitations are the complexity, variety and heterogeneity of the human tumor environment (Fennema et al., 2013; Edmonson et al., 2014; Chatzinikolaidou, 2016; Klicks et al., 2017).

Other technology is 3D bioprinting, that is based on three main approaches: design and production of materials or/and structures, replication of biological tissue using embryonic organ development, and the construction of small and functional blocks. Basically, it consists on the printing of different layers of a desired material such as hydrogel or biodegradable scaffolds to form those architectures. Cells can be added on these geometries to form biological structures. In addition, thanks to that system, structures like 3D neural tissues or tumor cell-bearing tissues for angiogenesis model can be created (Murphy and Atala, 2014; Klicks et al., 2017; Xia, Jin, and Ye, 2018).

Organ-on-a-chip system is the remodeling of tissue and organs by culturing living cells in a microscale environment controlling space and time. The aim of this technology is not to create a whole living organ, but rather to build a minimal functional unit that sum functions of tissue and organs. Skin organ-on-a-chip, for example, can be used to test drugs crossing through the stratum corneum (Klicks et al., 2017; Ronaldson-Bouchard and Vunjak-Novakovic, 2018).

However, the principal technique for constructing the models is the use of hydrogels to form the scaffold for dermal fibroblasts, that is co-cultured with keratinocytes on the surface. Collagen I is the most used hydrogel material. In addition, hydrogel systems are used to build full thickness human skin models (FTM), a generally used of HSE. FTM is formed by primary

fibroblasts in the dermal equivalent and primary keratinocytes in the epidermal equivalent growing on collagen I matrices, using filter inserts and multiwell culture plates. In these models, the fibroblast-keratinocyte communication is indispensable for epidermal morphogenesis and formation of the basement membrane (Breitkreutz et al., 2013; Klicks et al., 2017; Mieremet et al., 2017). FTM can be used for the study of skin disorders. In recent years, a diversity of reconstructed human epidermis models and full thickness human skin models, such as Phenion Full Thickness Skin Model, have been developed (Ackermann et al., 2010). Some other researchers have developed three-dimensional artificial skin models for disorders of keratinization like psoriasis and Harlequin ichthyosis (Thomas et al., 2009; Duque-Fernandez et al., 2016). Also, Eckl et al. (2011) developed 3D human skin models for autosomal recessive congenital ichthyosis in 2011, using *TGMI*-Knock Down models (Figure 8).

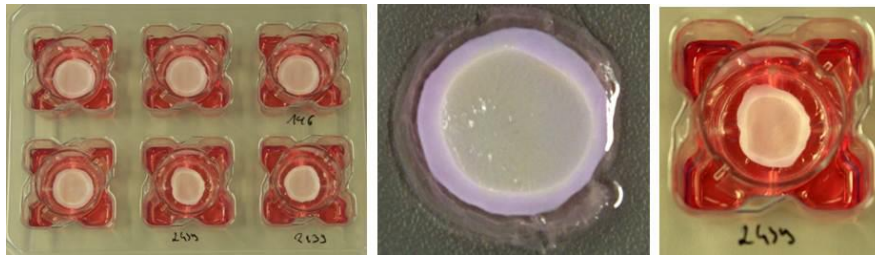


Figure 8. Full thickness skin models.

1.4. SKIN EXPLANTS

For ethical reasons, the use of experimental animals for some studies such as skin irritation for cosmetic products or chemical substances is not desired. Due to that, new alternative methods are required. Some of these methods use human keratinocyte culture to study the metabolism of dimethyl-thiazoldiphenyltetrazolium bromide (MTT) by cellular lactate dehydrogenase (LDH) connections or neutral red from preloaded cells. But those methods have disadvantages such as the fact that they have to be made in a short time range and only diluted products are used. A new method has been proposed and it is the use of human organotypic skin explanted culture (hOSEC). hOSEC are models similar to *in vivo* human skin, as a 3D human skin model, formed by melanocytes, keratinocytes, Langerhans cells, and the entire structure of fibroblasts, collagen and glycosaminoglycans. These characteristics are important, and they differ from the 3D skin models, that are only made of fibroblasts and keratinocytes on an extracellular matrix.

Also, skin biopsies can be kept for several days or weeks in culture medium when incubated at 37°C in an atmosphere of 95% air and 5%CO₂. This system permits the application of creams, ointments and substances that are lipid-soluble, and the study of the homeostasis and inflammatory/immune reactions. (Nakamura et al., 1990; Kataranovski and Karadagic, 1999; Varani et al., 2007; Varani, 2012; Andrade et al., 2015; Frade et al., 2015).

Human skin in large quantities is not usually available, reason why other alternatives have to be found. Skin organ-culture systems from different animal species like rodents, rabbits and pigs, have been described and used for biochemical studies (Bartnik et al., 1990; Jacobs et al., 2000; Varani et al., 2002; Dame et al., 2009).

2. AIM OF THE STUDY

Symptomatic treatment including a daily and time consuming strict routine of bathing with removal of excess skin scales and recurrent moisturising of the whole body gives some relieve to the ARCI (a rare cornification disorder) patients. However, this is not enough, as these available treatments only relieve the symptoms, but they do not eliminate them. A causative therapy is therefore necessary for these patients, and a causative treatment like the substitution of the diseased protein would mean an increase of the quality of life.

TGMI is the major gene in which mutations can cause ARCI, due to damaged linkage of lipids and proteins in the upper layer of the epidermis, and consequently the disturbance of the epidermal barrier. Therefore, *TGMI* is the gene chosen as a first target to test the possible replacement of the protein. Dendritic molecules, such as polyglycerol or polyester, have been shown to be useful as potential carriers in biomedical and pharmaceutical areas. TGase1 protein was previously loaded onto the developed PNIPAM-dPG nanogel for the delivery of the therapeutic protein in the epidermis, and its effectiveness has been studied. PNIPAM-dPG nanogel is a novel biocompatible thermoresponsive nanocarrier expected to be advantageous for epidermal deliveries due to its temperature responses.

The main goal of this project is the study of the fate of the protein-loaded thermoresponsive PNIPAM-dPG nanogel for cutaneous protein TGase1 delivery in skin model restoring the skin barrier function in ARCI patients with *TGMI* mutation.

To accomplish this, the construction of three-dimensional skin models built by primary keratinocytes and dermal fibroblasts will be carried out. These models mimic the architectural features and behaviour of human skin, therefore they are supposed to be useful for the development of patient-specific 3D skin models. Following this way, the molecular features of the diseases can be replicated, and the restoration of epidermal function with the TGase1/NG complex can be studied.

In parallel, studies with primary keratinocytes grown in a 2D monolayer will be performed to study the expression of different genes during epidermal differentiation, and also the specific subcellular location of the therapeutic protein and carrier when they are delivered to keratinocytes.

Due to the difficulties to obtain human skin samples, these studies will be also carried out with pig skin samples, as human and porcine skin share many similarities like histological,

immunological and physiological characteristics. In this way, we could compare the delivery of the TGase1 protein and the nanogel in our 3D skin models to its fate in *ex vivo* skin resulting from the culture of skin explants.

With this project we expect to better understand how the designed protein-loaded thermoresponsive PNIPAM-dPG nanogel for cutaneous protein TGase1 delivery, and the protein TGase1, are being delivered in the epidermis, as this would have a great impact towards a causative therapy for ARCI.

3. MATERIALS AND METHODS

3.1. ETHICAL APPROVAL

The study was approved by the Research Integrity and Ethics Committee from the University of Huddersfield (Huddersfield, United Kingdom).

All human primary cells lines used in this project were extracted and amplified from skin biopsies obtained after informed consent of healthy donors in accordance with Declaration of Helsinki. Three human cell lines were used, two of them were obtained from the Huddersfield Hospital in collaboration, and the other cell line was purchased in Lonza.

Patient samples were provided by the Department of Dermatology, Medical University of Innsbruck, Austria, after obtaining written informed consent. The study was approved by the Institutional Review Board (Ethics Committee) of the Medical University of Innsbruck.

Porcine cell lines were obtained from adult pigs from a Spanish abattoir located in Galaroza (Matadero de Jabugo-Galaroza), after permission from the Ethics Committee from the University of Huddersfield.

3.2. MATERIALS

Reagents and components:

Reagents	Company	Order ID
500 mL Filter-System	Corning	430758
Adenin	Sigma	A2786-5G
Albumin Fraction V, protease free (BSA)	CarlRoth	T844.3
Bacillol-AF	Hartmann	973389
Betaisodona	Mundipharma	15.973
Biopsy Punch 8mm	PFM	48601
CaCl ₂	Sigma	C2661-500G
Cell Safe Biopsy Capsules	Leica	14039430014
Cell strainer 100µm	Corning	352360
Cell strainer 70µm	Corning	352350
Cholera Toxin from <i>Vibrio cholera</i> (CT)	Sigma	C8052-1MG
Collagenase D	Roche	11088866001
Cryo-Embedding NEG50	ThermoFisher Scientific	6502
DAPI	Sigma	10236276001
Deep 6 well plate	Corning	355467
Dimethylsulfoxid (DMSO) Rotipuran	CarlRoth	4720.4

Dispase II	Roche	04942078001
Distilled water (DNase/RNase free)	Gibco	10977-035
DMEM	Gibco	11960-044
DMEM F12 (1:1) (1x)	Gibco	21331-020
DPBS (1x)	Gibco	14190-094
Entellan®	Sigma	1079610100
Eosin	CarlRoth	X883.2
Ethanol absolute	Acros Organics	445740010
Fetal Bovine Serum (FBS)	Gibco	10270-106
Fluoromount Aqueous Mounting Medium	Sigma	F4680-25ML
Formalin neutral solution salt buffered pH 7	VWR chemicals	351638K
Fungizone Amphotericin B	Gibco	15290-026
Gentamicin (10mg/mL)	Sigma	G1272-100mL
Hämalaun Lsg, sauer nach Meyer	CarlRoth	T865.3
HBSS (10x)	Gibco	14180-046
Histo-cassettes	Leica	14039440000
Human Epidermal Growth Factor (EGF)	Sigma	E9644-.2mg
Hydrocortisone (HC)	Sigma	H0888-1G
Inserts (high tensility, translucent PET membrane)	Corning	353092
Insulin from bovine pancreas	Sigma	I1882-100mg
Keratinocyte Basal Medium (KBM)	Lonza	CC-3101
KGM Single Quot Kit Supplements and Growth Factors	Lonza	CC-4131
L-Glutamine 200mM (100x)	Gibco	25030-123
LysoTracker Deep Red	Invitrogen	L12492
Metal lids for histo-cassettes	Leica	14039441014
NaOH	Sigma	71687-100G
Paraffin	Leica	037432124
PBS pH 7.2 (1x)	Gibco	20012-019
Penicillin-Streptomycin (P/S)	Gibco	15140-122
Poly-L-Lysine hydrobromide	Sigma	P1399-25MG
ProFreeze NAO/CD Freeze (2x)	Lonza	12-769E
Pure Col Type I Bovine Collagen	Advanced BioMatrix	5005-100mL
Scalpel	Braun	5518016
TaqMan® Fast Universal PCR Master Mix (2X)	Applied Biosystems	4364103
TaqMan® Gene Expression Assays*	Applied Biosystems	4351370 (GAPDH) 4331182 (others)
Triton X-100	CarlRoth	3051.3
Trypsin EDTA 0.05% (1x)	Gibco	25300-096
Trypsin Inhibitor Soybean	Gibco	17075-029
Tween 20	CarlRoth	9127.1
Xylene pure	Acros Organics	383930050

Kits:

Kit	Company	Order ID
High-Capacity RNA-to-cDNA™ Kit	Applied biosystems	4387406
PureLink™ RNA Mini Kit	Ambion	12183018A

Antibodies:

Antibodies	Dilution	Isotope	Company	Order ID
Anti-Mouse Involucrin	1:100	Monoclonal IgG1	Genetex	GTX17610
Anti-Mouse TGase 1	1:100	Monoclonal IgG _{2a}	Santa Cruz	Sc-1664674
Anti-Rabbit K10	1:150	Polyclonal IgG	abcam	ab53124
Goat anti-Mouse Alexa Fluor® 633	1:1000	Polyclonal IgG	Invitrogen	A21050
Goat anti-Mouse Alexa Fluor® 546	1:400	Polyclonal IgG	Invitrogen	A11003
Goat anti-Rabbit Alexa Fluor® 546	1:400	Polyclonal IgG	Invitrogen	A11035
Mouse anti-E-cadherin	1:50	Monoclonal IgG _{2a}	BD Biosciences	610181
Mouse anti-EEA1	1:50	Monoclonal IgG1	BD Biosciences	6120456
Mouse anti-GM130	1:50	Monoclonal IgG1	BD Biosciences	610822

TaqMan® Gene Expression Assays:

TaqMan® Gene Expression Assays	Details	Assay ID
<i>ALOX12B</i>	Specie: Human; Transcripts: 1; Amplicon Length: 73; Location Chromosome: Chr.17: 8072636-8087703; Gene Aliases: 12R-LOX, ARCI2	Hs00153961_m1
<i>ALOXE3</i>	Specie: Human; Transcripts: 2; Amplicon Length: 112; Location Chromosome: Chr.17: 8095900-8118916; Gene Aliases: ARCI3, E-LOX, eLOX-3, eLOX3	Hs00222134_m1
<i>GAPDH</i> (Housekeeper)	Specie: Human; Transcripts: 2; Amplicon Length: 122; Location Chromosome: Chr.12: 6534405-6538375; Gene Aliases: G3PD, GAPD, HEL-S-1623eP	Hs99999905_m1
<i>TGMI</i>	Specie: Human; Transcripts: 1; Amplicon Length: 99; Location Chromosome: Chr.14: 24249114-24263210; Gene Aliases: ARCI1, ICR2, KTG, LI, LI1, TGASE, TGK	Hs01070310_m1
<i>TGMI</i>	Specie: Human; Transcripts: 1; Amplicon Length: 86; Location Chromosome: Chr. 14: 24249114-24263210; Gene Aliases: ARCI1, ICR2, KTG, LI, LI1, TGASE, TGK	Hs00165929_m1

3.3. METHODS

3.3.1. CELL CULTURE

The growth of primary cells, human and porcine primary cells, as well as cell culture experiments have been carried out. An overview of the reagents used for the culture of these cells can be seen in Table 4.

Table 4. Reagents used in cell culture (companies mentioned above in chapter 3.2).

Category and use	Culture medium and its content	Final concentration
Basal Keratinocytes grown feeder free.	KGM™ 100% of KBM™ Basal Medium 100% of KGM™ SingleQuotKit Supplements and Growth Factors (BPE, hEGF, insulin, HC, GA-100)	
Basal Keratinocytes grown on feeders.	KCM: 43% of DMEM/F12 43% of DMEM 10% of FBS 2% of L-Glutamine 1% of Penicillin-Streptomycin 1% of Hydrocortisone 1% of hEGF 0.1% of Insulin 0.1% of Adenin 0.01% of Cholera Toxin	4 mM 100 U/mL 400 ng/mL 10 ng/mL 5 µg/mL 0.018 mM 10 ng/mL
Fibroblasts and 3T3-J2 feeders growth	3T3-CM: 88% of DMEM 10% of FBS 1% of L-Glutamine 1% of Penicillin-Streptomycin	2 mM 100 U/mL
Porcine skin explant growth	PECM: 95.5% of DMEM 1% of Penicillin-Streptomycin 1% of Hydrocortisone 1% of L-Glutamine 1% of Fungizone 0.5% of Gentamicin	100 U/mL 100 µg/mL 292 µg/mL 2.5 µg/mL 50 µg/mL
Transportation of skin samples	TPM (Transportation Medium): 86.8% of DMEM 10% of FBS 2% of Fungizone 1% of Penicillin-Streptomycin	5 µg/mL 100 U/mL

	0.2% of Gentamicin	20 µg/mL
Washing skin samples	AA-PBS (Wash-Buffer): 96.8% of PBS 2% of Fungizone 1% of Penicillin-Streptomycin 0.2% of Gentamicin	5 µg/mL 100 U/mL 20 µg/mL
Freezing cells	Freezing medium: 90% of ProFreeze NAO/CD Freeze Media 10% of DMSO	
Stopping trypsin/EDTA activity when splitting keratinocytes feeder-free	Trypsin inhibitor: 500 mL of DPBS 0.125 mg of Trypsin Inhibitor Soybean	
Differentiation of keratinocytes	KGM TM 0.114% of CaCl ₂ for human keratinocytes 0.095% of CaCl ₂ for pig keratinocytes	1.2 mM 1 mM

3.3.1.1. ISOLATION OF HUMAN AND PORCINE PRIMARY SKIN CELLS

Human skin samples were extracted from biopsies, and pig skin samples were collected from a Spanish abattoir. The samples were transported in 50 mL Falcon tube with cold transportation medium (TPM) and then it was washed once in the laboratory with Betaisodona solution for 2-3 minutes, followed by three wash steps in AA-PBS for 7 minutes.

The sample was placed with epidermal side down in a petri dish, and some drops of AA-PBS were added until sample was lightly covered. The fat and hair were removed with some scissors. The sample was then cut using a biopsy punch instrument and placed in a new petri dish, epidermis side down. 2 mL of Dispase II solution were mixed with 18 mL of KGM (dilution 1:10) in a Falcon tube and then added until sample was submerged.

The petri dish was placed overnight in a fridge (4°C).

At the same time, 3T3 feeders were plated in 6-well plates for the keratinocytes culturing next day.

The following day, dermis and epidermis were separated using two pairs of forceps. If the separation was not easy, the sample was placed in the incubator at 37°C, 5% CO₂ level and 95% relative humidity (RH) for 2 hours. The epidermis was placed in the lid of a 6 cm petri

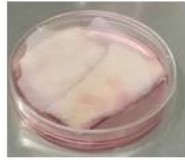
dish filled with some drops of trypsin/EDTA and left for 10 min at room temperature (RT). The sample was minced, and trypsin activity was stopped with some mL of trypsin inhibitor.

Everything was transferred to a 50 mL Falcon tube and centrifuged at 1000 rpm for 4 min at RT. At the same time, medium was removed from the feeder cell plates and KCM was added. Pellet was resuspended in 10 mL of KCM medium and filtered through a 70 µm cell stainer. The cells from the epidermis were plated in the 6-well plates.

During trypsin-incubation, the dermal part of the sample was placed in a new petri dish, added some drops of collagenase D solution, until submerged, and placed in an incubator at 37°C, 5% CO₂ level and 95% RH until the next day.

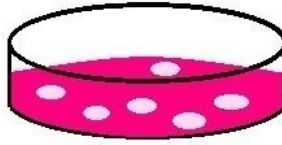
At the next day, medium was changed for the keratinocytes. Collagenase D solution was removed for dermal specimen, washed once with PBS, and added trypsin/EDTA until all dermis was fully covered. Dermis was cut in very small pieces and samples were left for 10 minutes at room temperature in trypsin. The sample was minced using scalpels, trypsin activity was stopped with 3T3 culture medium, and the solution was transferred to a 50 mL Falcon tube. The sample was centrifuged at 1000 rpm for 4 min at RT, resuspended with 10 mL of 3T3 culture medium, filtered through a 100 µm cell stainer and cells were plated in T25 flasks.

On first day, medium was changed for the fibroblasts. For the first week, medium was changed for keratinocytes every third day, and for fibroblasts when necessary (Figure 9).



Transport skin sample in Falcon tubes with transportation medium. Wash with Betaisodona solution for 2-3 min. Wash thrice with PBS (with antibiotics) for 7 min.

Remove fat and hair
Cut the sample in small pieces and place epidermal side down



Place the sample in Dispase II solution (dilution 1:10 in KGM) until submerged. Place overnight in a fridge

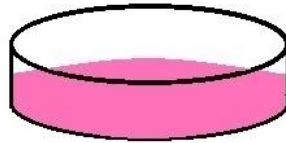
Plate feeder cells for next day

Following day:



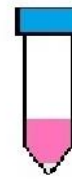
Separate dermis and epidermis.

Place epidermis in a petri dish filled with some drops of trypsin/EDTA
Leave for 10 min at RT and mince



Stop trypsin activity with trypsin inhibitor

Collect all volume in a Falcon
Centrifuge at 1000 rpm for 4 min at RT



Resuspend pellet in KCM medium
Filter through a 70 um cell stainer

Place dermal part in petri dish with some drops of collagenase D solution until submerged.
Incubate at 37°C, 5% CO₂ and 95% RH.

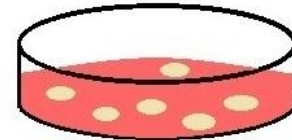
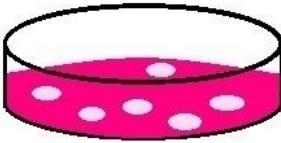
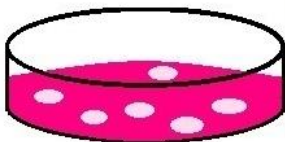


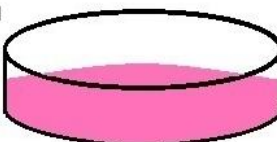
Plate cells (keratinocytes)

Next day:



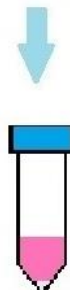
Dermal part in collagenase D solution

Wash with PBS1.x
Add trypsin/EDTA until all dermis is covered
Cut dermis in small pieces
Leave for 10 min at RT and mince



Stop trypsin activity with 3T3 culture medium

Collect all volume in a Falcon
Centrifuge at 1000 rpm for 4 min at RT



Resuspend pellet in 3T3 medium
Filter through a 100 um cell stainer



Plate cells (fibroblasts)

Figure 9. Schematic representation of extraction of pig skin cells.

3.3.1.2. SPLITTING FIBROBLASTS

Fibroblasts were thawed and resuspended in 3T3 culture medium in a Falcon tube for the plating. Cells were mixed carefully and incubated at 37°C, 5% CO₂ level and 95% relative humidity.

When cells were confluent and ready for splitting, the medium was removed and washed once with 25 mL of PBS 1x. 10 mL of Trypsin were added to the flask, which was incubated at the same temperature, CO₂ and RH until cells were completely detached. Once cells were detached, 10 mL of media were added to inactivate Trypsin activity. All volume was collected to a Falcon tube and centrifuged for approximate 4 minutes at 1000 rpm, pellet was resuspended in 20 mL of media, and cells were counted with Neubauer chamber. To count the cells, the cover slip was placed on chamber, and the cell-Trypan Blue mix (10 µL) was transferred into counting chamber. The cell-Trypan Blue mix was prepared adding 20 µL of well-mixed cell suspension to 20 µL of Trypan Blue in an Eppendorf tube. The desired density and the correct media were added to each new flask. Cells were placed in the incubator at 37°C (Figure 10).

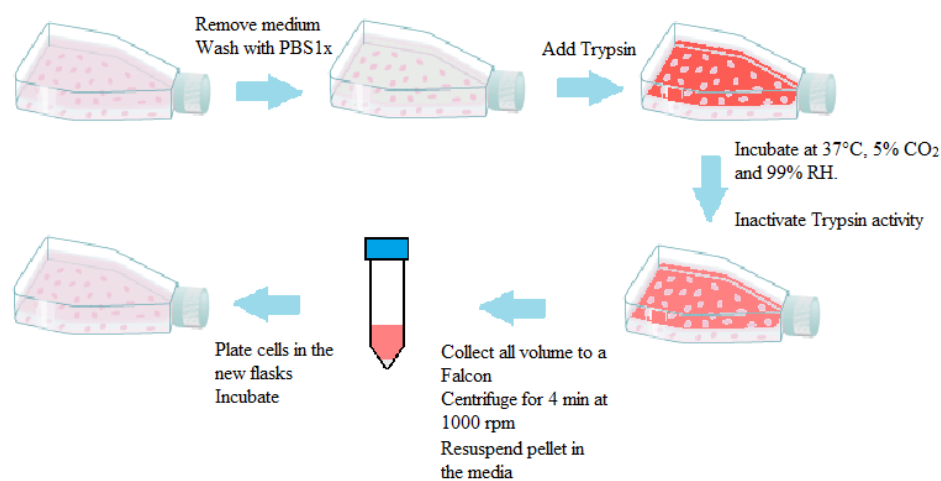


Figure 10. Schematic representation of splitting.

3.3.1.3. SPLITTING KERATINOCYTES

The protocol carried out to split keratinocytes was similar to the one used to split fibroblasts. Keratinocytes were growing in dishes so when cells were confluent and ready for splitting, KGM medium was removed and washed once with 4 mL of PBS 1x. 5 mL of Trypsin were added, and cells were incubated at 37°C until cells were detached. After that, 10 mL of trypsin inhibitor medium were added to inactivate Trypsin activity. All volume was collected to a

Falcon tube and centrifuged for 4 minutes at 1000 rpm. Pellet was resuspended in 10 mL of media. The desired density and the correct media were added to each new dish. Cells were placed in the incubator at 37°C.

3.3.1.4. TREATMENT WITH MITOMYCIN C

Embryonic 3T3-J2 fibroblasts were used as feeder cells to support the growth of primary keratinocytes in culture. To inhibit the feeder layer growth in long-term culture, embryonic fibroblast feeder cells were treated with Mitomycin C. The Mitomycin C was dissolved in 10 mL of distilled water to a final concentration of 4 µg/mL. Cells were washed with PBS 1x and incubated with 1 mL of Mitomycin C and 49 mL of medium for 3 hours. The solution was removed and washed three times with PBS 1x. Right after 10 mL of Trypsin were added to detach cells from the plate. 10 mL of 3T3 media were added as soon as cells were detached. Volume was accumulated in a Falcon tube and centrifuged 4 minutes at 1000 rpm, and pellet was resuspended in 20 mL of media.

A cell counter was used to count the number of cells. To do that, 20 mL of diluent and 100 µL of the sample were added into a special flask, the lid was closed, it was mixed well, and the flask was inserted inside the cell counter so that the probe was submerged in liquid.

The next step was to centrifuge again at the same conditions and resuspend the pellet in Profreeze medium (90% Profreeze solution and 10% DMSO). The volume of Profreeze medium was calculated depending on the total number of cells. Each vial should have 1 mL and 6×10^6 cells, so the correspondent volume of Profreeze medium was added to a Falcon tube to resuspend the pellet carefully. Vials were stored overnight at -80°C inside Mr Frosty, and on the next day, vials were moved to the liquid nitrogen tank.

3.3.1.5. FREEZING FIBROBLASTS AND KERATINOCYTES

First steps were the same in splitting and freezing cells. Once the pellet was resuspended in the correct media, cells were counted with Cell counter using 20 mL of diluent and 100 µL of the sample.

After counting, cells were centrifuged again for 4 minutes at 1000 rpm and resuspended in Profreeze medium (90% Profreeze solution and 10% DMSO). The volume of Profreeze medium was calculated depending on the total number of cells, and 4 Million cells per vial were frozen. 1 mL of the sample was added to the vial and stored inside Mr Frosty overnight at -80°C freezer. On the next day, vials were stored in the liquid nitrogen tank.

3.3.1.6. CALCIUM DIFFERENTIATION OF KERATINOCYTES

Calcium concentrations are involved in keratinocytes control. For this reason, a calcium differentiation of these skin cells is carried out. Keratinocytes were growing in KGM media, and when they reached about 70-80% confluent, the differentiation was started (day 0). Cells from one of the dishes were washed with 3 mL of PBS 1x, 2 mL of Trypsin were added, and cells were incubated at 37°C until detached. Trypsin activity was stopped with 3 mL of trypsin inhibitor, and all volume was collected to a Falcon tube to be centrifuged at 1000 rpm for 4 minutes. Pellet was resuspended in 3 mL of KGM media and number of cells was counted using a cell counter. Cells were centrifuged at the same condition and the supernatant obtained after centrifugation was discarded. Final pellet was stored at -20°C and used to extract RNA. 3 mL of KGM with CaCl₂ were added to the rest of the dishes to differentiate the keratinocytes. The protocol followed for every time point was the same than for the day 0.

3.3.1.7. 3D FULL THICKNESS SKIN MODELLING

Growing 3D full thickness skin models in cell culture is a complex process that involves the use of different cells and mediums, and special devices need to be combined in order to build the dermal end epidermal layers that allow the models to so closely resemble *in vivo* skin.

Fibroblasts and basal keratinocytes without the support of feeder cells were grown until they were nearly confluent in 3T3 and KGM medium, respectively.

The dermal layer, including fibroblasts and collagen, was prepared on top of a permeable membrane with a pore size of 3 µm. For that, fibroblasts were trypsinized on the day of skin modelling, counted and resuspended in serum (FBS) using 1.8 x 10⁶ fibroblasts/6 well plate in 1.8 mL serum. Inserts were placed into each well of a deep 6 well plate before 2.5 mL of the following fibroblast/collagen mix was added. The collagen I matrix was prepared adding 1.8

mL of 10x HBSS to 14.4 mL of Pure Col Type 1 Bovine Collagen. While swirling this mixture, 2M NaOH was added drop by drop to the bright yellow colour mix, until the pH indicator was back to pH 7, resulting in a red colour similar to the DMEM medium.

The 6-well plate was incubated during 2 hours in a CO₂-free incubator at 37°C. Under these conditions the matrix hardened to a pink gel. After the incubation, 2 mL of KGM medium were added from above to each matrix, and 14 mL were pipetted directly around each filter insert. The plate was then incubated for another 2 hours in an incubator at 37°C, 5% CO₂ level and 95% RH. After incubation, keratinocytes were then trypsinized, counted, and resuspended in KGM. The medium was removed from the top of the matrix and the keratinocyte-suspension was added onto the center of the matrix, with a density of 4-5 x 10⁶ cells per mL of medium. Deep-well plates with filter inserts were incubated at 37°C, 5% CO₂ level and 95% RH until day after.

The following day, medium was removed from deep-well plate. This was followed by the “airlift”, where the medium is removed from the top of the cells. 10 mL of KCM were added to the deep-well plate of each model, and 3D skin models were transferred to the incubator. Medium was changed every other day. The final skin model was usually harvested on the day 13 (Figure 11).

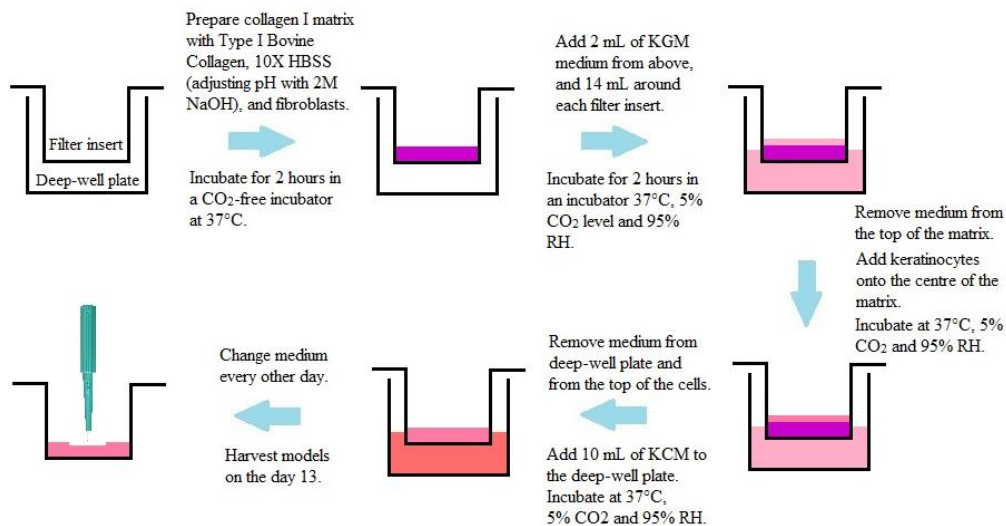


Figure 11. Schematic representation of skin models.

3D skin models were treated with labelled TGase1 (Alexa Fluor 488)/NG (Rhodamin) (10 µg nanogel loaded with 100 µg TGase1 in 1 mL PBS) every second day starting on the day 5 after

airlift. Before the treatment, medium was changed, and skin models were incubated for some time at 32°C to adjust them to the new conditions. 50 µL of the labelled complex were pipetted on top of the skin model, pipetting a droplet of 10 µL onto the centre of the model, followed by four other droplets around the first droplet. After application, each droplet was gently connected. Once the models were treated, they were exposed to a temperature gradient starting 1 hour at 32°C, followed by 1 hour at 34°C, before normal incubation at 37°C, 5% CO₂ level and 95% RH.

3.3.1.8. PIG SKIN EXPLANT CULTURE

Skin pig samples were collected from a Spanish abattoir. The sample was transported in 50 mL Falcon tube with cold transportation medium (TPM), and then it was washed once in the laboratory with Betaisodona solution for 2-3 minutes, followed by three wash steps in AA-PBS for 7 minutes.

The sample was placed with epidermal side down in a petri dish, and some drops of AA-PBS were added until sample was lightly covered. The fat and hair were removed with some scissors, and the sample was then cut using a biopsy punch instrument. In parallel, filter-inserts were placed into a deep-6-well plate using the single-use plastic forceps. For organ culture, the skin samples cut with a biopsy punch were placed, with dermal side down, on the sterile filter-inserts. 10 mL of PSE culture medium was added to the plate, from above (Figure 12).

The skin culture was maintained at 37°C, 5% CO₂ level and 95% RH and medium was changed every day.



Figure 12. Schematic representation of pig skin explant.

3.3.2. ANALYSIS OF 2D KERATINOCYTES

In order to study the location of the therapeutic protein complex TGase1/nanogel, porcine and human control keratinocytes were cultured and treated in a 2D monolayer.

3.3.2.1. COVERSLIPS COATING

Coverslips washed with ethanol were placed into p30 dishes. When the ethanol was evaporated, 1mL of Poly-L-Lysine solution was added to each dish. After sitting for 10 minutes at room temperature, Poly-L-Lysine solution was removed, and dishes were washed three times with sterile water. When they were dried, they were irradiated with UV light for 45 minutes.

Keratinocytes from pig and human control samples were plated on coverslips and grown in KGM medium. When the cells were about 70% confluent, they were treated with 5 μ L of 2% labelled TGase1(Alexa Fluor 488)/NG (Rhodamin) complex (50 μ g nanogel loaded with 0.5 μ g TGase1) in 1 mL of culture medium.

3.3.2.2. IMMUNOCYTOCHEMISTRY

After treatment, cells were washed once with PBS, and when the dishes were dried, 100% ice-cold methanol was added. Cells were washed with washing buffer (1% BSA in PBS) twice after incubation overnight at -20°C, and permeabilized with 0.1% Triton X-100 in PBS for 10 minutes at room temperature. Cells were then washed one with PBS/BSA and incubated for 2 hours at room temperature with blocking solution (10% FBS, 1% BSA in PBS). Primary antibody was diluted in blocking solution and 400 μ L of it were added to each dish. Next day, after incubation overnight at 4°C in a wet chamber, primary antibody was removed, cells were washed four times with washing buffer, and 400 μ L of secondary antibody, previously diluted in blocking buffer, were added. Cells were incubated for 2 hours at room temperature in the dark. After that, cells were washed once with washing buffer, incubated with DAPI for 5 minutes, washed three times with washing buffer, twice with PBS only, and once with distilled water. Fluoromount Mounting Medium was used to preserve samples before visualisation under confocal microscope.

All primary and secondary dilutions and antibodies details are shown in section 3.1.

3.3.3. HARVESTING AND ANALYSIS OF 3D SKIN MODELS

After growth of control skin models, they were analysed. The harvest was carried out on the 13th day after airlift, and then washed with PBS.

3.3.3.1. PARAFFIN- AND CRYO-EMBEDDING

Two biopsy punches were taken from the middle of the model with an 8mm punch for structure analysis and immune-histochemical stainings. The biopsies were then placed on top of a drop of PBS, which was on top of a petri-dish-lid, being cut in two halves using a scalpel. One of the halves was used for paraffin embedding while the other one was used for cryo-embedding.

The sample designated for paraffin embedding was transferred into one CellSafe biopsy capsule, closed, and transferred to one histo-cassette. The cassette was submerged in 10% formalin before fixation and dehydration in the tissue processing machine (Leica), where the following program was used (6h formalin) (Table 5).

Table 5. Program used for paraffin embedding.

Number of repeats	Time (hours)	Chemical
1x	4	Formalin
1x	2	Formalin
1x	1.5	70% ethanol
1x	1.5	80% ethanol
1x	1.5	90% ethanol
2x	1	100% ethanol
2x	1.5	Xylene
3x	1.5	Liquid 60°C paraffin

When tissue processor finished, samples were embedded in first liquid paraffin, the sample was placed with the straight side of the half circle skin punch facing up on the liquid paraffin, and when cold, more liquid paraffin was added until sample was covered. Once hardened on a

cooling plate (4°C), samples were cut into 5 µm sections on a microtome, placed in microscope slides, and dried in a free-CO₂ incubator for posterior haematoxylin and eosin (HE) stainings.

The sample selected for cryo-embedding was taken to the cryotom (precooled -25°C). Some drops of NEG50 embedding medium were added on a stamp at the cryotom at -25°C, and let freeze until nearly hard. The biopsy half was placed with the straight side of the half circle skin punch facing up. After hardening of the embedding medium with the sample, some more drops of NEG50 embedding medium were added to cover the sample. Once hard, samples were stored at -80°C.

3.3.3.2. HAEMATOXYLIN AND EOSIN STAININGS

In order to evaluate the structure of our skin models, haematoxylin and eosin staining were performed on paraffin cuts. Haematoxylin stains the cellular nuclei dark purple, while eosin dyes the non-nuclear cells and structures pink/orange.

The slides were placed into a staining rack and deparaffined with xylene during 40 minutes before they were submerged in the descending ethanol series (100%, 80% and 30% ethanol solution) for 4 minutes each. After that, slides were rinsed in tap water, and then placed in Haematoxylin for 8 minutes. Slides were rinsed in running tap water for 2 minutes, placed in Eosin for 4 minutes, and rinsed in tap water for 1 minute. Slides were then submerged in the ascending ethanol series (30%, 80%, 100% ethanol solution) for 4 minutes each before they were briefly submerged in xylene. Coverslips were then mounted on slides with Entellan Mounting Medium and dried in the fume hood for posterior analysis.

3.3.3.3. IMMUNOHISTOCHEMISTRY

Immunohistochemistry stainings were carried out for the study of specific expression markers on cryosections.

Slides were transferred for 10 minutes into ice-cold acetone and then washed with PBS. Sections were blocked with blocking solution for 2 hours at room temperature. After the incubation, all liquid was dried, slides were placed in a wet chamber, specimens were circle with Dako pen, and 50 µL of primary antibody diluted in blocking solution were added. After incubation overnight at 4 °C, sections were washed three times with washing buffer (0.5%

Tween in PBS) and once with PBS. Secondary antibody was diluted in blocking solution, 50 μ L of which were added to slides, and they were incubated for 2 hours at room temperature in the dark, in the wet chamber. Slides were then washed with washing buffer and incubated with DAPI for 5 minutes. Sections were washed three times with washing buffer, twice with PBS only, and once with distilled water.

All primary and secondary dilutions and antibodies details are shown in section 3.1.

Sections were mounted with fluorescent protecting mounting medium before stainings were analysed in a fluorescence microscope.

3.3.4. RNA EXTRACTION

PureLink™ RNA Mini Kit (by Ambion) protocol was followed to extract RNA from pellets obtained from cultured cells. The purpose of the RNA extraction is the analysis of different genes in samples extracted from primary keratinocytes.

60 mL of 100% ethanol were added to the Wash Buffer II when used for the first time. Lysis Buffer was prepared adding 10 μ L of 2-mercaptoethanol for every 1 mL of Lysis Buffer to contain 1% of 2-mercaptoethanol.

After the preparation of both buffers, protocol for $\leq 5 \times 10^6$ suspension cells were followed to carry out with binding, washing and elution. 0.3 or 0.6 mL of Lysis Buffer with 2-mercaptoethanol (Table 6) were added to the sample according to the cell number. Suspension was vortex to disperse the pellet.

Table 6. Required volume of Lysis Buffer.

Cell number	Lysis Buffer required for each sample (mL)
$\leq 1 \times 10^6$	0.3
$1 \times 10^6 - 5 \times 10^6$	0.6
$5 \times 10^6 - 5 \times 10^7$	0.6 for 5×10^6 cells (e.g., 1.2 per 1×10^7 cells)

Once cells were lysed, one volume of 70% ethanol was added to each volume of cell homogenate. Cells were mixed thoroughly by vortex, and 700 μL of them were transferred up to the spin cartridge with the collection tube. Each sample was centrifuged at 12000 x g for 15 seconds at room temperature. The flow-through was discarded, and the spin cartridge was reinserted into the same collection tube. Each sample was centrifuged at the same conditions, and the flow-through was discarded again.

700 μL of “Wash Buffer I” were added to the spin cartridge, and cells were centrifuged at 12000 x g for 15 seconds at room temperature. The flow-through and the collection tube were discarded, and the spin cartridge was placed into a new collection tube.

A DNase treatment was accomplished. 350 μL of “Wash Buffer I” were added to the spin cartridge containing the bound RNA and the spin was centrifuged at 12000 x g for 15 seconds at room temperature. The flow-through and the collection tube were discarded. The spin cartridge was inserted into a new collection tube.

80 μL of PureLink® DNase mixture (Table 7) were added directly onto the surface of the spin cartridge membrane and incubated at room temperature for 15 minutes. 350 μL of “Wash Buffer I” was added to the spin cartridge. After centrifuging at 12000 x g for 15 seconds at room temperature, the flow-through and the collection tube were discarded. The spin cartridge was inserted into a new collection tube.

Table 7. Composition of PureLink® DNase mixture.

Component	Volume (μL)
10X DNase I Reaction Buffer	8
Resuspended DNase (~ 3U/μL)	10
RNase Free Water	62
Final Volume	80

500 μL of Wash Buffer II with ethanol were added to the spin cartridge and centrifuged at 12000 x g for 15 seconds at room temperature. The flow-through was discarded. These steps were repeated once.

The spin cartridge was centrifuged at 12000 x g for 2 minutes to dry the membrane with bound RNA. The collection tube was discarded, and the spin cartridge was inserted into a recovery tube. 70 µL of RNase-free water were added to the centre of the spin cartridge and incubated for 1 minute at room temperature. The spin cartridge was centrifuged at 12000 x g for 2 minutes at room temperature to elute the RNA from the membrane into the recovery tube. The eluates were collected in a single tube (Figure 13). Purified RNA was stored and used to evaluate RNA quality and for cDNA synthesis.

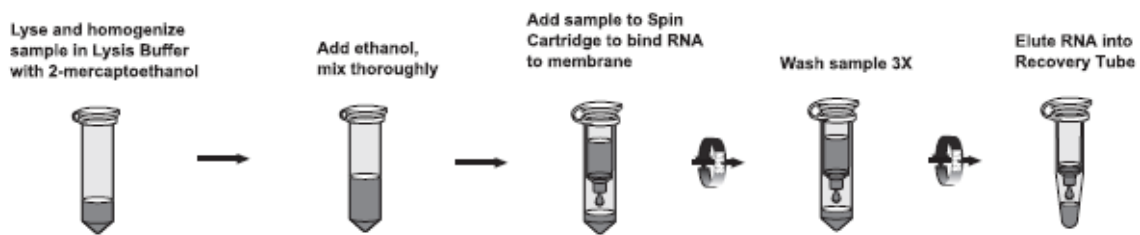


Figure 13. Schematic representation of RNA extraction.

3.3.5. cDNA SYNTHESIS

RNA concentration was estimated using "Nanodrop 2000/200c Spectrophotometer V1.0 User Manual." (2009).

The Nucleic Acid application was open in the NanoDrop Spectrophotometer. 1 µL of distilled water was loaded as a blank onto the lower measurement pedestal and the sampling arm was lowered. "Blank" was clicked to measure and store the reference spectrum. When the measurement was completed, a dry, lint-free lab wipe was used to remove the buffer from both the top and bottom measurement surfaces. An aliquot of the buffer was pipetted onto the pedestal, the arm was lowered and "Measure" was clicked. The surfaces were cleaned.

After the blank measurement, 1 µL of every sample was pipetted directly onto the measurement pedestal. The sampling arm was lowered, and a spectral measurement was initiated using the software on the PC. When the measurement was completed, the sampling arm was raised, and the sample was wiped from both the upper and lower pedestals.

500 ng of RNA were used to perform cDNA-synthesis with the High-Capacity RNA-to-cDNATM Kit. Each reaction contained 10 µL of Reverse Transcriptase buffer mix (2x), 1 µL of

Reverse Transcriptase enzyme mix (20x) as well as the RNA and was topped up with RNase/DNase free water to a total volume of 20 μL . The reaction was put for 1 hour at 37°C and 5 minutes at 95°C to complete cDNA-synthesis in the PCR machine/Thermocycler. cDNA was diluted afterwards 1:10 in RNase/DNase free water and stored for using to analyse the different genes through qRT-PCR.

3.3.6. TaqMan REAL TIME PCR (qRT-PCR)

qRT-PCR was carried out for analysing different primers and housekeeping genes on keratinocyte samples. A reaction mix for the Master Mix plus the assay primer and probe mix was prepared. Furthermore, a sample mix for each cDNA was prepared as well.

Table 8. Quantities of Master Mix, primer, cDNA and distilled water for every plate.

Reaction	Component	1x reaction	25x reaction (for 24 wells on one plate)
Reaction Mix	Master Mix	5 μL	125 μL
	Assay primer and probe mix	0.5 μL	12.5 μL
Sample Mix	cDNA diluted	1 μL	10 μL
	Distilled water	3.5 μL	35 μL

A fresh PCR fast plate was put on ice and 5.5 μL of the reaction mix were pipetted into the correct well until the plate was full. When it was ready 4.5 μL of sample mix were added to each row (Figure 14). Then the plate was covered with an adhesive film and centrifuged. The plate was put into the StepOnePlus™ Real-Time PCR System and the template was adjusted to the correct samples to be run and to analyse the results.

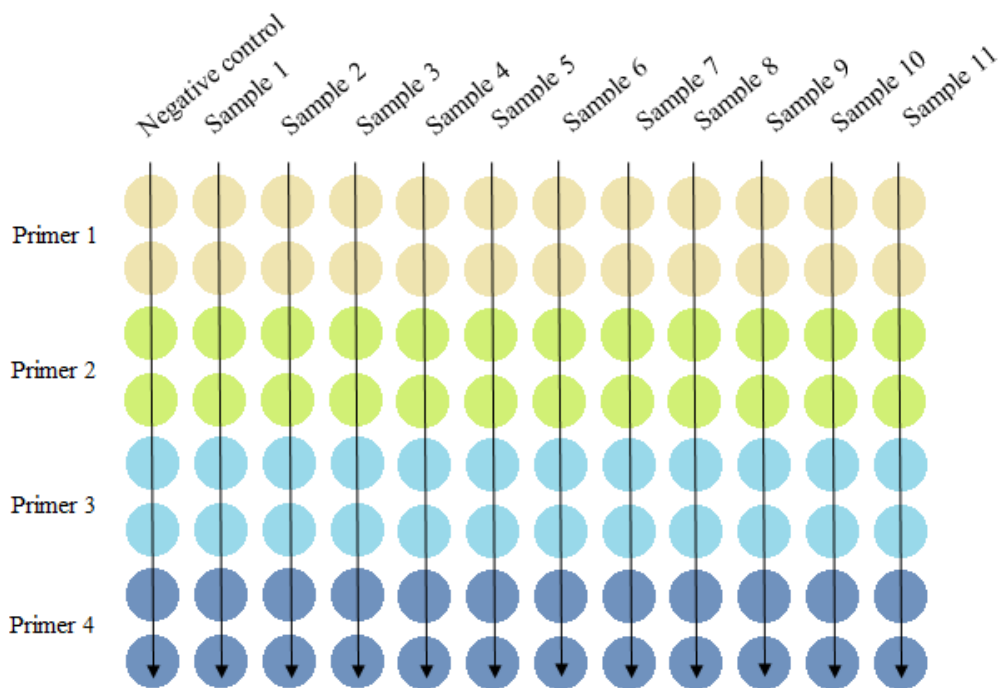


Figure 14. Drawing of the plate with the samples and primers.

The StepOne™ Software included with the StepOnePlus™ Real-Time PCR System runs on the Windows® XP operating system and provides instrument control, data collection, and data analysis capabilities.

Table 9. Cycling conditions to run RT-PCR.

StepOnePlus™ Instrument:	96-well Real-Time PCR
Type of experiment:	Quantitation
Quantitation method:	Comparative C_T ($\Delta\Delta C_T$)
Reagents to detect the target sequence:	TaqMan® Reagents
Ram speed:	Fast (~ 40 minutes to complete a run)
Run method:	cDNA
Run method:	Reaction volume per well: 10 μ L Holding stage: 25°C → 95°C (20 seconds) Step 1 Cycling Stage: 40 cycles: 95 °C (1 second) Step 1 60 °C (20 seconds) Step 2

3.3.7. STATISTICAL ANALYSIS

Mean and standard error were calculated for each data set from duplicates. Statistical analysis was performed using Independent T-test analysis in SPSS (SPSS Inc., Chicago, IL, U.S.A.).

4. RESULTS

4.1. GENE EXPRESSION IN DIFFERENTIATED AND NON-DIFFERENTIATED PRIMARY KERATINOCYTES.

Calcium has been showed to induce keratinocyte differentiation, which is associated with the moving of keratinocytes through the strata of the epidermis to form the skin barrier.

Because calcium is considered a main factor in the regulation of keratinocyte differentiation, we have studied how different genes act in keratinocytes differentiating with calcium induction.

Primary human and pig normal epidermal keratinocytes (hKC15 and pKC1) were grown in KGM medium and differentiated with calcium induction when cells were about 80% confluent, following the protocol described in section 3.3.1.6. Three time points, which are day 0, day 7, and day 14, were carried out in the calcium differentiation, RNA was extracted from the differentiated cells cultured in the laboratory, and cDNA was synthesized and analysed through qRT-PCR. Three genes and one housekeeper were used for the analysis. Those genes were *TGM1*, *ALOXE3* and *ALOX12B*, and the housekeeping gene was *GAPDH*. These results were also compared to an ARCI patient with mutation in *TGM1*, which cells were grown in a 2D monolayer, and treated with TGase1.

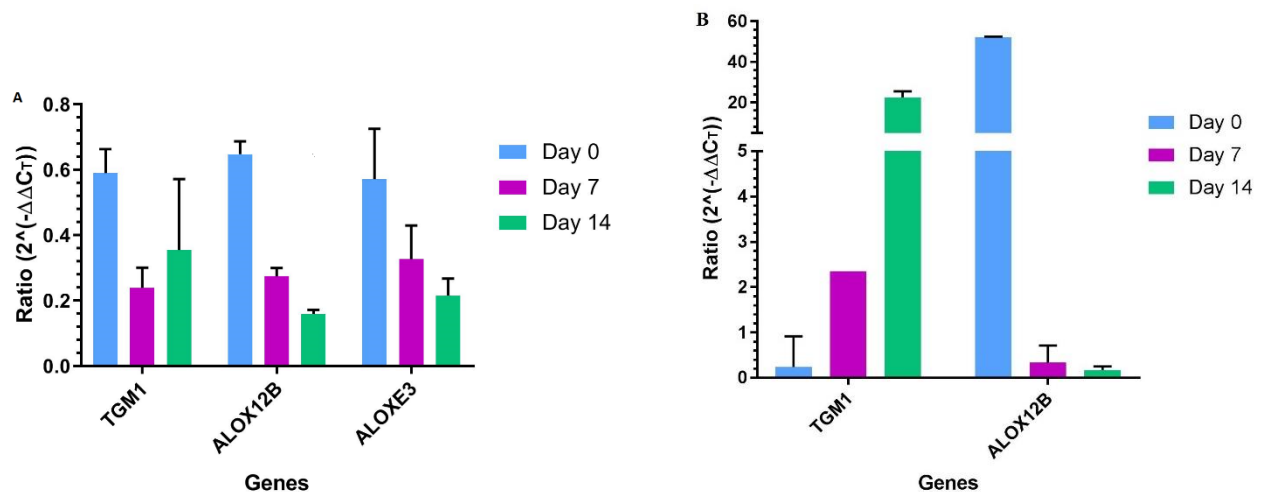


Figure 15. Gene expression in differentiated primary keratinocytes. RNA was extracted from keratinocytes derived from human and pig tissue, differentiated with 1.2 mM and 1 mM calcium chloride, respectively. qRT-PCR was performed for specific markers. Resulting C_T values were normalized using housekeeping gene *GAPDH* and to the respective control sample (non differentiated primary keratinocytes) which expression values are 1. Graphics show the

relative gene expression (ratio) of specific genes for human (A) and porcine (B) primary keratinocytes. Duplicates from the same donor were used for the analysis. Error bars indicate standard deviation.

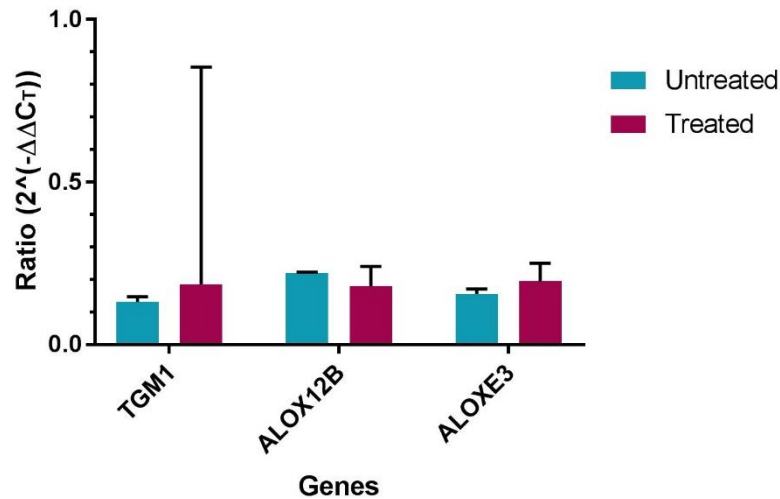


Figure 16. Gene expression in basal primary keratinocytes. RNA extraction was carried out from keratinocytes derived from an ARCI patient with mutation in *TGM1*. Cells were treated with TGase1 and analysed by qRT-PCR. C_T values, given as results of the analysis, were normalized using *GAPDH* as housekeeping gene and to an untreated control sample (non differentiated primary keratinocytes), which expression values are 1. Graphic shows the relative gene expression (ratio) of specific genes for treated and untreated primary keratinocytes. Duplicates from the same donor were used for this analysis. Error bars indicate standard deviation.

C_T values were obtained by the StepOne™ Software included with the StepOnePlus™ RT-PCR system, where C_T is defined as the number of cycles needed for the fluorescence to reach a specific threshold level of detection and is inversely correlated with the amount of template nucleic acid present in the reaction. Replicates from the same donor were used, so an average with C_T values was calculated to determinate the difference between the C_T value of the target gene and the C_T value of the housekeeper (reference gene) (value called delta C_T or ΔC_T). The ΔC_T value of the test sample minus the ΔC_T value of the control sample, which are non differentiated primary keratinocytes gave as result what is called $\Delta\Delta C_T$, the value used to calculate the ratio or the relative gene expression ($2^{-\Delta\Delta C_T}$). To summarise: $\Delta\Delta C_T = \Delta C_{T \text{ test sample}}$

- ΔC_T control sample, where $\Delta C_T = C_{T \text{ target gene}} - C_{T \text{ reference gene}}$. The relative gene expression was the one used to analyse the results shown in the figures 15 and 16.

As it can be seen in Figure 15, despite all markers present a higher expression when human (A) and pig (B) keratinocytes (A) are not differentiated (day 0), except when analysing *TGMI* (Figure 15B), where an increase in the differentiation can be seen, *TGMI* increases with the keratinocyte differentiation in both cell lines. However, the opposite occurs with *ALOX12B* and *ALOXE3*, as their expression decreases in the late stages of the differentiation.

In Figure 16, where keratinocytes from an ARCI patient with mutation in *TGMI* were used for the study, a slightly increase of expression can be observed for *TGMI* and *ALOXE3* when cells were treated with TGase1, while expression was higher for untreated keratinocytes than treated for *ALOX12B*.

4.2. 3D SKIN MODELS CHARACTERIZATION

3D skin models of human skin are used in biomedical and pharmacological research for drug development and for the study of skin disease, being an alternative method to animal experimentation (Mathes, Ruffner, and Graf-Hausner, 2014). 3D full thickness skin models are constructed by a collagen and fibroblasts matrix, which is equivalent to the dermis, with keratinocytes growing on it to mimic the epidermis. These models can resemble most of the characteristics of the native human skin and we have used them to test the effect of the therapeutic TGase1/NG complex.

To accomplish this, fibroblasts and keratinocytes derived from healthy human donors were used to construct control 3D skin models. Models were cultured for 13 days and then characterized regarding structure and protein expression.

Furthermore, we compared those models from healthy human donors with diseased skin models. The fibroblasts and keratinocytes used for the diseased skin models were derived from ARCI patients with mutations in *TGMI*, and they were cultured for 13 days by a colleague from our research group.

4.2.1. EVALUATION OF SKIN STRUCTURE IN 3D SKIN MODELS

To evaluate the structure of 3D skin models, H&E staining (as explained in chapter 3.3.3.2.) was carried out on control and diseased models (Figure 17).

After culturing the 3D skin models for 13 days, two biopsy punches were taken from their middle, processed in the tissue processing machine, and paraffin-embedded (as mentioned in paragraph 3.3.3.1.). Samples were sectioned with a microtome for evaluation of their structure by H&E staining.

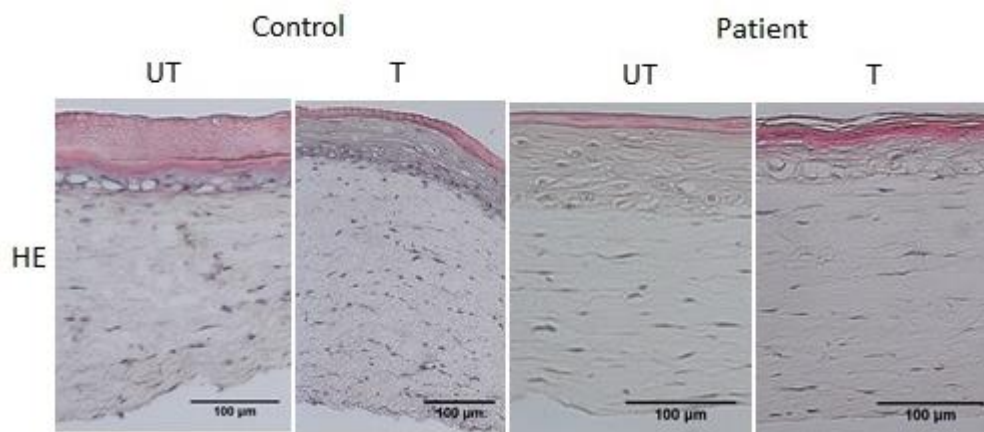


Figure 17. Characterization of untreated and treated control, and ARCI-patient derived 3D skin models (day 13). H&E staining shows structure of models by staining nuclei in dark purple, and corneal layer in pink. Bars 100 µm.

H&E staining shows a well-established structure in all untreated and treated control and diseased skin models. Untreated and treated control models present a multi-layered thick epidermis with nuclei in the stratum granulosum, while *TGMI*-patient skin models manifest an epidermis that has become flatter. The number of nuclei in the stratum granulosum is also lower in the case of diseased models.

4.2.2. CHALLENGES IN 3D SKIN MODEL CONSTRUCTION

The construction of 3D skin models is a complex and sensitive process, and the generation of good skin models is challenging. The main factor that generates changes in the skin models are the keratinocytes. Well-structured models are produced when the correct number of basal

keratinocytes is used, and when those keratinocytes are not starting to look differentiated, which can happen when high passages are used.

Other factor to take in consideration is the Pure Col Type 1 Bovine Collagen used and possible changes in the humidity in the incubators. After preparing matrix and incubating in the CO₂-free incubator, a non-hardened matrix was sometimes produced, affecting the quality of the skin model produced.

Therefore, only well-structured models are suitable to reproduce skin *in vitro* and will be used for experiments.

4.3. APPLICATION OF TGase1/NG COMPLEX IN CELLS GROWN ON A 2D MONOLAYER

To assess the cellular distribution of TGase1 and the NG in primary cells, isolated keratinocytes from porcine and human healthy controls were cultured on a 2D monolayer. Cells were cultured on Poly-L-Lysine-treated coverslips inserted in culture dishes and fed with KGM medium. When cells were about 70% confluent, 5 µL of 2% labelled TGase1(Alexa Fluor 488)/NG (Rhodamin) complex (50 µg nanogel loaded with 1 µg TGase1) were added in 1 mL of culture medium. Three conditions were carried out for this experiment: untreated (UT) cells, cells treated for 3 hours at 37°C, and cells treated for 24 hours at 37°C. After incubation times, cells were fixed following the protocol described in section 3.3.2.2., stained with 4 specific antibodies (anti E-cadherin, anti EEA1, anti GM130, and LysoTracker Deep Red), counterstained with DAPI, and analysed by confocal microscopy (Figure 18-25). As LysoTracker Deep Red is a fluorescent dye, secondary antibody was not needed for its stain, and its application was performed in live cells after TGase1/NG treatment and before fixation. Specifically, anti E-cadherin detects the membrane, anti EEA1 shows the endoplasmic reticulum, anti GM130 is specific for Golgi, and LysoTracker Deep Red tracks lysosomes. As TGase1 and the nanogel are labelled, this method is an effective way to check their progress in keratinocytes.

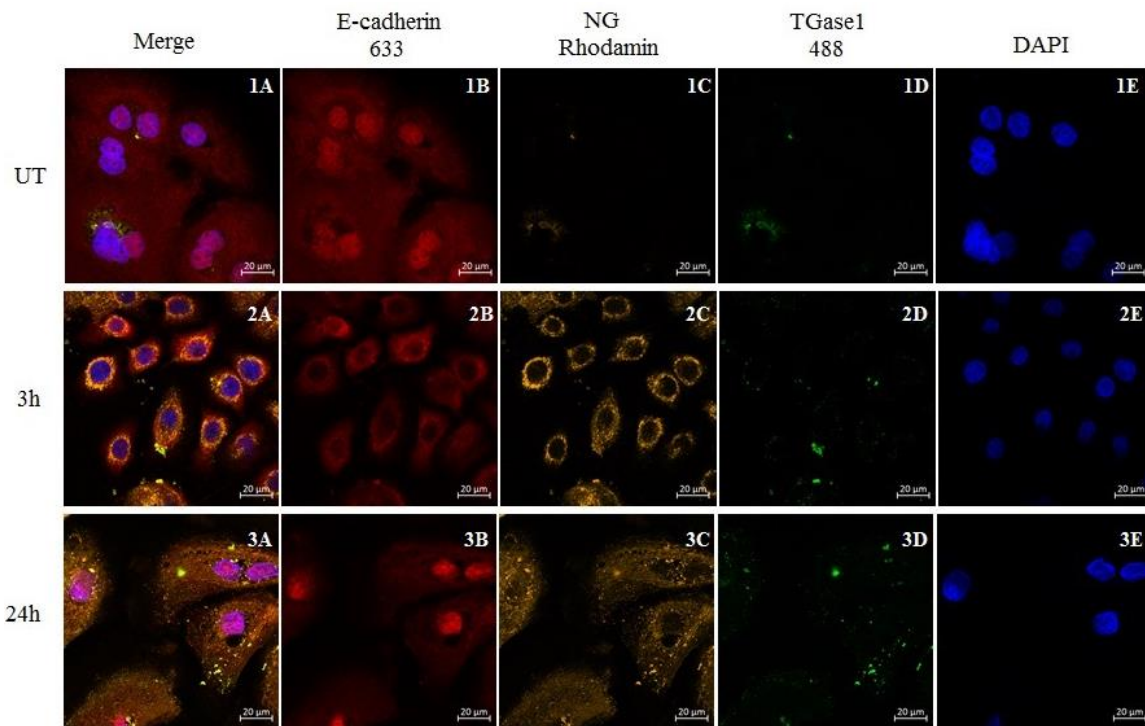


Figure 18. Anti E-cadherin staining when application of labelled TGase1/NG complex in basal, control human keratinocytes. Untreated and treated cells (after 3 hours or 24 hours of incubation with 2% TGase1/NG complex) were stained with anti E-cadherin antibody, a marker specific for membrane, using Alexa Fluor® 633 (red) as secondary antibody. TGase1 was labelled with Alexa Fluor® 488 (green) and the nanogel was labelled with Rhodamin (red, pseudo-colored orange). Nuclear counterstaining was performed with DAPI (blue). Bars 20 μm .

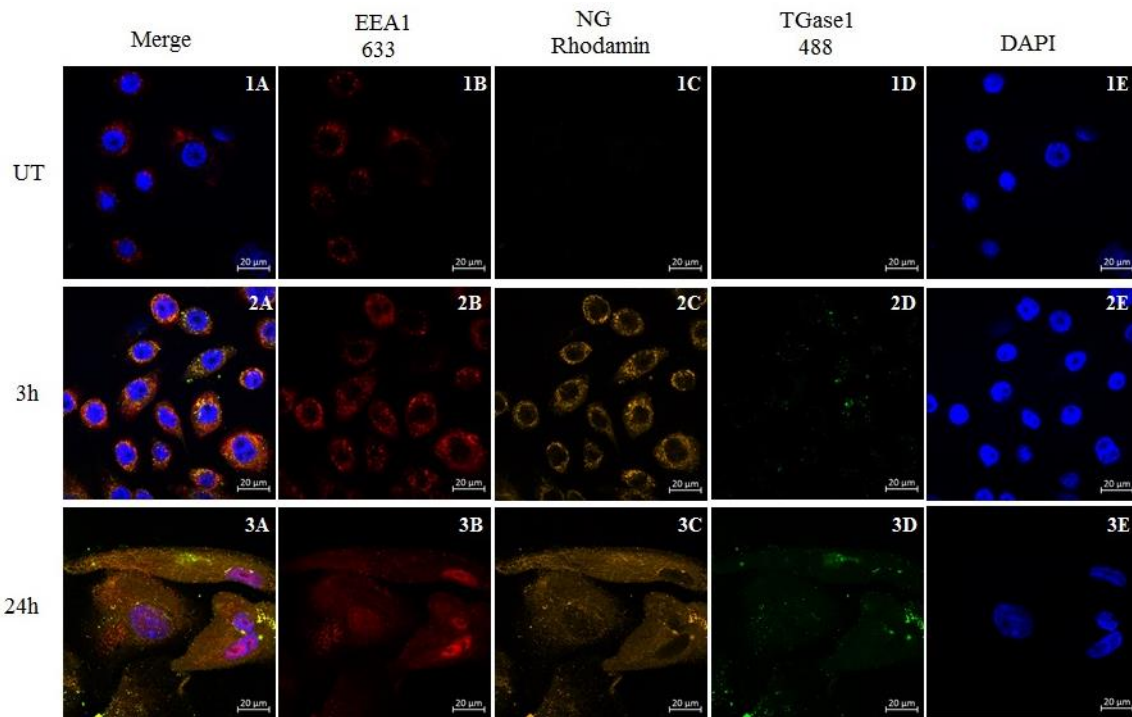


Figure 19. Anti EEA1 staining when application of labelled TGase1/NG in basal, control human keratinocytes. Cells were stained with anti EEA1 antibody, a marker specific for endoplasmic reticulum, using Alexa Fluor® 633 (red) as secondary antibody. TGase1 was labelled with Alexa Fluor® 488 (green) and the nanogel was labelled with Rhodamin (red, pseudo-colored orange). DAPI (blue) was used for nuclear staining. Bars 20 μ m.

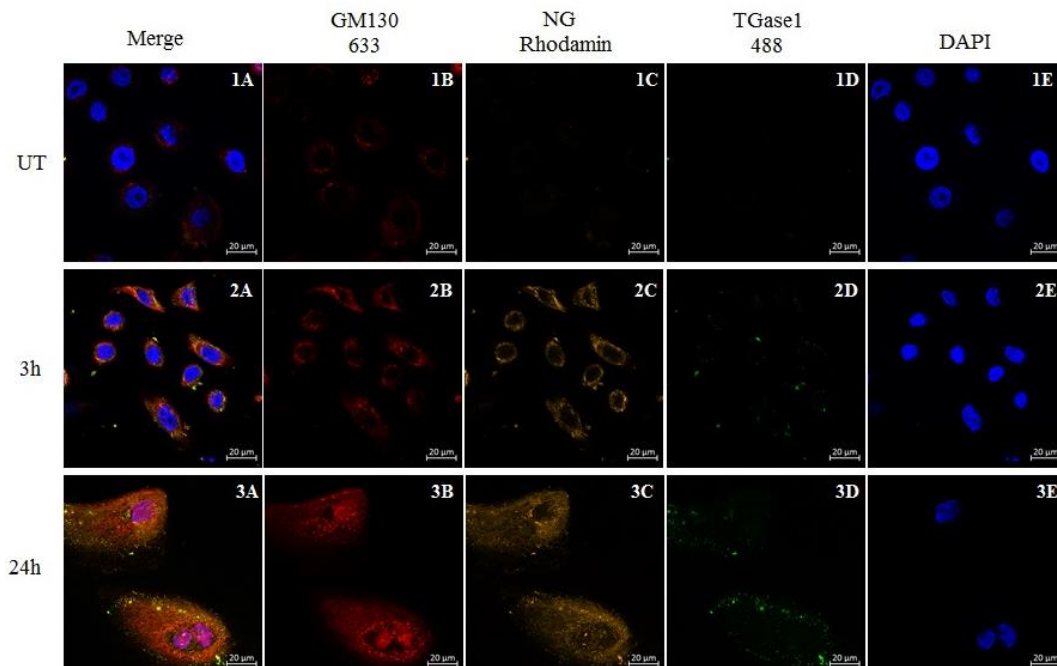


Figure 20. Anti GM130 staining when application of labelled TGase1/NG in basal, control human keratinocytes. Untreated cells, as well as treated, were stained with anti GM130

antibody, a specific marker for Golgi, using Alexa Fluor® 633 (red) as secondary antibody. The TGase1/NG complex was labelled with Alexa Fluor® 488 (green) for TGase1 and with Rhodamin (red, pseudo-colored orange) for the nanogel. Nuclear counterstaining was performed with DAPI (blue). Bars 20 μm .

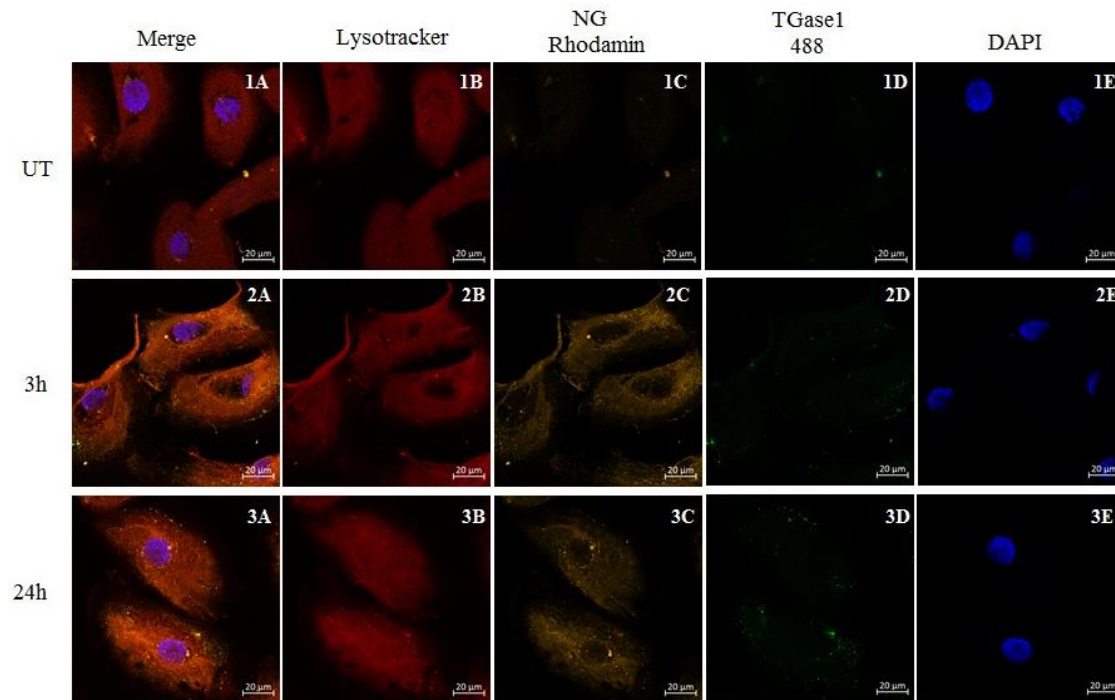


Figure 21. LysoTracker deep red staining when application of labelled TGase1/NG in basal, control human keratinocytes. Untreated and treated cells were stained with LysoTracker Deep Red (red), a specific dye for lysosomes, before fixation of the cells and after treatment with the TGase1/NG complex, labelled with Alexa Fluor® 488 (green) for TGase1 and with Rhodamin (red, pseudo-colored orange) for the nanogel. To stain the nuclei, DAPI (blue) was used. Bars 20 μm .

After culture of untreated and treated cells cultured in a 2D monolayer and staining with different antibodies specific for some organelles, analysis was carried out with confocal microscope. TGase1 enters the keratinocytes, as expected, and the nanogel also enters the cytoplasm. When comparing the intensity of TGase1 and nanogel signals, the signal for the complex is stronger when the treatment was carried out for 24 hours. Upon 3 hours treatment, TGase1/NG complex is located around the nuclei, and in the cytoplasm and membrane. Subsequently, when treatment is carried out for 24 hours, TGase1/NG complex seems to stay

around the nuclei, cytoplasm and membrane, therefore the complex does not seem to enter the nuclei any time.

Senescent cell appearance can be observed at 24 hours for each antibody. In addition, keratinocytes are in senescence when no treatment was used for the lysotracker staining. An atypical distribution of lysotracker staining is also seen, and anti E-cadherin staining is not very accurate, as not only the membrane is stained. Nuclei appear stained when anti E-cadherin was used.

Due to the fact that the complex is a 2% TGase1 solution in the nanogel, the fluorescent signal of the rhodamine always appeared stronger than the Alexa Fluor® 488 signal.

As pigs share many physiological and anatomical similarities with humans, like a structurally similar skin, we compare human and pig keratinocytes from healthy controls, grown and treated with the TGase1/NG complex in the same conditions.

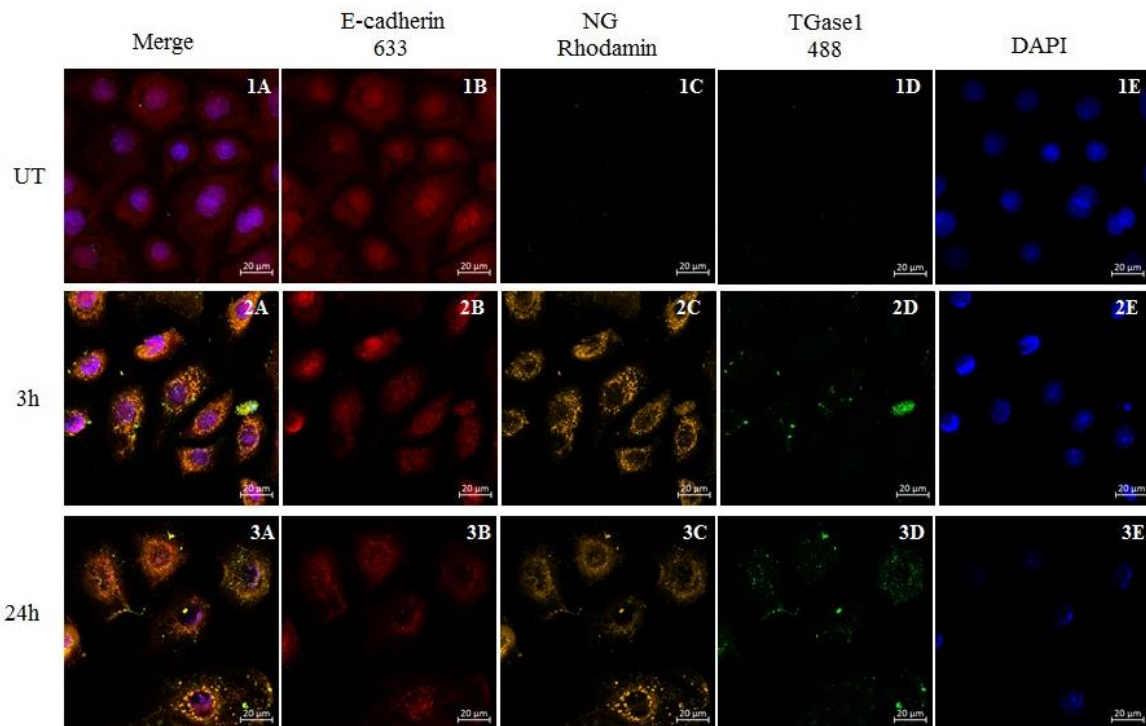


Figure 22. Anti E-cadherin staining when application of labelled TGase1/NG complex in basal, control porcine keratinocytes. Untreated and treated cells were stained with anti E-cadherin antibody, using Alexa Fluor® 633 (red) as secondary antibody. TGase1, part of the treatment complex, was labelled with Alexa Fluor® 488 (green), and the nanogel was labelled

with Rhodamin (red, pseudo-colred orange). To stain the nuclei, DAPI (blue) was used. Bars 20 μm .

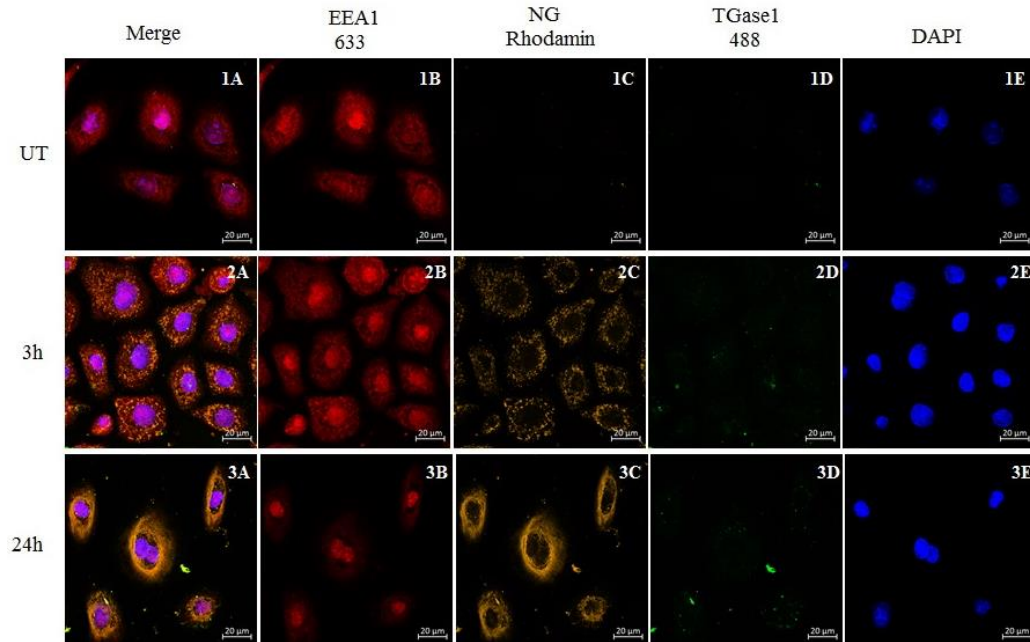


Figure 23. Anti EEA1 staining when application of labelled TGase1/NG complex in basal, control porcine keratinocytes. Untreated cells, and cells treated with 2% labelled TGase1/NG complex, were stained with anti EEA1 antibody using Alexa Fluor® 633 (red) as secondary antibody. TGase1 was labelled with Alexa Fluor® 488 (green), while the nanogel was labelled with Rhodamin (red, pseudo-colred orange). Nuclear counterstaining was performed with DAPI (blue). Bars 20 μm .

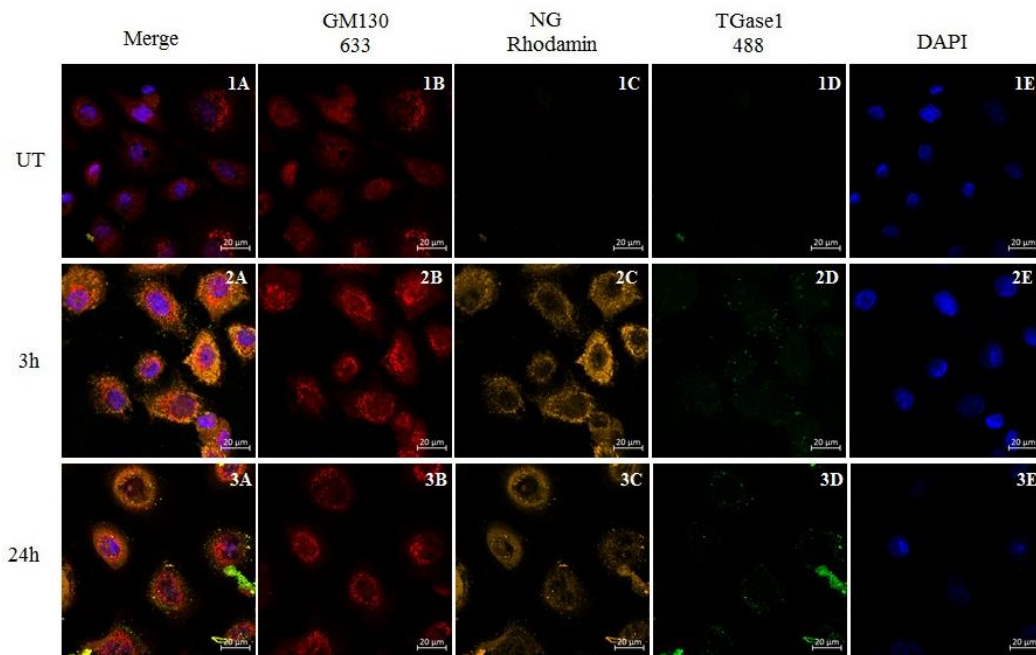


Figure 24. Anti GM130 staining when application of labelled TGase1/NG complex in basal, control porcine keratinocytes. Cells were stained with anti GM130 primary antibody, using the secondary antibody Alexa Fluor® 633 (red). TGase1 was labelled with Alexa Fluor® 488 (green) and the nanogel was labelled with Rhodamin (red, pseudo-colored orange). DAPI was used to counterstain the nuclei. Bars 20 μm.

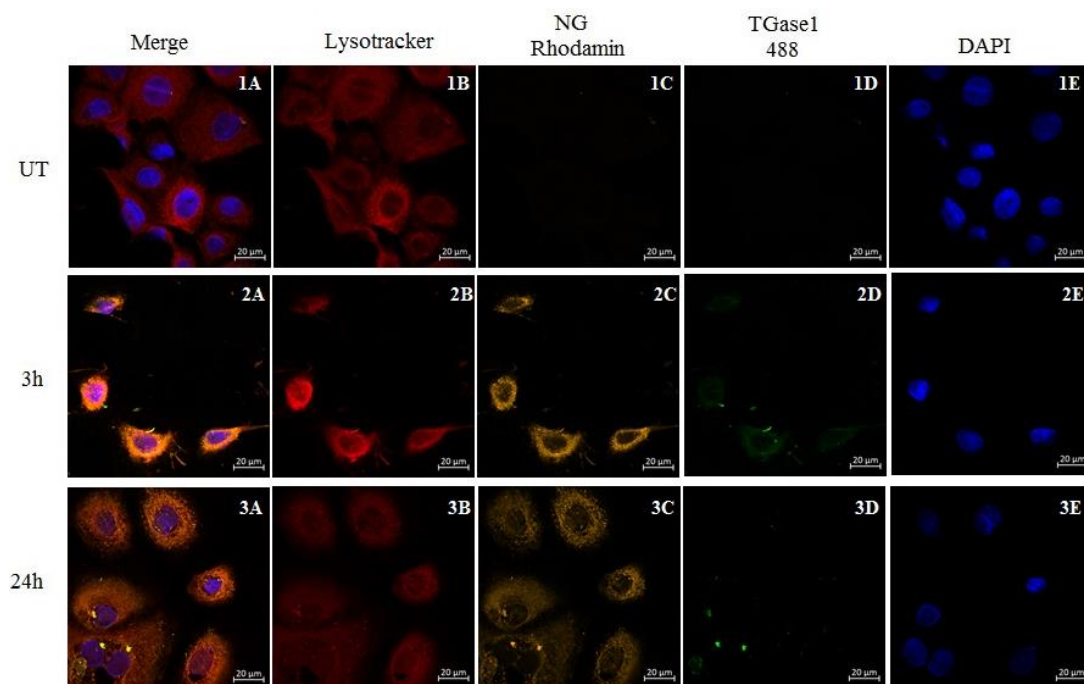


Figure 25. LysoTracker deep red staining when application of labelled TGase1/NG complex in basal, control porcine keratinocytes. Keratinocytes were stained with

LysoTracker Deep Red dye (red) before cells were fixed, and after application of TGase1/NG complex, which was labelled with Alexa Fluor® 488 (green) for the TGase1, and Rhodamin (red, pseudo-colored orange) for the nanogel. Nuclei were stained with DAPI (blue). Bars 20 μm .

When using porcine keratinocytes, our TGase1/NG complex enters the keratinocytes, with both our protein and the nanogel entering the cytoplasm. After 24 hours, the signals for the complex are stronger than when cells were incubated for 3 hours with the treatment. As in human keratinocytes, TGase1/NG complex does not seem to enter the nuclei when 3 hours treatment or 24 hours treatment, being located in the cytoplasm and membrane.

In this case, senescent cell appearance is not observed in any condition. As in human primary keratinocytes, an atypical distribution of lysotracker staining is seen, and anti E-cadherin is stained in both membrane and nuclei.

4.4. CHARACTERIZATION OF PIG SKIN EXPLANTS

Skin explants are models close to *in vivo* skin, and they are made by keratinocytes, melanocytes, Langerhans cells, fibroblasts, collagen and glycosaminoglycans, while the 3D skin models are only formed by keratinocytes and fibroblasts. Also, skin explants can be used immediately, there is no need of time to prepare them. Because human skin in large quantities is not easy to obtain, we thought that porcine skin could be an alternative to test our therapeutic TGase 1 protein and see how it behaves in *in vivo* circumstances.

Several skin samples from different pigs were received from a Spanish abattoir and cultured in the laboratory as skin explants. Medium was changed every day and incubated at 37°C in an atmosphere of 95% air and 5% CO₂.



Figure 26. Pig skin explants.

Pig skin explants (Figure 26) were cultured for 13 days, but their culture has been a challenge. In first place, tissue samples must be fresh. No changes in skin explants are in fact observed when skin samples have been obtained subsequently treatment and processes (e.g. removing hair) run before slaughtering the animal. Those and old samples cannot be used for the experiments due to cells being already dead.

Consequently, obtaining the skin samples turned to be a great challenge that influenced our study. No local abattoirs in fact agreed to provide us the requested samples. In order to overcome this problem, we contacted a slaughterhouse in Galaroza (Spain), who agreed to supply us the fresh (alive) pig skin samples. However, the career used and the shipping time, mainly due to the hot temperature and holidays season, turned out to be inadequate. Once received in fact, explants resulted to be contaminated after 2 days of being in culture.

5. DISCUSSION

ARCI is a diverse group of diseases that share some characteristics such as autosomal recessive pattern of inheritance, newborns presenting collodion membrane, and overlap in causative gene (Oji et al., 2010). ARCI is a rare disease, therefore less than 2 in 100000 of the population present the disease. Around 7000 rare diseases are known, and 80% are genetic. Rare diseases are often misdiagnosed or diagnosed with a major delay, however The World Health Organization (WHO) has expressed concern about them (Puiu and Dan, 2010).

In the case of ARCI, eleven genes have been associated with different ARCI phenotypes, being mutations in *TGMI* the most common cause of ARCI. *TGMI* encodes for TGase1, that catalyses the N^ε-(γ -glutamyl) lysine crosslinking of precursor proteins, such as loricrin or involucrin, during the formation of the cytoplasmic layer of the cornified cell envelope, structure important for the skin's barrier function. Subsequently, defects in the cornified cell envelope in the epidermis and altered expression of these proteins are shown in patients with ARCI, mostly due to *TGMI* mutations (Herman et al., 2009).

Unfortunately, the only current available treatment for this skin disease is symptomatic, providing symptomatic relief to the patient, but not eliminating the symptoms. Therefore, a causative treatment has to be developed. Witting et al. (2015) synthesized a thermoresponsive PNIPAM-dPG nanogel for cutaneous protein TGase1 delivery in skin models, a personalized TGase1 substitution therapy, to restore the skin barrier function in ARCI patients with mutations in *TGMI*.

With this project, we aimed to better understand the fate of the PNIPAM-dPG nanogel and the loaded TGase1 protein when they are delivered in the skin. In parallel, these studies have been also carried out with porcine skin samples due to its similarities with human skin.

5.1. COMPARISON OF HUMAN AND PIG KERATINOCYTES GROWTH CONDITIONS

Comparing the cell lines used, human and porcine keratinocytes were isolated following the same protocol and cultured in the same culture medium (KGM medium when cultured without feeder cells, and KCM medium when cultured on feeders) and same conditions. After splitting, at first day, only a few colonies of porcine keratinocytes were observed. It was not until day 6-7 when proliferating keratinocytes were observed, as it was previously seen in Ponce's research (2017). Porcine keratinocytes were then taking more time than human keratinocytes in replicating. We also observed that porcine keratinocytes were growing nicer and faster when on feeder cells, as sometimes, when growing them without the support of feeders, they started to look differentiated. This could be due to the medium used to culture them. Regarding the morphology (figures not shown), no differences between human and porcine keratinocytes were observed.

In future studies, other keratinocytes growth medium could be tested, as EpiLife or KGM Gold, to evaluate if the proliferation of keratinocytes extracted from porcine skin samples is faster and their morphology is nicer. Concerning morphology, human and porcine keratinocytes look very similar. No differences can be appreciated.

5.2. TGase1 IS EXPRESSED ON RNA LEVEL IN 2D KERATINOCYTES

We aimed to examine the expression of three genes associated with ARCI when primary keratinocytes are differentiated and when they are non-differentiated in vitro. Also, we wanted to analyse those genes in samples from ARCI-patients with *TGMI* mutation. Skin sample of the patient was extracted by upper arm biopsy. This patient, a 43 years old male, had disease causing mutations in *TGMI* leading to lamellar ichthyosis. He features a homozygous mutation in exon 3, c.428G>A corresponding to p.(Arg143His).

To accomplish this, different cell lines (human and porcine primary keratinocytes) were grown and when they were about 70% confluent, differentiation was induced by calcium application. After several days of culture, pellet was collected to extract RNA, for the posterior synthesis of cDNA to finally perform the qRT-PCR through which we will be able to analyse the relative gene expression.

The three genes used to study the gene expression were *TGMI*, *ALOX12B* and *ALOXE3*. *TGMI* is a member of the transglutaminase family and codes for the TGase 1 enzyme, which catalyses the crosslinking between polypeptides. TGase1 is involved in the assembly of the cornified envelope at the cell periphery of corneocytes, and it is the most common cause of ARCI (Haneda et al., 2016). *ALOX12B* and *ALOXE3* are lipoxygenases genes that encode two LOX proteins, 12R-LOX and eLOX3, which are involved in the conversion of linoleoyl ceramide in the cornified envelope, into cornified envelope, which plays an important role in the maintenance of epidermal barrier formation (Krieg and Fürstenberger, 2014; Mashima and Okuyama, 2015). Genetic failures of these processes lead to ARCI (Eckl et al., 2009).

Target gene expression was calculated relatively to a stably expressed gene, which should be uniformly expressed during all experimental conditions. The housekeeping gene used was GAPDH, which is a highly expressed multifunctional protein that participated in diverse activities as glycolysis, transcriptional and posttranscriptional gene regulation, maintenance of DNA integrity, vesicular transport, and chromatin structure (Khan et al., 2013).

Quantitative real time PCR shows an increase in the gene expression of *TGMI* in the late stages of the keratinocyte differentiation for both cell lines, human and porcine controls (Figure 15A-B). In figure 15A, a high *TGMI* expression in day 0 can be seen, that decreases when keratinocytes start the differentiation (day 7) and that increases at later stages (day 14). In figure 15B, *TGMI* expression is very low when differentiation was not started (day 0), expression that increases during the differentiation (*TGMI* expression in day 7 is lower comparing to expression in day 14).

The expression of TGase1 in the differentiation was expected, as differentiation requires the expression of this protein for the crosslinking of protein through the formation of covalent isopeptide bonds. Recent studies have also proved the variation of *TGMI* expression in keratinocyte differentiation. Enomoto et al. (2003) indicated a high gene expression of *TGMI* after the initiation of differentiation in primary human keratinocytes, compared with its expression before the differentiation. Yamane et al. (2016) showed that the activity of TGase1 at the early stages of the differentiation was maintained at a similar level and increased in differentiating keratinocytes together with other catalysed substrates.

A reduction in the gene expression of *ALOX12B* and *ALOXE3* during the differentiation can be observed (Figure 15 A-B). Our findings suggest, for both human and porcine differentiated keratinocytes, a decrease of *ALOX12B* expression until day 7 (early stage of the differentiation), that keeps decreasing at day 14 (later stage).

In 2009, Kim et al. demonstrated, in primary keratinocytes isolated from new-born mice, that the expression of *Alox12b* is directly induced by Δ Np63, contributing to epidermal barrier formation. This induction is dependent on intact *p63* binding sites in the *Alox12* promoter and only occurs in differentiating keratinocytes (Kim et al., 2009). The fact that Δ Np63 induces *ALOX12B* can explain our results, as Δ Np63 is mostly involved at the beginning of the differentiation (Koh et al. 2015). In contrast with our results, it is also suggested that *ALOX12B* and *ALOXE3* are expressed in the terminal differentiation of keratinocytes. However, it is still unclear, if the role of LOX-dependent pathway is structural, or if it is involved in signalling, in epidermal differentiation (Jobard et al., 2002; Moran et al., 2007).

ALOX12B and *ALOXE3* have also been seen to participate in the keratinocyte differentiation by the formation of products which act in the differentiation. Therefore, they are involved in the regulation of proliferation and differentiation of keratinocytes. This is also supported by studies showing that inactivating mutations in these genes are linked to the development of ARCI (Yu et al., 2003; Epp et al., 2007).

When looking at the patient samples (Figure 16), a higher *ALOX12B* expression can be seen when patient keratinocytes were not treated, comparing to treated cells, while *ALOXE3* expression is increased in treated patient cells than in untreated. A significant reduction of *TGMI* expression on the RNA level can be seen, as well as of the other genes. This decrease of the gene expression is also observed when the patient is treated with the TGase1/NG complex. This patient is known to carry a homozygous mutation in exon 3 leading to nonsense mediated decay meaning that he does not express the protein at all. The fact of that the therapeutic complex did not increase the expression of *TGMI*, could be due to the application itself topically, so we are not expected to see a direct change on the *TGMI* expression because it is still mutated. We would expect *TGMI* expression to go up if would have done gene editing and corrected the mutation, other strategy for therapeutic development that has been done for epidermolysis bullosa (Hainzl et al., 2017).

These analyses therefore confirm the expression of *TGMI* on RNA level in control and diseased 2D keratinocytes. Also, the use of primary keratinocytes isolated from biopsies of patients is a very valuable model for investigating proteins and genes involved in epidermal differentiation, and they contribute to the basic knowledge of the mechanism of different skin diseases.

It has also been seen that some of these markers are induced by other proteins. As previously mentioned, the expression of *ALOX12B* is directly induced by Δ Np63, contributing to epidermal barrier formation (Kim et al., 2000). In addition, *TGMI* expression can be induced by tumor necrosis factor-related apoptosis-inducing ligand (TRAIL), which is involved in the initiation of keratinocyte differentiation by p63. p63, which is a reliable keratinocyte stem cell marker, plays a major role in ectodermal development, in the maintenance of a basal cell population and in the terminal differentiation of stratified epithelia, where it can also induce the expression of involucrin, Reis-Filho et al., 2002; Koster, 2010; Wu et al., 2011).

Furthermore, mutations in the genes causing ARCI, like *ALOX12B* or *ALOXE3*, can also influence the expression of some differentiation markers such as filaggrin (Eckl et al., 2011).

In future studies, it would be also interesting for our research to analyse the gene expression of different differentiation markers of the skin, such as involucrin, filaggrin, and p63 and its two main isoforms (Δ Np63 and Tap63) in undifferentiated and differentiated cells grown in 2D monolayer, but also in treated and untreated skin cells for a better comprehension of them and of the TGase1/NG complex treatment.

It has also to be mentioned that no literature concerning studies with transglutaminase 1 of porcine skin has been found, so that we assumed that TGase1 is very similar in pig and human skin, as *TGMI* in porcine skin is highly homologous to *TGMI* in human skin. In a first instance we analysed gene expression with a human specific *TGMI* TaqMan assay (assay ID Hs01070310_m1, designed by Applied Biosystems), obtaining undetermined values when cDNA from pig cell line was used. Therefore, as predesigned pig assays did not seem to be available, one specific for human but similar to pig sequence was used (assay ID Hs00165929_m1, designed by Applied Biosystems). Subsequently, with this second TaqMan assay for human *TGMI*, gene expression values were obtained for the pig samples, but not for the human samples, so that for the posterior analysis of the gene expression and obtaining the results shown in Figure 15(A-B), a combination of both assays was made.

To compare human and porcine samples, a series of independent t tests was run to compare the different conditions of *TGMI* and *ALOX12B* expression at days 0, 7 and 14. T test showed no statistically significant differences (P value > 0.05) when comparing both genes between the two species, and at the different time points. However, this analysis is just preliminary, as only duplicates were run for each gene.

Despite the statistical analysis did not show any significant differences, when looking at the qPCR data (figures 15A-B), a difference in the ratio at day 0 for *ALOX12B* may be observed. This is unexpected, and it might be due to the control used for the qPCR analysis, or the TaqMan assay used, as it could be specific only for human. Therefore, further replicates are needed to run a more powerful statistical analysis and eliminate any calibration error, in order to better clarify and understand the similarities of differences between these genes in human and porcine samples.

Large error bars can be observed in figures 15A and 16 for some of the samples (*TGMI* at day 14 in human keratinocytes differentiation, and *TGMI* in treated sample), which can be due to errors when pipetting to prepare the qPCR experiment.

In further studies, new suitable TaqMan assays for both cell lines, porcine and human primary keratinocytes, should be found for a better understanding of how *TGMI* is expressed in porcine cells. Furthermore, undetermined values were obtained when using a human specific *ALOXE3* TaqMan assay (assay ID Hs00222134_m1, designed by Applied Biosystems), therefore new TaqMan probes suitable for porcine cells would be helpful for future experiments. Also, a comparison between the studied samples (differentiated cells) to other calibrator samples used for the analysis of the qPCR data will be used in future experiments. In addition, more time points will be carried out in the differentiation to further understand the role of the genes in the differentiation, and in the different species.

5.3. CONTROL AND DISEASED 3D SKIN MODELS ARE GOOD SYSTEMS TO TEST PROTEIN SUBSTITUTION

After proved that *TGMI* is expressed in both porcine and human primary keratinocytes, we constructed human control 3D skin models and evaluated their characteristics through H&E and immunohistochemistry staining for epidermal markers. Also, this evaluation was carried out on human diseased 3D skin models previously made by a colleague from our research

group. The diseased 3D skin models were built with keratinocytes and fibroblasts from an ARCI patient with mutation in *TGMI*.

H&E staining seems to show hyperkeratosis in the control model, which is not seen in the treated control, where we would not expect a major difference; the untreated patient model shows a perfect epidermis, while the treated patient shows some hypoplasia and a mild hyperkeratosis. The treated models are as expected, while the non-treated models are not as expected. These differences can be due to the age of the keratinocytes used for the models, as models can differ from each other if keratinocytes are in high passages or if they start to differentiate.

Despite H&E staining shows that the morphology of the diseased model is slightly different to the morphology of the control skin model, assessment of epidermal markers like K14 and K10 in immunohistochemistry stainings carried out by one of our colleagues, reveals that their expression was optima as they were correctly distributed through all the models. Therefore, the keratinocyte differentiation was in accordance with what it was expected, as K14 expression was present in the basal layer, and K10 in the supra basal layer. When comparing with human skin, the expression for some markers like K14 was less well-defined for the 3D skin equivalents.

Keratins are the principal components of the intermediate filament cytoskeleton in epithelial cells. K14 is expressed in the mitotically active basal cells, but when cells enter the terminal differentiation, it is substituted by K10 (Santos et al., 2002). Barker et al. (2004) showed the expression patterns of K10 in all supra basal layers. Similar results were obtained by Jung et al. (2014), who presented K14 expression in the basal layer, and K10 expression in the supra basal keratinocyte layer of the KeraSkinTM-VM model, showing an extended staining for these keratins through all layers. Ojeh et al. (2017) also revealed K14 expression in the basal layer of the epidermis, while K10 expression was in the supra basal layer.

When staining with TGase1 antibody, a clear difference is shown comparing control and diseased skin models. As expected, the expression of the TGase1 in diseased models was lower than in the control equivalents, which expressed an active membrane-bound TGase1 in the upper layers of the epidermis. These differences are due to *TGMI* mutation in the diseased skin models, which means that because *TGMI* is mutated, a lower or no expression is going to be shown after stainings. This was also observed by Aufenvenne et al.'s research (2013), who showed a defeat of activity stainings in models generated from TGase1-deficient skin. Akiyama

et al. (2010) carried out studies with 4 patients with lamellar ichthyosis caused by *TGMI*. Only the two patients with missense mutations and mild hyperkeratosis showed TGase1 staining and activity.

In conclusion, 3D skin models were successfully constructed and characterised by histology, and gene expression and for their functional barrier (by a colleague from the group, results not shown) to demonstrate the equivalency to *in vivo* conditions.

However, it has to be taken in consideration that the construction of 3D skin models is challenging. One of the main issues has been the undesirable differentiation of keratinocytes when cultured in 2D monolayers without feeder cells before transferring them onto the fibroblast/collagen matrix for building 3D skin models. This influenced the structure of the models, because when keratinocytes are not basal keratinocytes, the model does not grow as desirable. This was shown by Carlson et al. (2008), whose group carried out the development of 3D human skin equivalents of normal and diseased skin. Carlson et al. (2008) also indicated that despite nearly all keratinocytes seeded onto the skin model attached to the connective tissue substrate, only those cells that were replicating grew after seeding. Keratinocytes that were differentiating also adhered to the connective tissue substrate, but they did not proliferate to form the stratified human skin equivalent. For this reason, is important to work with low passage keratinocytes, as most of the keratinocytes will grow as basal cells and with a preminent growth potential. It has also been described by Carlson et al. (2008), that with a long period of time of incubation, the uppermost layers of the epithelium began to be thicker, being the suggested period of time of incubation for 7 to 14 days.

Another notable factor that changes the quality of the 3D skin equivalents is the type of collagen that is used to fabricate the matrix, as with some of the collagen batches, a non-jellified matrix was obtained after the period of incubations in our protocol. To avoid this trouble, Carlson et al. (2008) suggest keeping on ice all the compounds needed for the construction of the collagen matrix until the gel mixture is placed onto the insert. On this way, the collagen should not prematurely precipitate.

In future evaluation of 3D skin equivalents, further differentiation markers of the skin, such as involucrin and other cytokeratins, in untreated and treated skin models should be studied. Well-developed stratum corneum can be confirmed by scanning electron microscopy. Also, markers that are known to induce or decrease TGase1 expression could be important in this study. Moreover, different doses of the TGase1/NG complex, longer treatment, potential effects of

the complex in immune responses and toxicity tests would help to understand disease and therapy mechanisms. To achieve this, Haneda et al. (2016), for example, analysed gene expression of wildtype and *TGMI* ^{-/-} epidermis using microarrays to observe genes involved in innate immune system such as some cytokines or G-CSF, but cytokines and chemokines can also be analysed by ELISA. Cellular viability of 2D and 3D cultured keratinocytes and cytotoxicity can be assessed by MTT. Flow cytometry can be used to study the extent of apoptosis and necrosis in response to the nanocarrier. Also, to test dermal toxicity in 3D skin equivalents protocols like the one described by Jung et al. (2014) could be tested. To test skin irritation, Jung et al. (2014) unpacked the tissues on delivery and transferred them into 6 well plates with culture medium to expose the tissues to the chemicals. D-PBS and SDS were used as negative and positive control, respectively. After incubation with the test materials, tissues were treated with MTT. Afterwards, Formazan extraction was carried out before optical density was measured (Jung et al., 2014). Finally, to evaluate DNA lesions, an alkaline single-cell gel electrophoresis can be assessed.

In addition, as we did with the studies of RNA level in keratinocytes grown in a 2D monolayer, we wanted to compare human skin models with skin models built by porcine keratinocytes and fibroblasts. Pig skin has been used in previous studies as models for wound healing, transdermal penetration and delivery, radiation and UV effects, and dermal toxicology (Abd et al., 2016). However, no literature concerning 3D skin equivalents from porcine skin samples have been found.

To accomplish this, we obtained tissue samples from a Spanish abattoir for the isolation of skin cells. The first samples that we obtained were old, and even if we isolated them and left in culture for 14 days, no cells grew. More skin samples were acquired from the same slaughterhouse, and after isolation, only keratinocytes grew in culture. Afterwards, more samples were received, but all them arrived contaminated. We hypothesized that this was due to shipment conditions. Despite precautions were taken to keep the samples between 2 and 8°C, as instructed by manufacturer guidelines, the exceptional and unforeseeable high temperatures affected the medium temperature raising it over the recommended storage temperature. We proceed with the extraction of the skin cells, as we needed fibroblasts to perform the skin models on the same way we constructed the human skin equivalents, but no fibroblasts grew, so we could not build the 3D skin models from pig samples.

One of the issues were the contaminations obtained when extracting skin cells (keratinocytes and fibroblasts). Apart from the high temperatures during the transport of the samples, this could be also explained by the fact that skin biopsy conditions were not done in sterile conditions like in humans (in a surgery room with sterile instruments). Before the animal was slaughtered, a skin sample was biopsied with non-sterile instruments and in a non-sterile room. Sample was not disinfected until it was delivered in the laboratory. Other explanation to the contaminations can be our protocol for extracting skin cells. We adapted our protocol for the isolation of fibroblasts and keratinocytes from human skin biopsies to the protocols suggested by Hengge et al. (1996) and Ponce et al. (2017) for the extraction of porcine skin cells.

In further studies, we will keep looking for local abattoirs that will be willing to provide us skin samples to avoid the long transport and reduce the risk of contamination. If the difficulties in finding local abattoirs will persist, an optimization of the transport condition, such as special packaging will be needed. Also, if samples from Spain are still been delivered, the protocol for the isolation of fibroblasts and keratinocytes should be also optimized. Thanks to the aforementioned modification in sourcing the skin samples and in the protocols, we expect the successfully extraction of skin cells from pigs, in order to develop equivalents 3D skin models. This would allow us to widen the knowledges of porcine skin and at the same time it will help us to overcome the difficulties in getting human skin samples, giving us the opportunity to better comprehend protein substitution, specifically of our TGase1/NG complex and its delivery in the epidermis, and to the development of new treatments for skin diseases.

5.4. TGase1/NG COMPLEX ENTERS THE KERATINOCYTES

We have seen that *TGMI* is expressed in our cells on RNA level, and that the TGase1/NG complex used to treat the 3D skin equivalents penetrates into the epidermis.

To assess the specific location of the recombinant protein TGase1 and the nanogel, which is the main goal of the project, keratinocytes isolated from human control biopsies, and from porcine control skin samples, were cultured in a 2D monolayer on top of coverslips. When cells were about 70% confluent, cells were treated with the 2% labelled TGase1 (Alexa Fluor® 488)/NG (Rhodamin) complex (50 µg nanogel loaded with 1 µg TGase1) either for 3 hours or 24 hours. After incubation times, cells were either stained with LysoTracker Deep Red for posterior fixation, as LysoTracker Deep Red is a fluorescent dye which application has to be

performed in live cells, or directly fixated with ice-cold methanol for immunohistochemistry. After a succession of washes, permeabilization, and blocking, cells were incubated with the primary antibody (anti GM130, anti E-cadherin or anti EEA1). Anti GM130 is a specific marker for Golgi, anti E-cadherin tracks the membrane, anti EEA1 detects the endoplasmic reticulum, and LysoTracker Deep Red shows the lysosomes. After incubation overnight, cells were incubated with the secondary antibody (Alexa Fluor® 633) and counterstained with DAPI (to stain the nuclei) for the visualisation under the confocal microscope.

The confocal fluorescence microscope can remove blur from outside of the focal plane of the image (Jonkman and Brown, 2015). Confocal microscopy is an optimal imaging technique that scans a focused point of light around a sample to reconstruct an image in a point-by-point manner. For the detection, a pinhole is used, increasing the resolution and contrast compared to wide field illumination. Researchers have used the different confocal microscopies for skin imaging (Calzavara-Pinton et al., 2008; Gareau, 2011; Rodríguez-Leyva et al., 2014). Rodríguez-Leyva et al. (2014), for example, analysed keratinocytes from skin samples with a confocal laser scanning microscope.

We analysed our samples with a Zeiss LSM 800, a confocal laser scanning microscope, observing that TGase1, as well as the nanogel, enters the keratinocytes (Figure 18-25). When human and pig cells were stained with anti E-cadherin, anti EEA1, anti GM130, and LysoTracker Deep Red (Figure 18 and 22, 19 and 23, 20 and 24, and 21 and 25, respectively), TGase1 and nanogel seem to be associated to the membrane, but also to be in the cytoplasm, in each of those organelles. This could be due to the fact that TGase1 is also present in proliferating cells and in intact or proteolytically processed cytosolic or membrane-anchored forms. For this reason, our findings suggest that TGase1 and nanogel are present in cytosol, as well as in plasma membrane.

Steinert et al. (1996) showed that the location of TGase1 in cytosol or in membrane is influenced by myristate and palmitate modifications. During TGase1 synthesis, it is N-myristoylated, and in proliferating or differentiating cells, it is modified. Candi et al. (1998) suggested that TGase1 is an enzyme presented also as both forms, cytosolic and membrane-bound. In addition, TGase1 is involved in the catalysing of lysine crosslinking of precursor proteins during the formation of the cytoplasmic layer of the cornified cell envelope (Herman et al., 2009). Therefore, our results seem to corroborate the location of TGase1 in cytosol and in membrane.

The fluorescent signal of rhodamine appears always to be stronger than Alexa Fluor® 488 signal, which is due to a 2% TGase solution in the nanogel.

When the human keratinocytes were treated for 3 hours, TGase1/NG complex seems to be located around the nuclei, in the cytoplasm, and associated to membrane, as well as when cells were treated for 24 hours. Same results are shown for pig keratinocytes. Also, we can see that the TGase1 has a different distribution pattern through the cells when comparing to the nanogel, which means that the TGase1 is released from the nanogel PNIPAM-dPG.

In addition, senescent cell appearance was shown mainly in human primary keratinocytes after 24 hours of the treatment. This suggests that treatment could be causing senescence on the cells. However, nearly no senescence was shown in pig primary keratinocytes, therefore the senescent cell appearance could be also due to the age of the cells, as human primary keratinocytes were relatively older than the pig keratinocytes. Despite these differences, replicates of the experiment with cells of the same passage and more time points should be carried out to finally understand the treatment.

Atypical distribution of some antibodies such as lysotracker and anti E-cadherin were observed for both human and pig primary keratinocytes. This can be due to a wrong concentration of the reagents used. Other antibodies and concentrations should be used in future experiments to replicate these data and analyse them for a better comprehension of the cellular location of the TGase1 and nanogel.

To avoid senescence in future experiments, cells can be treated with the TGase1/NG when they are about 50% confluent. Also, different concentrations and time points of the protein and the nanogel could be used to compare the effect of the treatment on the cells when more or less protein is added. Furthermore, optimisation of the antibody concentrations would be an important step to further understand the TGase1/NG location in the cells.

Gerecke et al. (2017) carried out studies with the PNIPAM-dPG for 3 hours, 24 hours, and 48 hours incubation times showing intracellular localization in keratinocytes, corroborating our findings. Also, their stains, and ours using LysoTracker Deep Red, indicated strong colocalization of the nanogel with lysosomal compartments when cells are exposed to a long incubation times, which was mentioned too by Iversen, Skotland and Sandvig in 2011. This reveals that the final or major part of the intracellular fate of the nanogels in HaCaT cells and keratinocytes are the lysosomes. Rancan et al. (2017) carried out studies with intact and

disrupted skin barrier, indicating that the nanogel is capable of penetrating to deeper layers of the stratum corneum, and also in the viable epidermis and dermis when the skin barrier was disrupted. They also showed that the nanogel enters the keratinocytes and HaCaT cells, therefore in line with other studies mentioned.

Because TGase1 has been shown to be membrane-associated and expressed in the epidermis, specifically in the granular layer (Kim et al. 1995; Jeon, Dijan and Green, 1998), Aufenvenne et al. (2013) developed sterically stabilized liposomes with encapsulated recombinant human TGase1, equipped with a highly cationic lipopeptide, showing the delivery of the TGase1 in the keratinocyte's plasma membrane as a causative therapy for ARCI. However, liposomes can be unstable under environmental stress, while PNIPAm is soluble at room temperature but its phase separates at body temperature (Calderon et al., 2010; Cuggino et al., 2011).

To further evaluate tracking of TGase1 and PNIPAM-dPG nanogel, transmission electron microscopy can be used. In this microscopy technique a beam of electrons is transmitted through a specimen to form an image. For that, immunogold labelling and stainings can be carried out and images can be compared to the ones obtained with confocal microscopy. Also, other microscopy technique is atomic force microscopy, a very-high-resolution type of scanning probe microscopy that provide images of atoms on or in surfaces.

In addition, other markers can be evaluated in pig and human keratinocytes, to keep comparing them, as there is not so much literature concerning them. Protein expression and location could be analysed by flow cytometry. Also, the study of all these markers with keratinocytes isolated from ARCI-patients would allow us to understand the fate of the PNIPAM-dPG nanogel and TGase1.

5.5. PIG SKIN EXPLANTS

Because small skin samples can be propagated in culture with the advantage of that all type of cells from the skin are present in the skin explant (Mathes, Ruffner and Graf-Hausner, 2014), we planned on carrying out studies to test our therapeutic TGase1 in *ex vivo* conditions, in skin explants. Due to the obstacles for obtaining human skin samples, we opted for culturing porcine skin explants. We wanted to culture the skin explants for 13 days, the same period of time as 3D skin equivalents were in culture and compare untreated and treated skin explants by harvesting and posterior immunohistochemistry and immunocytochemistry. Skin explants

were going to be treated with 2% of labelled TGase1/NG, the same concentration used for the skin models. Pig skin explants were first cultured for 13 days, with no TGase1/NG treatment, but no signals of skin explant growing were observed. Some changes were expected, for example observable modifications in the colour medium when the culture medium was not changed for a couple of days, which means that explants need more nutrients; therefore a medium change, as literature for human skin equivalents suggest changing medium every other day (Varani et al., 2007). This was due to the fact that samples were old, and/or they were treated and processed before slaughtering.

In consequence, obtaining skin samples became a challenge influencing our research as previously mentioned.

In future studies, other sources and optimization of the transport conditions will be evaluated. In addition, with skin explants in culture, paraffined sections from human or porcine skin explants can be stained with HE to evaluate the morphology, followed by qualitative analysis, and compare it with the 3D skin equivalents constructed. Immunohistochemistry experiments with TGase1, keratins, and other markers involved in differentiation should be tested. With human and porcine explants, we can also evaluate the depth of penetration of the TGase1/NG complex. Characterising skin explants will give us a more accurate knowledge of the therapy.

6. CONCLUSION

ARCI is a rare and severe skin disease marked by genetic heterogenicity, and with no causative treatments available, making a targeted therapy extremely necessary.

Different expression markers involved in ARCI were analysed in keratinocytes isolated from human controls and ARCI-patients with mutation in *TGMI*, and keratinocytes extracted from porcine skin samples on RNA level. After observing expression of *TGMI* on RNA level for all samples, we constructed three-dimensional skin models to successfully characterize control and *TGMI* patient 3D skin models using haematoxylin and eosin stainings, and immunohistochemical stainings. We also tested the fate of PNIPAM-dPG, a thermosensitive nanocarrier optimal for delivering proteins in the epidermis, developed by our group. This nanocarrier was labelled together with TGase1 for the detection of its delivery in the skin.

After confirmation of the delivery of TGase1 in the skin, we confirmed using confocal microscopy that TGase1, as well as the nanogel, enters the keratinocytes. After 3 hours and 24 hours treatment, the complex is located around the nuclei, therefore not toxicity should be detected, in the cytoplasm and in the plasma membrane for both porcine and human keratinocytes.

To summarize, we provide new results not previously shown in the literature to contribute the overall goal of developing therapeutic approaches using protein replacement. We therefore corroborate the expression of differentiation markers involved in ARCI in human differentiated keratinocytes and in treated and untreated ARCI-patient cells, and we propose some results concerning the expression of those genes in pig differentiated keratinocytes. In addition, we present some analysis concerning the expression of some keratins and TGase1 in developed 3D skin models from control samples. Furthermore, we add new data indicating the organelle location of TGase1 and PNIPAM-dPG nanocarrier in keratinocytes derived from human and porcine control skin samples, contributing to the main objective of this project. And finally, it has to be mentioned the not achievement of *ex vivo* data due to already mentioned issues.

However, further studies to confirm this and to establish the protein substitution for ARCI patients are important steps to be taken in consideration. Examples of these studies are the evaluation of differentiation markers of the skin in untreated and treated healthy and diseased primary keratinocytes grown in a 2D monolayer, in control and diseased skin models, and in skin explants. Different doses and longer treatment should also be tested to determine optimal

delivery conditions. It is also important to analyse the depth of penetration of the TGase1/NG complex, and its possible toxic effects through toxicity experiments such as MTT assay or flow cytometry to study apoptosis. Specifically, to study the depth of penetration, obtaining skin explants would be very important, as it would provide us more accurate results. Finally, we would also like to look at the potential effects of the therapeutic complex in immune responses, as it has been seen in previous studies (Haneda et al., 2016) that in *TGMI* ^{-/-} epidermis the expression of genes involved in innate immune system is increased. This can be assess using microarrays. In addition, studies with different cell lines for both control and patient samples, and executing the experiments with replicates, would be very important points to be taken in consideration. Different microscopy techniques such as Atomic force microscopy, transmission electron microscopy, and confocal microscopy will be also used to track the therapeutic protein TGase1 and the nanocarrier.

The work presented in this thesis provides a better comprehension of a possible new protein replacement therapy for ARCI patients with *TGMI* mutations, as we provide new results concerning the tracking of the delivery of the TGase1/PNIPAM-dPG complex. Furthermore, this strategy could be used to develop further therapeutic approaches for other proteins that are defective in other cases of ARCI or even other monogenic skin diseases.

7. BIBLIOGRAPHY

Abd, E., Yousef, S. A., Pastore, M. N., Telaprolu, K., Mohammed, Y. H., Namjoshi, S., ... & Roberts, M. S. (2016). Skin models for the testing of transdermal drugs. *Clinical pharmacology: advances and applications*, 8, 163.

Abdallah, M. A. E., Pawar, G., & Harrad, S. (2015). Evaluation of 3D-human skin equivalents for assessment of human dermal absorption of some brominated flame retardants. *Environment international*, 84, 64-70.

Ackermann, K., Borgia, S. L., Korting, H. C., Mewes, K. R., & Schäfer-Korting, M. (2010). The Phenion® full-thickness skin model for percutaneous absorption testing. *Skin pharmacology and physiology*, 23(2), 105-112.

Ahn, A. C., & Kaptchuk, T. J. (2011). Spatial anisotropy analyses of subcutaneous tissue layer: potential insights into its biomechanical characteristics. *Journal of anatomy*, 219(4), 515-524.

Akbari, M. T., & Ataei-Kachoui, M. (2015). Triallelic Inheritance of TGM1 and ALOXE3 Mutations Associated with Severe Phenotype of Ichthyosis in an Iranian Family-A Case Report. *Iranian journal of public health*, 44(7), 1004.

Akiyama, M. (2010). ABCA12 mutations and autosomal recessive congenital ichthyosis: A review of genotype/phenotype correlations and of pathogenetic concepts. *Human mutation*, 31(10), 1090-1096.

Akiyama, M. (2011). Updated molecular genetics and pathogenesis of ichthyoses. *Nagoya journal of medical science*, 73(3-4), 79.

Akiyama, M., Sakai, K., Yanagi, T., Fukushima, S., Ihn, H., Hitomi, K., & Shimizu, H. (2010). Transglutaminase1 preferred substrate peptide K5 is an efficient tool in diagnosis of lamellar ichthyosis. *The American journal of pathology*, 176(4), 1592-1599.

Akiyama, M., Sawamura, D., & Shimizu, H. (2003). The clinical spectrum of nonbullous congenital ichthyosiform erythroderma and lamellar ichthyosis. *Clinical and Experimental Dermatology: Experimental Dermatology*, 28(3), 235-240.

Akiyama, M., Sugiyama-Nakagiri, Y., Sakai, K., McMillan, J. R., Goto, M., Arita, K., ... & Sawamura, D. (2005). Mutations in lipid transporter ABCA12 in harlequin ichthyosis and

functional recovery by corrective gene transfer. *The Journal of clinical investigation*, 115(7), 1777-1784.

Alberts, B., Johnson, A., Lewis, J., Raff, M., Roberts, K., & Walter, P. (2002). Fibroblasts and their transformations: the connective-tissue cell family.

Al-Naamani, A., Al-Waily, A., Al-Kindi, M., Al-Awadi, M., & Al-Yahyaee, S. A. (2013). Transglutaminase-1 mutations in Omani families with lamellar ichthyosis. *Medical Principles and Practice*, 22(5), 438-443.

Andrade, T. A., Aguiar, A. F., Guedes, F. A., Leite, M. N., Caetano, G. F., Coelho, E. B., ... & Frade, M. A. (2015). Ex vivo model of human skin (hOSEC) as alternative to animal use for cosmetic tests. *Procedia Engineering*, 110, 67-73.

Annilo, T., Shulenin, S., Chen, Z. Q., Arnould, I., Prades, C., Lemoine, C., ... & Rosier, M. (2002). Identification and characterization of a novel ABCA subfamily member, ABCA12, located in the lamellar ichthyosis region on 2q34. *Cytogenetic and genome research*, 98(2-3), 169-176.

Arda, O., Göksügür, N., & Tüzün, Y. (2014). Basic histological structure and functions of facial skin. *Clinics in dermatology*, 32(1), 3-13.

Aufvenne, K., Larcher, F., Hausser, I., Duarte, B., Oji, V., Nikolenko, H., ... & Traupe, H. (2013). Topical enzyme-replacement therapy restores transglutaminase 1 activity and corrects architecture of transglutaminase-1-deficient skin grafts. *The American Journal of Human Genetics*, 93(4), 620-630.

Aufvenne, K., Rice, R. H., Hausser, I., Oji, V., Hennies, H. C., Del Rio, M., ... & Larcher, F. (2012). Long-term faithful recapitulation of transglutaminase 1-deficient lamellar ichthyosis in a skin-humanized mouse model and insights from proteomic studies. *The Journal of investigative dermatology*, 132(7), 1918.

Avon, S. L., & Wood, R. E. (2005). Porcine skin as an in-vivo model for model for ageing of human bite marks. *J. Forensic Odontostomatol*, 23, 30-39.

Barker, C. L., McHale, M. T., Gillies, A. K., Waller, J., Pearce, D. M., Osborne, J., ... & Pringle, J. H. (2004). The development and characterization of an in vitro model of psoriasis. *Journal of investigative dermatology*, 123(5), 892-901.

- Bartnik, F. G., Pittermann, W. F., Mendorf, N., Tillman, U., & Künstler, K. (1990). Skin organ culture for the study of skin irritancy. *Toxicology in vitro*, 4(4-5), 293-301.
- Bastaki, F., Mohamed, M., Nair, P., Saif, F., Mustafa, E. M., Bizzari, S., ... & Hamzeh, A. R. (2017). Summary of mutations underlying autosomal recessive congenital ichthyoses (ARCI) in Arabs with four novel mutations in ARCI-related genes from the United Arab Emirates. *International journal of dermatology*, 56(5), 514-523.
- Binamer, Y. (2016). Ichthyin (NIPAL4)-autosomal recessive congenital ichthyosis with atopic diathesis: *Case report and literature review. Journal of Dermatology & Dermatologic Surgery*, 20(1), 55-57.
- Boer, M., Duchnik, E., Maleszka, R., & Marchlewicz, M. (2016). Structural and biophysical characteristics of human skin in maintaining proper epidermal barrier function. *Advances in Dermatology and Allergology/Postępy Dermatologii i Alergologii*, 33(1), 1.
- Calderón, M., Quadir, M. A., Sharma, S. K., & Haag, R. (2010). Dendritic polyglycerols for biomedical applications. *Advanced materials*, 22(2), 190-218.
- Calzavara-Pinton, P., Longo, C., Venturini, M., Sala, R., & Pellacani, G. (2008). Reflectance confocal microscopy for in vivo skin imaging. *Photochemistry and photobiology*, 84(6), 1421-1430.
- Candi, E., Melino, G., Lahm, A., Ceci, R., Rossi, A., Kim, I. G., ... & Steinert, P. M. (1998). Transglutaminase 1 Mutations in Lamellar Ichthyosis LOSS OF ACTIVITY DUE TO FAILURE OF ACTIVATION BY PROTEOLYTIC PROCESSING. *Journal of Biological Chemistry*, 273(22), 13693-13702.
- Candi, E., Schmidt, R., & Melino, G. (2005). The cornified envelope: a model of cell death in the skin. *Nature reviews Molecular cell biology*, 6(4), 328.
- Carlson, M. W., Alt-Holland, A., Egles, C., & Garlick, J. A. (2008). Three-dimensional tissue models of normal and diseased skin. *Current protocols in cell biology*, 41(1), 19-9.
- Chatzinikolaidou, M. (2016). Cell spheroids: the new frontiers in in vitro models for cancer drug validation. *Drug discovery today*, 21(9), 1553-1560.

- Cichorek, M., Wachulska, M., Stasiewicz, A., & Tymińska, A. (2013). Skin melanocytes: biology and development. *Advances in Dermatology and Allergology/Postępy Dermatologii I Alergologii*, 30(1), 30.
- Craiglow, B. G. (2013, February). Ichthyosis in the newborn. *In Seminars in perinatology* (Vol. 37, No. 1, pp. 26-31). Elsevier.
- Cuggino, J. C., Strumia, M. C., Welker, P., Licha, K., Steinhilber, D., Mutihac, R. C., & Calderón, M. (2011). Thermosensitive nanogels based on dendritic polyglycerol and N-isopropylacrylamide for biomedical applications. *Soft Matter*, 7(23), 11259-11266.
- Dahlqvist, J., Klar, J., Hausser, I., Anton-Lamprecht, I., Pigg, M. H., Gedde-Dahl, T., ... & Dahl, N. (2007). Congenital Ichthyosis: mutations in ichthyin associated with specific structural abnormalities in the granular layer of epidermis. *Journal of medical genetics*.
- Dame, M. K., Paruchuri, T., DaSilva, M., Bhagavathula, N., Ridder, W., & Varani, J. (2009). The Göttingen minipig for assessment of retinoid efficacy in the skin: comparison of results from topically treated animals with results from organ-cultured skin. *In Vitro Cellular & Developmental Biology-Animal*, 45(9), 551-557.
- Dick, A., Tantcheva-Poór, I., Oji, V., Giehl, K. A., Fischer, J., Krieg, P., ... & Rauh, M. (2017). Diminished protein-bound ω -hydroxylated ceramides in the skin of patients with ichthyosis with 12R-lipoxygenase (LOX) or eLOX-3 deficiency. *British Journal of Dermatology*, 177(4), e119-e121.
- DiGiovanna, J. J., & Robinson-Bostom, L. (2003). Ichthyosis. *American journal of clinical dermatology*, 4(2), 81-95.
- DiGiovanna, J. J., Mauro, T., Milstone, L. M., Schmuth, M., & Toro, J. R. (2013). Systemic retinoids in the management of ichthyoses and related skin types. *Dermatologic therapy*, 26(1), 26-38.
- Dökmeci-Emre, S., Taşkıran, Z. E., Yüzbaşıoğlu, A., Önal, G., Akarsu, A. N., Karaduman, A., & Özgüç, M. (2017). Identification of two novel PNPLA1 mutations in Turkish families with autosomal recessive congenital ichthyosis. *The Turkish journal of pediatrics*, 59(4).

Duque-Fernandez, A., Gauthier, L., Simard, M., Jean, J., Gendreau, I., Morin, A., ... & Pouliot, R. (2016). A 3D-psoriatic skin model for dermatological testing: The impact of culture conditions. *Biochemistry and biophysics reports*, 8, 268-276.

Eaglstein, W. H., & Mertz, P. M. (1978). New method for assessing epidermal wound healing: the effects of triamcinolone acetonide and polyethelene film occlusion. *Journal of Investigative Dermatology*, 71(6).

Eckert, R. L., & Rorke, E. A. (1989). Molecular biology of keratinocyte differentiation. *Environmental health perspectives*, 80, 109.

Eckert, R. L., Sturniolo, M. T., Broome, A. M., Ruse, M., & Rorke, E. A. (2005). Transglutaminase function in epidermis. *Journal of Investigative Dermatology*, 124(3), 481-492.

Eckl, K. M., Alef, T., Torres, S., & Hennies, H. C. (2011). Full-thickness human skin models for congenital ichthyosis and related keratinization disorders. *The Journal of investigative dermatology*, 131(9), 1938-42.

Eckl, K. M., De Juanes, S., Kurtenbach, J., Nätebus, M., Lugassy, J., Oji, V., ... & Harel, A. (2009). Molecular analysis of 250 patients with autosomal recessive congenital ichthyosis: evidence for mutation hotspots in ALOXE3 and allelic heterogeneity in ALOX12B. *Journal of Investigative Dermatology*, 129(6), 1421-1428.

Eckl, K. M., Krieg, P., Küster, W., Traupe, H., André, F., Wittstruck, N., ... & Hennies, H. C. (2005). Mutation spectrum and functional analysis of epidermis-type lipoxygenases in patients with autosomal recessive congenital ichthyosis. *Human mutation*, 26(4), 351-361.

Eckl, K. M., Tidhar, R., Thiele, H., Oji, V., Hausser, I., Brodesser, S., ... & Becker, K. (2013). Impaired epidermal ceramide synthesis causes autosomal recessive congenital ichthyosis and reveals the importance of ceramide acyl chain length. *Journal of Investigative Dermatology*, 133(9), 2202-2211.

Edmondson, R., Broglie, J. J., Adcock, A. F., & Yang, L. (2014). Three-dimensional cell culture systems and their applications in drug discovery and cell-based biosensors. *Assay and drug development technologies*, 12(4), 207-218.

- El Ghalbzouri, A., Commandeur, S., Rietveld, M. H., Mulder, A. A., & Willemze, R. (2009). Replacement of animal-derived collagen matrix by human fibroblast-derived dermal matrix for human skin equivalent products. *Biomaterials*, 30(1), 71-78.
- Elias, P. M., Gruber, R., Crumrine, D., Menon, G., Williams, M. L., Wakefield, J. S., ... & Uchida, Y. (2014). Formation and functions of the corneocyte lipid envelope (CLE). *Biochimica et Biophysica Acta (BBA)-Molecular and Cell Biology of Lipids*, 1841(3), 314-318.
- Enomoto, K., Enomoto, Y., Ishii, Y., Araie, M., & Kanda, T. (2003). Genes up-or down-regulated by expression of keratinocyte-specific POU transcription factor hSkn-1a. *Biochemical and biophysical research communications*, 303(2), 580-585.
- Epp, N., Fürstenberger, G., Müller, K., de Juanes, S., Leitges, M., Hausser, I., ... & Krieg, P. (2007). 12R-lipoxygenase deficiency disrupts epidermal barrier function. *The Journal of cell biology*, 177(1), 173-182.
- Falany, C. N., He, D., Dumas, N., Frost, A. R., & Falany, J. L. (2006). Human cytosolic sulfotransferase 2B1: isoform expression, tissue specificity and subcellular localization. *The Journal of steroid biochemistry and molecular biology*, 102(1-5), 214-221.
- Farasat, S., Wei, M. H., Liewehr, D. J., Herman, M., Steinberg, S. M., Bale, S., ... & Toro, J. (2008). Novel Transglutaminase-1 mutations and genotype-phenotype investigations of 104 patients with autosomal recessive congenital ichthyosis in the United States. *Journal of medical genetics*.
- Fennema, E., Rivron, N., Rouwkema, J., van Blitterswijk, C., & de Boer, J. (2013). Spheroid culture as a tool for creating 3D complex tissues. *Trends in biotechnology*, 31(2), 108-115.
- Fischer, J. (2009). Autosomal recessive congenital ichthyosis. *Journal of investigative dermatology*, 129(6), 1319-1321.
- Fischer, J., Faure, A., Bouadjar, B., Blanchet-Bardon, C., Karaduman, A., Thomas, I., ... & Prud'homme, J. F. (2000). Two new loci for autosomal recessive ichthyosis on chromosomes 3p21 and 19p12-q12 and evidence for further genetic heterogeneity. *The American Journal of Human Genetics*, 66(3), 904-913.

- Fore, J. (2006). A review of skin and the effects of aging on skin structure and function. *Ostomy/wound management*, 52(9), 24-35.
- Frade, M. A. C., Andrade, T. A. M. D., Aguiar, A. F. C. L., Guedes, F. A., Leite, M. N., Passos, W. R., ... & Das, P. K. (2015). Prolonged viability of human organotypic skin explant in culture method (hOSEC). *Anais brasileiros de dermatologia*, 90(3), 347-350.
- Fradette, J., Larouche, D., Fugère, C., Guignard, R., Beauparlant, A., Couture, V., ... & Roy, A. (2003). Normal human Merkel cells are present in epidermal cell populations isolated and cultured from glabrous and hairy skin sites. *Journal of investigative dermatology*, 120(2), 313-317.
- Fujita, A. K. L., da Rocha, R. W., Escobar, A., de Nardi, A. B., Bagnato, V. S., & de Menezes, P. F. C. (2018). Correlation between Porcine and Human Skin Models by Optical Methods.
- Gareau, D. S. (2011). Automated identification of epidermal keratinocytes in reflectance confocal microscopy. *Journal of biomedical optics*, 16(3), 030502.
- Gelse, K., Pöschl, E., & Aigner, T. (2003). Collagens—structure, function, and biosynthesis. *Advanced drug delivery reviews*, 55(12), 1531-1546.
- Gerecke, C., Edlich, A., Giulbudagian, M., Schumacher, F., Zhang, N., Said, A., ... & Ma, N. (2017). Biocompatibility and characterization of polyglycerol-based thermoresponsive nanogels designed as novel drug-delivery systems and their intracellular localization in keratinocytes. *Nanotoxicology*, 11(2), 267-277.
- Gilbert, S. F. (2000). The epidermis and the origin of cutaneous structures. *Developmental biology*, 6.
- Glick, J. B., Craiglow, B. G., Choate, K. A., Kato, H., Fleming, R. E., Siegfried, E., & Glick, S. A. (2016). Improved management of harlequin ichthyosis with advances in neonatal intensive care. *Pediatrics*, e20161003.
- Grall, A., Guaguère, E., Planchais, S., Grond, S., Bourrat, E., Hausser, I., ... & Lagoutte, L. (2012). PNPLA1 mutations cause autosomal recessive congenital ichthyosis in golden retriever dogs and humans. *Nature genetics*, 44(2), 140.

- Grond, S., Eichmann, T. O., Dubrac, S., Kolb, D., Schmuth, M., Fischer, J., ... & Lass, A. (2017). PNPLA1 deficiency in mice and humans leads to a defect in the synthesis of omega-O-acylceramides. *Journal of Investigative Dermatology*, 137(2), 394-402.
- Gruber, R., Rainer, G., Weiss, A., Udvardi, A., Thiele, H., Eckl, K. M., ... & Volc-Platzer, B. (2017). Morphological alterations in two siblings with autosomal recessive congenital ichthyosis associated with CYP 4F22 mutations. *British Journal of Dermatology*, 176(4), 1068-1073.
- Gutierrez, K., Dicks, N., Glanzner, W. G., Agellon, L. B., & Bordignon, V. (2015). Efficacy of the porcine species in biomedical research. *Frontiers in genetics*, 6, 293.
- Hainzl, S., Peking, P., Kocher, T., Murauer, E. M., Larcher, F., Del Rio, M., ... & Reichelt, J. (2017). COL7A1 editing via CRISPR/Cas9 in recessive dystrophic epidermolysis bullosa. *Molecular Therapy*, 25(11), 2573-2584.
- Haneda, T., Imai, Y., Uchiyama, R., Jitsukawa, O., & Yamanishi, K. (2016). Activation of molecular signatures for antimicrobial and innate defense responses in skin with transglutaminase 1 deficiency. *PloS one*, 11(7), e0159673.
- Hengge, U. R., Chan, E. F., Hampshire, V., Foster, R. A., & Vogel, J. C. (1996). The derivation and characterization of pig keratinocyte cell lines that retain the ability to differentiate. *Journal of investigative dermatology*, 106(2).
- Herman, M. L., Farasat, S., Steinbach, P. J., Wei, M. H., Toure, O., Fleckman, P., ... & Toro, J. R. (2009). Transglutaminase-1 gene mutations in autosomal recessive congenital ichthyosis: summary of mutations (including 23 novel) and modeling of TGase-1. *Human mutation*, 30(4), 537-547.
- Herron, A. J. (2009, December). Pigs as dermatologic models of human skin disease. In *Proceeding of the ACVP/ASVCP Concurrent Annual Meetings December* (pp. 5-9).
- Hovnanian, A. (2005). Harlequin ichthyosis unmasked: a defect of lipid transport. *The Journal of clinical investigation*, 115(7), 1708-1710.
- Iizuka, R., Chiba, K., & Imajoh-Ohmi, S. (2003). A novel approach for the detection of proteolytically activated transglutaminase 1 in epidermis using cleavage site-directed antibodies. *Journal of investigative dermatology*, 121(3), 457-464.

- Israeli, S., Khamaysi, Z., Fuchs-Telem, D., Nousbeck, J., Bergman, R., Sarig, O., & Sprecher, E. (2011). A mutation in LIPN, encoding epidermal lipase N, causes a late-onset form of autosomal-recessive congenital ichthyosis. *The American Journal of Human Genetics*, 88(4), 482-487.
- Iversen, T. G., Skotland, T., & Sandvig, K. (2011). Endocytosis and intracellular transport of nanoparticles: present knowledge and need for future studies. *Nano Today*, 6(2), 176-185.
- Jacobi, U., Kaiser, M., Toll, R., Mangelsdorf, S., Audring, H., Otberg, N., ... & Lademann, J. (2007). Porcine ear skin: an in vitro model for human skin. *Skin Research and Technology*, 13(1), 19-24.
- Jacobs, J. J., Lehé, C., Cammans, K. D., Das, P. K., & Elliott, G. R. (2000). Methyl green-pyronine staining of porcine organotypic skin explant cultures: an alternative model for screening for skin irritants. *Alternatives to laboratory animals: ATLA*, 28(2), 279-292.
- Jaitley, S., & Saraswathi, T. R. (2012). Pathophysiology of Langerhans cells. *Journal of oral and maxillofacial pathology: JOMFP*, 16(2), 239.
- Jeon, S., Djian, P., & Green, H. (1998). Inability of keratinocytes lacking their specific transglutaminase to form cross-linked envelopes: absence of envelopes as a simple diagnostic test for lamellar ichthyosis. *Proceedings of the National Academy of Sciences*, 95(2), 687-690.
- Jobard, F., Lefèvre, C., Karaduman, A., Blanchet-Bardon, C., Emre, S., Weissenbach, J., ... & Fischer, J. (2002). Lipoygenase-3 (ALOXE3) and 12 (R)-lipoygenase (ALOX12B) are mutated in non-bullous congenital ichthyosiform erythroderma (NCIE) linked to chromosome 17p13. 1. *Human Molecular Genetics*, 11(1), 107-113.
- Jonkman, J., & Brown, C. M. (2015). Any way you slice it—a comparison of confocal microscopy techniques. *Journal of biomolecular techniques: JBT*, 26(2), 54.
- Jung, K. M., Lee, S. H., Jang, W. H., Jung, H. S., Heo, Y., Park, Y. H., ... & Seok, S. H. (2014). KeraSkin™-VM: A novel reconstructed human epidermis model for skin irritation tests. *Toxicology in Vitro*, 28(5), 742-750.
- Karim, N., Murtaza, G., & Naem, M. (2017). Whole-exome sequencing identified a novel frameshift mutation in SDR9C7 underlying autosomal recessive congenital ichthyosis in a Pakistani family. *British Journal of Dermatology*, 177(5), e191-e192.

- Kataranovski, M., & Karadagic, D. (1999). Skin organ culture: a review. *ACTA DERMATOVENEROLOGICA ALPINA PANONICA ET ADRIATICA*, 8(4), 131-140.
- Khan, F., Choong, W. L., Du, Q., & Jovanovi'c, A. (2013). Real-Time RT-PCR Ct Values for Blood GAPDH Correlate with Measures of Vascular Endothelial Function in Humans. *Clinical and translational science*, 6(6), 481-484.
- Kihara, A. (2016). Synthesis and degradation pathways, functions, and pathology of ceramides and epidermal acylceramides. *Progress in lipid research*, 63, 50-69.
- Kim, S. Y., Chung, S. I., Yoneda, K., & Steinert, P. M. (1995). Expression of transglutaminase 1 in human epidermis. *Journal of investigative dermatology*, 104(2), 211-217.
- Kim, S., Choi, I. F., Quante, J. R., Zhang, L., Roop, D. R., & Koster, M. I. (2009). p63 directly induces expression of Alox12, a regulator of epidermal barrier formation. *Experimental dermatology*, 18(12), 1016-1021.
- Klicks, J., von Molitor, E., Ertongur-Fauth, T., Rudolf, R., & Hafner, M. (2017). In vitro skin three-dimensional models and their applications. *Journal of Cellular Biotechnology*, 3(1), 21-39.
- Koh, L. F., Ng, B. K., Bertrand, J., & Thierry, F. (2015). Transcriptional control of late differentiation in human keratinocytes by TA p63 and Notch. *Experimental dermatology*, 24(10), 754-760.
- Kolarsick, P. A., Kolarsick, M. A., & Goodwin, C. (2011). Anatomy and physiology of the skin. *Journal of the Dermatology Nurses' Association*, 3(4), 203-213.
- Koster, Maranke I. "p63 in skin development and ectodermal dysplasias." *Journal of Investigative Dermatology* 130.10 (2010): 2352-2358.
- Krieg, P., & Fürstenberger, G. (2014). The role of lipoxygenases in epidermis. *Biochimica et Biophysica Acta (BBA)-Molecular and Cell Biology of Lipids*, 1841(3), 390-400.
- Krieg, T., & Aumailley, M. (2011). The extracellular matrix of the dermis: flexible structures with dynamic functions. *Experimental dermatology*, 20(8), 689-695.
- Lai-Cheong, J. E., & McGrath, J. A. (2009). Structure and function of skin, hair and nails. *Medicine*, 37(5), 223-226.

- Lai-Cheong, J. E., & McGrath, J. A. (2017). Structure and function of skin, hair and nails. *Medicine*, 45(6), 347-351.
- Landmann, L. (1988). The epidermal permeability barrier. *Anatomy and embryology*, 178(1), 1-13.
- Larsen, F. G., Jakobsen, P., Larsen, C. G., Kragballe, K., & Nielsen-Kudsk, F. (1988). Pharmacokinetics of etretin and etretinate during long-term treatment of psoriasis patients. *Pharmacology & toxicology*, 62(3), 159-165.
- Layton, A. (2009). The use of isotretinoin in acne. *Dermato-endocrinology*, 1(3), 162-169.
- Lefèvre, C., Audebert, S., Jobard, F., Bouadjar, B., Lakhdar, H., Boughdene-Stambouli, O., ... & Lathrop, M. (2003). Mutations in the transporter ABCA12 are associated with lamellar ichthyosis type 2. *Human molecular genetics*, 12(18), 2369-2378.
- Leist, M., Lidbury, B. A., Yang, C., Hayden, P. J., Kelm, J. M., Ringeissen, S., ... & Stolper, G. (2012). Novel technologies and an overall strategy to allow hazard assessment and risk prediction of chemicals, cosmetics, and drugs with animal-free methods. *Altex*, 29(4), 373-388.
- Lesueur, F., Bouadjar, B., Lefevre, C., Jobard, F., Audebert, S., Lakhdar, H., ... & Saker, S. (2007). Novel mutations in ALOX12B in patients with autosomal recessive congenital ichthyosis and evidence for genetic heterogeneity on chromosome 17p13. *Journal of Investigative Dermatology*, 127(4), 829-834.
- Li, H., Vahlquist, A., & Törmä, H. (2013). Interactions between FATP4 and ichthyin in epidermal lipid processing may provide clues to the pathogenesis of autosomal recessive congenital ichthyosis. *Journal of dermatological science*, 69(3), 195-201.
- Lima, L. H., Morales, Y., & Cabral, T. (2016). Poly-N-isopropylacrylamide (pNIPAM): a reversible bioadhesive for sclerotomy closure. *International journal of retina and vitreous*, 2(1), 23.
- Liu, J., Kim, D., Brown, L. D., Madsen, T., & Bouchard, G. F. (2009, September). Comparison of human, porcine, and rodent wound healing with new miniature swine study data. In *Journal of the American association for laboratory animal science* (Vol. 48, No. 5, pp. 581-581). 9190 CRESTWYN HILLS DR, MEMPHIS, TN 38125 USA: AMER ASSOC LABORATORY ANIMAL SCIENCE.

- López, O., Cócera, M., Wertz, P. W., López-Iglesias, C., & De La Maza, A. (2007). New arrangement of proteins and lipids in the stratum corneum cornified envelope. *Biochimica et Biophysica Acta (BBA)-Biomembranes*, 1768(3), 521-529.
- Lopez-Ojeda, W., & James, W. D. (2017). *Anatomy, Skin (Integument)*.
- Louhichi, N., Hadjsalem, I., Marrakchi, S., Trabelsi, F., Masmoudi, A., Turki, H., & Fakhfakh, F. (2013). Congenital lamellar ichthyosis in Tunisia is caused by a founder nonsense mutation in the TGM1 gene. *Molecular biology reports*, 40(3), 2527-2532.
- Lucker, G. P. H., Heremans, A. M. C., Boegheim, P. J., Van de Kerkhof, P. C. M., & STEIJLIN, P. (1997). Oral treatment of ichthyosis by the cytochrome P-450 inhibitor liarozole. *British Journal of Dermatology*, 136(1), 71-75.
- Maruthappu, T., Scott, C. A., & Kelsell, D. P. (2014). Discovery in genetic skin disease: the impact of high throughput genetic technologies. *Genes*, 5(3), 615-634.
- Mashima, R., & Okuyama, T. (2015). The role of lipoxygenases in pathophysiology; new insights and future perspectives. *Redox biology*, 6, 297-310.
- Mathes, S. H., Ruffner, H., & Graf-Hausner, U. (2014). The use of skin models in drug development. *Advanced drug delivery reviews*, 69, 81-102.
- McAnulty, R. J. (2007). Fibroblasts and myofibroblasts: their source, function and role in disease. *The international journal of biochemistry & cell biology*, 39(4), 666-671.
- Meigel, W. N., Gay, S., & Weber, L. (1977). Dermal architecture and collagen type distribution. *Archives of Dermatological Research*, 259(1), 1-10.
- Mertsching, H., Weimer, M., Kersen, S., & Brunner, H. (2008). Human skin equivalent as an alternative to animal testing. *GMS Krankenhaushygiene interdisziplinär*, 3(1).
- Mestas, J., & Hughes, C. C. (2004). Of mice and not men: differences between mouse and human immunology. *The Journal of Immunology*, 172(5), 2731-2738.
- Mieremet, A., Rietveld, M., Absalah, S., van Smeden, J., Bouwstra, J. A., & El Ghalbzouri, A. (2017). Improved epidermal barrier formation in human skin models by chitosan modulated dermal matrices. *PloS one*, 12(3), e0174478.

- Min, M., Chen, X. B., Wang, P., Landeck, L., Chen, J. Q., Li, W., ... & Man, X. Y. (2017). Role of keratin 24 in human epidermal keratinocytes. *PloS one*, 12(3), e0174626.
- Mithwani, A. A., Hashmi, A., Shahnawaz, S., & Al Ghamdi, Y. (2014). Harlequin ichthyosis: a case report of prolonged survival. *BMJ case reports*, 2014, bcr2013200884.
- Moll, I., Roessler, M., Brandner, J. M., Eispert, A. C., Houdek, P., & Moll, R. (2005). Human Merkel cells—aspects of cell biology, distribution and functions. *European journal of cell biology*, 84(2-3), 259-271.
- Moran, J. L., Qiu, H., Turbe-Doan, A., Yun, Y., Boeglin, W. E., Brash, A. R., & Beier, D. R. (2007). A mouse mutation in the 12R-lipoxygenase, Alox12b, disrupts formation of the epidermal permeability barrier. *Journal of Investigative Dermatology*, 127(8), 1893-1897.
- Mortazavi, H., Aghazadeh, N., Ghiasi, M., & Lajevardi, V. (2013). A review of three systemic retinoids in dermatology: acitretin, isotretinoin and bexarotene. *Iranian Journal of Dermatology*.
- Mukherjee, S., Date, A., Patravale, V., Korting, H. C., Roeder, A., & Weindl, G. (2006). Retinoids in the treatment of skin aging: an overview of clinical efficacy and safety. *Clinical interventions in Aging*, 1(4), 327.
- Murphy, S. V., & Atala, A. (2014). 3D bioprinting of tissues and organs. *Nature biotechnology*, 32(8), 773.
- Nakamura, M., Rikimaru, T., Yano, T., Moore, K. G., Pula, P. J., Schofield, B. H., & Dannenberg Jr, A. M. (1990). Full-Thickness Human Skin Explants for Testing the Toxicity of Topically Applied Chemicals. *Journal of investigative dermatology*, 95(3).
- Noguera-Morel, L., Feito-Rodríguez, M., Maldonado-Cid, P., García-Miñaur, S., Kamsteeg, E. J., González-Sarmiento, R., ... & Torrelo, A. (2016). Two Cases of Autosomal Recessive Congenital Ichthyosis due to CYP4F22 Mutations: Expanding the Genotype of Self-Healing Collodion Baby. *Pediatric dermatology*, 33(2), e48-e51.
- Numata, S., Teye, K., Krol, R. P., Karashima, T., Fukuda, S., Matsuda, M., ... & Ariffin, R. (2015). Mutation study for 9 genes in 23 unrelated patients with autosomal recessive congenital ichthyosis in Japan and Malaysia. *Journal of dermatological science*, 78(1), 82-85.

O'Brien, K., Bhatia, A., Tsen, F., Chen, M., Wong, A. K., Woodley, D. T., & Li, W. (2014). Identification of the critical therapeutic entity in secreted Hsp90 α that promotes wound healing in newly re-standardized healthy and diabetic pig models. *PLoS One*, 9(12), e113956.

O'Brien, K., Bhatia, A., Tsen, F., Chen, M., Wong, A. K., Woodley, D. T., & Li, W. (2014). Identification of the critical therapeutic entity in secreted Hsp90 α that promotes wound healing in newly re-standardized healthy and diabetic pig models. *PloS one*, 9(12), e113956.

Ohno, Y., Nakamichi, S., Ohkuni, A., Kamiyama, N., Naoe, A., Tsujimura, H., ... & Kihara, A. (2015). Essential role of the cytochrome P450 CYP4F22 in the production of acylceramide, the key lipid for skin permeability barrier formation. *Proceedings of the National Academy of Sciences*, 112(25), 7707-7712.

Ojeh, N., Akgül, B., Tomic-Canic, M., Philpott, M., & Navsaria, H. (2017). In vitro skin models to study epithelial regeneration from the hair follicle. *PloS one*, 12(3), e0174389.

Oji, V., & Traupe, H. (2009). Ichthyosis. *American journal of clinical dermatology*, 10(6), 351-364.

Oji, V., Tadini, G., Akiyama, M., Bardon, C. B., Bodemer, C., Bourrat, E., ... & Fleckman, P. (2010). Revised nomenclature and classification of inherited ichthyoses: results of the First Ichthyosis Consensus Conference in Soreze 2009. *Journal of the American Academy of Dermatology*, 63(4), 607-641.

Ormerod, A. D., Campalani, E., & Goodfield, M. J. D. (2010). British Association of Dermatologists guidelines on the efficacy and use of acitretin in dermatology. *British Journal of Dermatology*, 162(5), 952-963.

Pant, K., Pufe, J., Zarschler, K., Bergmann, R., Steinbach, J., Reimann, S., ... & Stephan, H. (2017). Surface charge and particle size determine the metabolic fate of dendritic polyglycerols. *Nanoscale*, 9(25), 8723-8739.

Pigg, M. H., Bygum, A., Gånemo, A., Virtanen, M., Brandrup, F., Zimmer, A. D., ... & Fischer, J. (2016). Spectrum of autosomal recessive congenital ichthyosis in Scandinavia: clinical characteristics and novel and recurrent mutations in 132 patients. *Acta dermato-venereologica*, 96(7), 932-938.

- Planz, V., Lehr, C. M., & Windbergs, M. (2016). In vitro models for evaluating safety and efficacy of novel technologies for skin drug delivery. *Journal of Controlled Release*, 242, 89-104.
- Ponce, L., Heintz, F., Schäfer, I., Klusch, A., Holloschi, A., Schmelz, M., ... & Hafner, M. (2017). Isolation and cultivation of primary keratinocytes from piglet skin for compartmentalized co-culture with dorsal root ganglion neurons. *Journal of Cellular Biotechnology*, 2(2), 93-115.
- Proksch, E., Brandner, J. M., & Jensen, J. M. (2008). The skin: an indispensable barrier. *Experimental dermatology*, 17(12), 1063-1072.
- Puiu, M., & Dan, D. (2010). Rare diseases, from European resolutions and recommendations to actual measures and strategies. *Mædica*, 5(2), 128-131.
- Radner, F. P., Marrakchi, S., Kirchmeier, P., Kim, G. J., Ribierre, F., Kamoun, B., ... & Heilig, R. (2013). Mutations in CERS3 cause autosomal recessive congenital ichthyosis in humans. *PLoS genetics*, 9(6), e1003536.
- Ranamukhaarachchi, S. A., Lehnert, S., Ranamukhaarachchi, S. L., Sprenger, L., Schneider, T., Mansoor, I., ... & Stoeber, B. (2016). A micromechanical comparison of human and porcine skin before and after preservation by freezing for medical device development. *Scientific reports*, 6, 32074.
- Rancan, F., Giulbudagian, M., Jurisch, J., Blume-Peytavi, U., Calderon, M., & Vogt, A. (2017). Drug delivery across intact and disrupted skin barrier: Identification of cell populations interacting with penetrated thermoresponsive nanogels. *European Journal of Pharmaceutics and Biopharmaceutics*, 116, 4-11.
- Rathore, S., David, L. S., Beck, M. M., Bindra, M. S., & Arunachal, G. (2015). Harlequin ichthyosis: Prenatal diagnosis of a rare yet severe genetic dermatosis. *Journal of clinical and diagnostic research: JCDR*, 9(11), QD04.
- Reijnders, C. M., van Lier, A., Roffel, S., Kramer, D., Scheper, R. J., & Gibbs, S. (2015). Development of a full-thickness human skin equivalent in vitro model derived from TERT-immortalized keratinocytes and fibroblasts. *Tissue Engineering Part A*, 21(17-18), 2448-2459.

Reis-Filho, Jorge S., et al. "p63 expression in normal skin and usual cutaneous carcinomas." *Journal of cutaneous pathology* 29.9 (2002): 517-523.

Richard, G. (2004, November). Molecular genetics of the ichthyoses. In *American Journal of Medical Genetics Part C: Seminars in Medical Genetics* (Vol. 131, No. 1, pp. 32-44). Wiley Subscription Services, Inc., A Wiley Company.

Richard, G. (2017). Autosomal recessive congenital ichthyosis.

Richardson, M. (2003). Understanding the structure and function of the skin. *Nursing times*, 99(31), 46-48.

Rodríguez-Leyva, I., Calderón-Garcidueñas, A. L., Jiménez-Capdeville, M. E., Rentería-Palomo, A. A., Hernandez-Rodriguez, H. G., Valdés-Rodríguez, R., ... & Santoyo, M. E. (2014). α -Synuclein inclusions in the skin of Parkinson's disease and parkinsonism. *Annals of clinical and translational neurology*, 1(7), 471-478.

Ronaldson-Bouchard, K., & Vunjak-Novakovic, G. (2018). Organs-on-a-chip: a fast track for engineered human tissues in drug development. *Cell stem cell*, 22(3), 310-324.

Salehin, S., Azizimoghadam, A., Abdollahimohammad, A., & Babaeipour-Divshali, M. (2013). Harlequin ichthyosis: Case report. *Journal of research in medical sciences: the official journal of Isfahan University of Medical Sciences*, 18(11), 1004.

Santos, M., Paramio, J. M., Bravo, A., Ramirez, A., & Jorcano, J. L. (2002). The expression of keratin k10 in the basal layer of the epidermis inhibits cell proliferation and prevents skin tumorigenesis. *Journal of Biological Chemistry*, 277(21), 19122-19130.

Schmook, F. P., Meingassner, J. G., & Billich, A. (2001). Comparison of human skin or epidermis models with human and animal skin in in-vitro percutaneous absorption. *International journal of pharmaceutics*, 215(1-2), 51-56.

Schmuth, M., Martinz, V., Janecke, A. R., Fauth, C., Schossig, A., Zschocke, J., & Gruber, R. (2013). Inherited ichthyoses/generalized Mendelian disorders of cornification. *European Journal of Human Genetics*, 21(2), 123.

Scientific, T. F. (2009). NanoDrop 2000/2000c Spectrophotometer V1. 0 User Manual. Wilmington, DE, 19810.

Sekkat, N., Kalia, Y. N., & Guy, R. H. (2002). Biophysical study of porcine ear skin in vitro and its comparison to human skin in vivo. *Journal of pharmaceutical sciences*, 91(11), 2376-2381.

Shigehara, Y., Okuda, S., Nemer, G., Chedraoui, A., Hayashi, R., Bitar, F., ... & Sleiman, M. B. (2016). Mutations in SDR9C7 gene encoding an enzyme for vitamin A metabolism underlie autosomal recessive congenital ichthyosis. *Human molecular genetics*, 25(20), 4484-4493.

Shruthi, B., Nilgar, B. R., Dalal, A., & Limbani, N. (2017). Harlequin ichthyosis: A rare case. *Turkish journal of obstetrics and gynecology*, 14(2), 138.

Specifications, Kit. "PureLink™ RNA Mini Kit."

Steinert, P. M., Kim, S. Y., Chung, S. I., & Marekov, L. N. (1996). The transglutaminase 1 enzyme is variably acylated by myristate and palmitate during differentiation in epidermal keratinocytes. *Journal of Biological Chemistry*, 271(42), 26242-26250.

Steven, A. C., & Steinert, P. M. (1994). Protein composition of cornified cell envelopes of epidermal keratinocytes. *Journal of cell science*, 107(2), 693-700.

Stout, T. E., McFarland, T., Mitchell, J. C., Appukuttan, B., & Stout, J. T. (2014). Recombinant filaggrin is internalized and processed to correct filaggrin deficiency. *Journal of Investigative Dermatology*, 134(2), 423-429.

Sugiura, K., & Akiyama, M. (2015). Update on autosomal recessive congenital ichthyosis: mRNA analysis using hair samples is a powerful tool for genetic diagnosis. *Journal of dermatological science*, 79(1), 4-9.

Suter, M. M., Schulze, K., Bergman, W., Welle, M., Roosje, P., & Müller, E. J. (2009). The keratinocyte in epidermal renewal and defence. *Veterinary dermatology*, 20(5-6), 515-532.

Swindle, M. M. (1998). Comparative anatomy and physiology of the pig. *Scand. J. Lab. Anim. Sci.*, 25, 11-21.

Swindle, M. M., Makin, A., Herron, A. J., Clubb Jr, F. J., & Frazier, K. S. (2012). Swine as models in biomedical research and toxicology testing. *Veterinary pathology*, 49(2), 344-356.

Takeichi, T., & Akiyama, M. (2016). Inherited ichthyosis: Non-syndromic forms. *The Journal of dermatology*, 43(3), 242-251.

- Takeichi, T., Nanda, A., Aristodemou, S., McMillan, J. R., Lee, J., Akiyama, M., ... & McGrath, J. A. (2015). Whole-exome sequencing diagnosis of two autosomal recessive disorders in one family. *British Journal of Dermatology*, 172(5), 1407-1411.
- Takeichi, T., Nomura, T., Takama, H., Kono, M., Sugiura, K., Watanabe, D., ... & Akiyama, M. (2017). Deficient stratum corneum intercellular lipid in a Japanese patient with lamellar ichthyosis with a homozygous deletion mutation in SDR 9C7. *British Journal of Dermatology*, 177(3), e62-e64.
- Tekin, M., Konca, Ç., Kahramaner, Z., & Erdemir, A. (2014). Harlequin ichthyosis: The third babies with harlequin ichthyosis in a family. *Turkish Archives of Pediatrics/Türk Pediatri Arşivi*, 49(3), 269.
- Terrinoni, A., Serra, V., Codispoti, A., Talamonti, E., Bui, L., Palombo, R., ... & Zambruno, G. (2012). Novel transglutaminase 1 mutations in patients affected by lamellar ichthyosis. *Cell death & disease*, 3(10), e416.
- Thomas, A. C., Tattersall, D., Norgett, E. E., O'Toole, E. A., & Kelsell, D. P. (2009). Premature terminal differentiation and a reduction in specific proteases associated with loss of ABCA12 in Harlequin ichthyosis. *The American journal of pathology*, 174(3), 970-978.
- Todo, H. (2017). Transdermal permeation of drugs in various animal species. *Pharmaceutics*, 9(3), 33.
- Tracy, L. E., Minasian, R. A., & Caterson, E. J. (2016). Extracellular matrix and dermal fibroblast function in the healing wound. *Advances in wound care*, 5(3), 119-136.
- Traupe, H., Fischer, J., & Oji, V. (2014). Nonsyndromic types of ichthyoses—an update. *JDDG: Journal der Deutschen Dermatologischen Gesellschaft*, 12(2), 109-121.
- Tsatmali, M., Ancans, J., & Thody, A. J. (2002). Melanocyte function and its control by melanocortin peptides. *Journal of Histochemistry & Cytochemistry*, 50(2), 125-133.
- Vahlquist, A. (2010). Pleomorphic ichthyosis: proposed name for a heterogeneous group of congenital ichthyoses with phenotypic shifting and mild residual scaling. *Acta dermato-venereologica*, 90(5), 454-460.
- Vahlquist, A., Bygum, A., Gånemo, A., Virtanen, M., Hellström-Pigg, M., Strauss, G., ... & Fischer, J. (2010). Genotypic and clinical spectrum of self-improving collodion ichthyosis:

ALOX12B, ALOXE3, and TGM1 mutations in Scandinavian patients. *Journal of Investigative Dermatology*, 130(2), 438-443.

Vaigundan, D., Kalmankar, N. V., Krishnappa, J., Gowda, N. Y., Kutty, A. V. M., & Krishnaswamy, P. R. (2014). A novel mutation in the transglutaminase-1 gene in an autosomal recessive congenital ichthyosis patient. *BioMed research international*, 2014.

Varani, J. (2012). Human skin organ culture for assessment of chemically induced skin damage. *Expert review of dermatology*, 7(3), 295-303.

Varani, J., Perone, P., Merfert, M. G., Moon, S. E., Larkin, D., & Stevens, M. J. (2002). All-trans retinoic acid improves structure and function of diabetic rat skin in organ culture. *Diabetes*, 51(12), 3510-3516.

Varani, J., Perone, P., Spahlinger, D. M., Singer, L. M., Diegel, K. L., Bobrowski, W. F., & Dunstan, R. (2007). Human skin in organ culture and human skin cells (keratinocytes and fibroblasts) in monolayer culture for assessment of chemically induced skin damage. *Toxicologic pathology*, 35(5), 693-701.

Venus, M., Waterman, J., & McNab, I. (2010). Basic physiology of the skin. *Surgery-Oxford International Edition*, 28(10), 469-472.

Verfaille, C. J., Borgers, M., & Van Steensel, M. A. (2008). Retinoic acid metabolism blocking agents (RAMBAs): a new paradigm in the treatment of hyperkeratotic disorders. *JDDG: Journal der Deutschen Dermatologischen Gesellschaft*, 6(5), 355-364.

Verfaille, C. J., Vanhoutte, F. P., Blanchet-Bardon, C., Van Steensel, M. A., & Steijlen, P. M. (2007). Oral liarozole vs. acitretin in the treatment of ichthyosis: a phase II/III multicentre, double-blind, randomized, active-controlled study. *British Journal of Dermatology*, 156(5), 965-973.

Vörsmann, H., Groeber, F., Walles, H., Busch, S., Beisert, S., Walczak, H., & Kulms, D. (2013). Development of a human three-dimensional organotypic skin-melanoma spheroid model for in vitro drug testing. *Cell death & disease*, 4(7), e719.

Wajid, M., Kurban, M., Shimomura, Y., & Christiano, A. M. (2010). NIPAL4/ichthyin is expressed in the granular layer of human epidermis and mutated in two Pakistani families with autosomal recessive ichthyosis. *Dermatology*, 220(1), 8-14.

- Wei, J. C., Edwards, G. A., Martin, D. J., Huang, H., Crichton, M. L., & Kendall, M. A. (2017). Allometric scaling of skin thickness, elasticity, viscoelasticity to mass for micro-medical device translation: from mice, rats, rabbits, pigs to humans. *Scientific reports*, 7(1), 15885.
- West, H. C., & Bennett, C. L. (2018). Redefining the role of langerhans cells as immune regulators within the skin. *Frontiers in immunology*, 8, 1941.
- Witting, M., Molina, M., Obst, K., Plank, R., Eckl, K. M., Hennies, H. C., ... & Hedtrich, S. (2015). Thermosensitive dendritic polyglycerol-based nanogels for cutaneous delivery of biomacromolecules. *Nanomedicine: Nanotechnology, Biology and Medicine*, 11(5), 1179-1187.
- Wu, Nan-Lin, et al. "TRAIL-induced keratinocyte differentiation requires caspase activation and p63 expression." *Journal of Investigative Dermatology* 131.4 (2011): 874-883.
- Xia, Z., Jin, S., & Ye, K. (2018). Tissue and Organ 3D Bioprinting. SLAS TECHNOLOGY: *Translating Life Sciences Innovation*, 2472630318760515.
- Yamada, K., Matsuki, M., Morishima, Y., Ueda, E., Tabata, K., Yasuno, H., ... & Yamanishi, K. (1997). Activation of the human transglutaminase 1 promoter in transgenic mice: terminal differentiation-specific expression of the TGM1-lacZ transgene in keratinized stratified squamous epithelia. *Human molecular genetics*, 6(13), 2223-2231.
- Yamane, M., Sugimura, K., Kawasaki, H., Tatsukawa, H., & Hitomi, K. (2016). Analysis on transglutaminase 1 and its substrates using specific substrate peptide in cultured keratinocytes. *Biochemical and biophysical research communications*, 478(1), 343-348.
- Yoneda, K. (2016). Inherited ichthyosis: syndromic forms. *The Journal of dermatology*, 43(3), 252-263.
- Yousef, H., & Sharma, S. (2017). Anatomy, Skin (Integument), Epidermis.
- Yu, Z., Schneider, C., Boeglin, W. E., Marnett, L. J., & Brash, A. R. (2003). The lipoygenase gene ALOXE3 implicated in skin differentiation encodes a hydroperoxide isomerase. *Proceedings of the National Academy of Sciences*, 100(16), 9162-9167.
- Zhang, Z., & Michniak-Kohn, B. B. (2012). Tissue engineered human skin equivalents. *Pharmaceutics*, 4(1), 26-41.